Title
AN ELECTROMAGNETIC (EM-60) SURVEY IN THE PANTHER CANYON AREA, GRASS VALLEY, NEVADA

Authors
Wilt, M.
Goldstein, N.
Stark, M.
et al.

Publication Date
1980-05-01

LBL-10993
UC-66b

AN ELECTROMAGNETIC (EM-60) SURVEY IN THE PANTHER CANYON AREA, GRASS VALLEY, NEVADA

M. Wilt, N. Goldstein, M. Stark, and R. Haught

Earth Sciences Division
Lawrence Berkeley Laboratory
University of California,
Berkeley, California 94720

DISCLAIMER

DISCLAIMER

AN ELECTROMAGNETIC (EM-60) SURVEY IN THE PANTHER CANYON AREA GRASS VALLEY, NEVADA

M. Wilt, N. Goldstein, M. Stark, and R. Haught

Abstract

Eight frequency domain electromagnetic soundings were measured over the Panther Canyon thermal anomaly in Grass Valley, Nevada. The data were collected with Lawrence Berkeley Laboratory's large moment horizontal loop system (EM-60). At the transmitter site located near the center of the thermal anomaly, square wave currents of up to 70 A were impressed into a four-turn 50 m radius coil at frequencies from 0.033 to 500 Hz. At the eight receiver sites, 0.5 to 1.5 km from the loop, magnetic fields were detected with a three-component SQUID magnetometer and vertical and radial magnetic field spectra were calculated. Data were interpreted with a computer program which fit filled spectra and associated ellipse polarization data to one-dimensional resistivity models and results were compared to interpretations from earlier dipole-dipole resistivity measurements. Comparison of these interpretations indicates fairly close agreement between the two, with both models clearly indicating the presence and dimensions of the conductivity anomaly associated with the thermal zone. Although the dc data was better able to resolve the high resistivity bedrock, the EM data were able to resolve all major features without distortion at shorter transmitter receiver separations and in about one-third of the field time.

Introduction

As part of the Department of Energy, Division of Geothermal Energy's (DOE/DGE) Industry-Coupled Program to stimulate geothermal resource development, Lawrence Berkeley Laboratory has conducted a series of electromagnetic (EM-60) sounding surveys over several promising geothermal sites in Nevada.

This report describes the results of a controlled-source EM survey in the Panther Canyon region of Grass Valley, Nevada (Figure 1). The soundings were performed with the EM-60 horizontal loop, frequency-domain electromagnetic system (Morrison et al., 1978). We performed eight frequency domain electromagnetic soundings within a 12 km^2 region surrounding a single four-turn, 50-m-radius horizontal loop. For each sounding, a layered model interpretation was made, and the layered interpretations were combined into resistivity

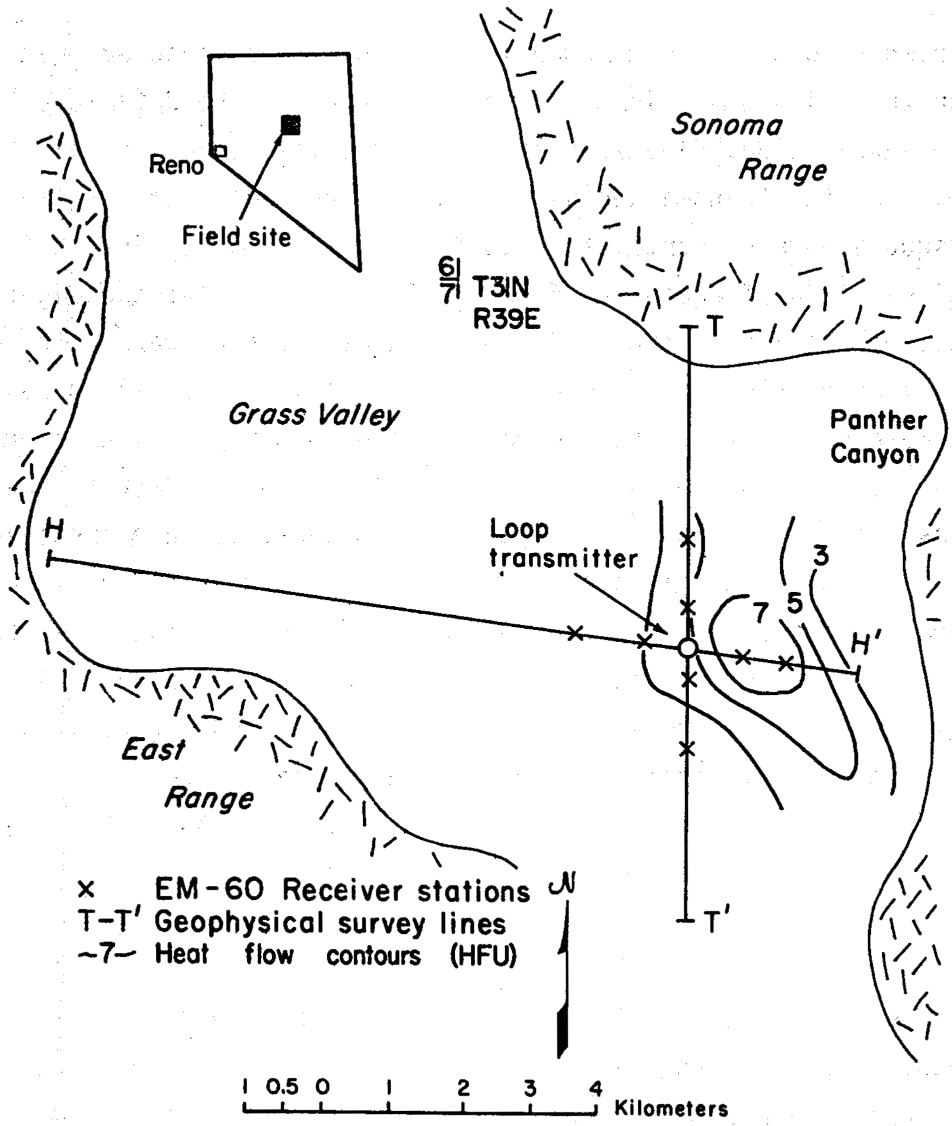

XBL 804-7050

Figure 1. Survey location map of Panther Canyon area, Grass Valley, Nevada.

sections. These interpretations are compared to other geophysical data for confirmation and as a way of evaluating the EM method.

Geology

Grass Valley is an elongate northerly-trending Basin and Range valley located in north-central Nevada. The region is characterized by higher-than-normal heat flow (Sass et al., 1971), active hot springs (Olmsted et al., 1975) and recent faulting (Noble, 1975; Majer, 1978). Grass Valley has been an area of active geothermal exploration for about the past eight years, but to date no major discovery has been made.

Surface geologic studies consisting of regional photogeology (Noble, 1975) and detailed field mapping (Olmsted et al., 1975; Silberling, 1975; Noble, 1975; and Nichols, 1972) were done partly in conjunction with geothermal studies (Beyer et al., 1976). A bedrock geologic map of the Leach Hot Springs quadrangle is given in Figure 2. This map is a composite from the sources cited and includes the area of the present survey.

The Panther Canyon area is located in the southwestern portion of Grass Valley near the intersection of the Tobin and Sonoma Ranges. Exposed rocks in these ranges consist mainly of the Paleozoic Havallah sequence of cherts, argillites and sandstones. Also present in the mountains are Tertiary Kiapoto formation rhyolite and trachitic tuffs and Triassic cherts, dolomites, and conglomerates of the Panther Canyon Formation. Figures 3 and 4 are idealized geologic cross sections along the orthogonal EM-60 survey lines. These composite profiles correspond to the lines shown in Figure 1.

Geophysics

Reconnaissance and detailed geophysical investigations have been performed throughout Grass Valley and several detailed studies were done in the Panther Canyon area. Work has included dipole-dipole resistivity and telluric profiles (Beyer, 1977), magnetotelluric soundings (Morrison et al., 1979), passive seismics (Majer, 1978), gravity (Goldstein and Paulsson, 1978) and heat flow (Sass et al., 1977). Composite profiles and syntheses of these and other data are given in Beyer (1977) and Morrison et al. (1978).

Geothermal interest in the Panther Canyon area was heightened after several shallow boreholes indicated anomalously high heat flow values of 7 heat flow units (HFU), about three times the regional average. Subsequent telluric and

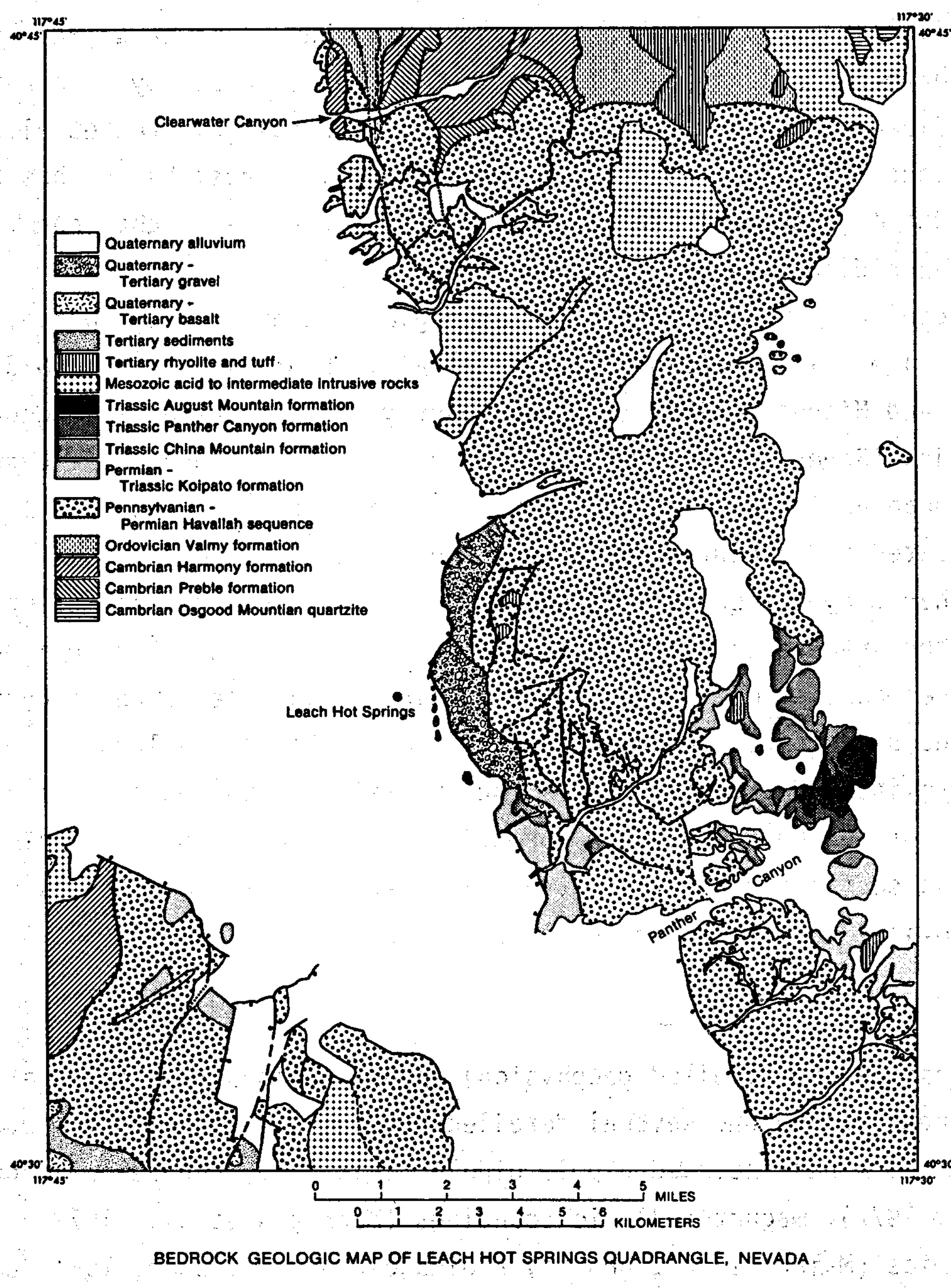

Figure 2. Bedrock geologic map of the Leach Hot Springs Quadrangle, Grass Valley Nevada (after Sass et al.. 1977).

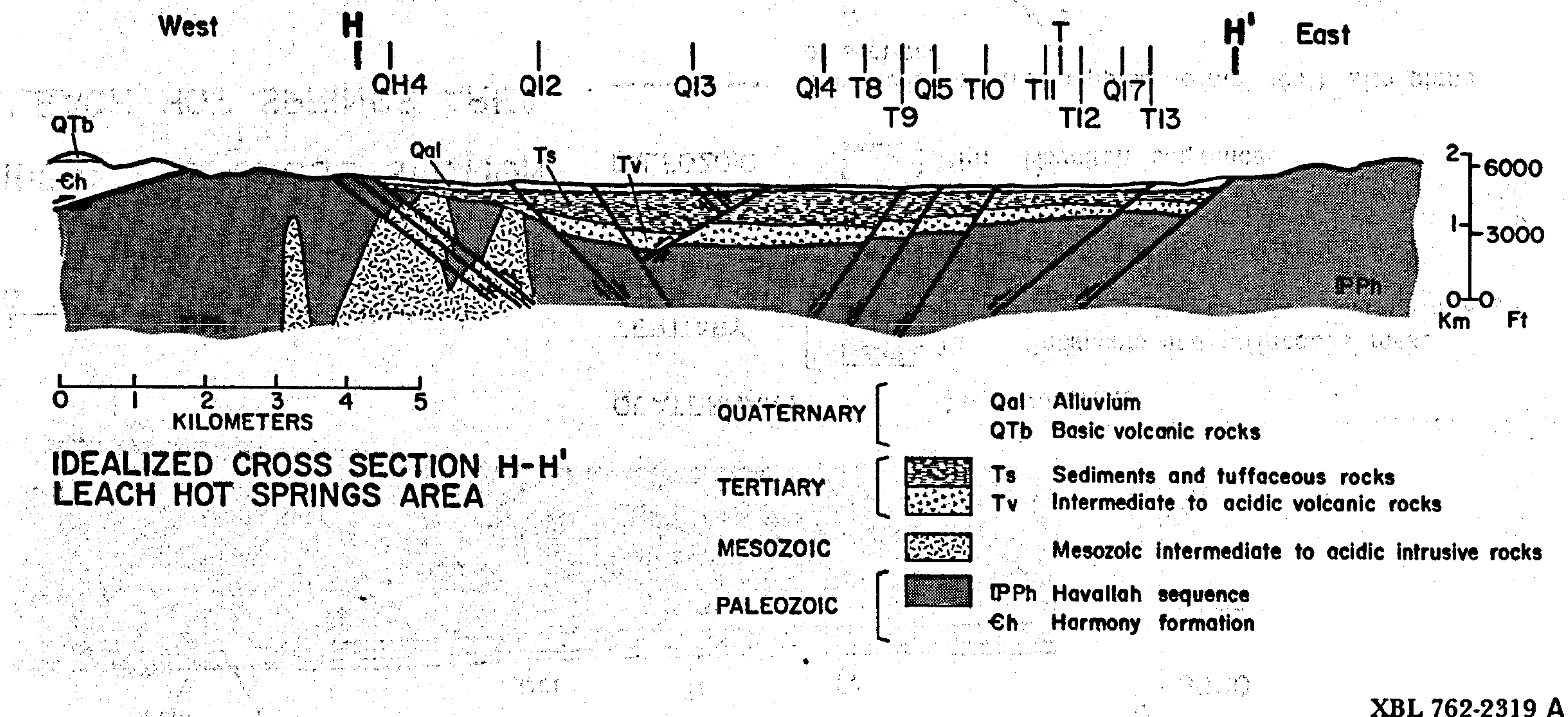

Figure 3. Idealized geologic cross section for survey line H-H' (after Sass et al., 1977). Markings (Q12) denote locations of heat flow boreholes.

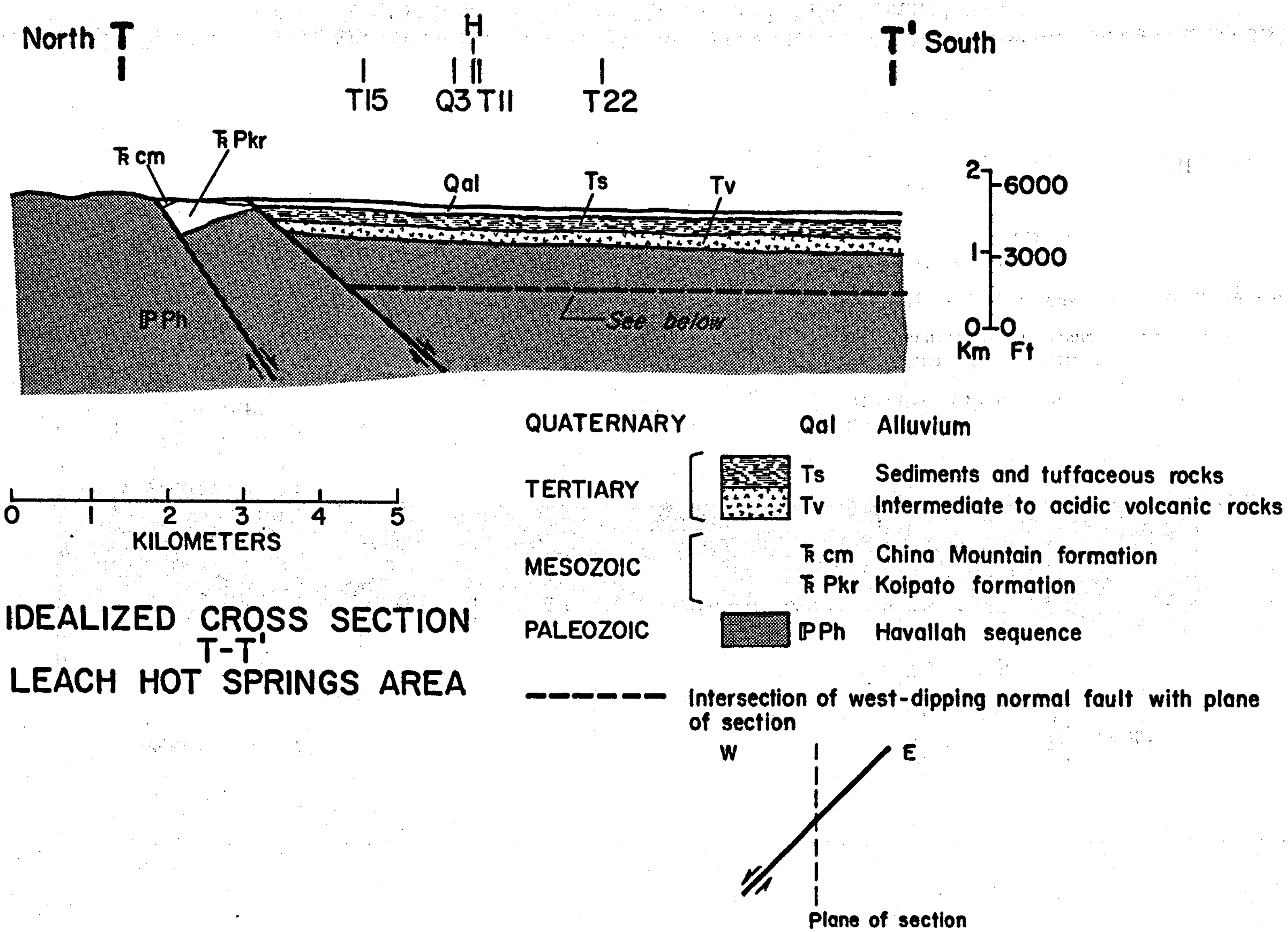

Figure 4. Idealized geologic cross section for survey line T–T' (after Sass et al., 1977). Markings (Q3) denote heat flow boreholes. XBL 763-622 A

resistivity studies over the heat flow anomaly revealed a low resistivity zone, thus suggesting the presence of geothermal waters at depth.

Field Survey

The EM-60 field survey in Panther Canyon consisted of eight soundings arranged in two orthogonal profiles about a central four-turn, 50-radius horizontal loop. Transmitter-receiver separations varied from 400 m to 1.6 km, and data at each site were recorded over at least two frequency decades within the frequency band 0.033-500 Hz. Since the depth of penetration for EM induction sounding is proportional to both the transmitter-receiver separation and the period of the transmitted wave, it was desirable to occupy receiver sites at different separations with respect to one loop. This permitted a more complete resistivity depth section and a better knowledge of surface inhomogeneities. At Panther Canyon four of the soundings were placed about 500 m from the loop source for shallow information, and four other sites were occupied at about 1.5 km for better resolution of deeper horizons. A crew of four completed the entire survey in six field days, including laying out and retrieving the transmitter coil and one day of system testing and debugging. The maximum production rate achieved was three soundings in a 12 hr work day. Recording times varied from about four hr per station at the more distant sites to one at the closer stations. Radial and vertical magnetic fields were measured at each station by means of a three-component SQUID magnetometer (Appendix A). The survey was performed under ideal weather conditions, and there was good vehicular access to stations.

Results

Data for the eight EM-60 soundings are given in Appendix B. Each sounding is presented in terms of normalized amplitudes and phases of the observed magnetic fields, as well as the polarization ellipse parameters of the fields; namely, ellipticity and tilt angle. The observed fields are normalized by the free-space primary field so that the secondary fields, due to the presence of the earth can be better visualized. The phases are given with respect to the phase of the current impressed into the loop. The ellipticity parameter is the ratio of the minor to major axis of the polarization ellipse traced out by the observed field; the sign of the ellipticity refers to the direction in which the ellipse is traced, a negative sign denotes anticlockwise rotation. The tilt angle parameter refers to the inclination from the vertical of the polarization ellipse. The polarization ellipse parameters are calculated from relative phases between the observed fields, and thus these measurements may be made without an absolute phase reference to the loop current.

Data listed in Appendix B indicate that accurate amplitude-phase data were obtained at Panther Canyon up to about 100 Hz, whereas good polarization ellipse data could sometimes be obtained to 500 Hz. The declining strength of the primary and secondary fields with frequency and the increasing noise in the reference wire cause amplitude-phase data to be particularly noisy above 100 Hz. Because polarization ellipse data can be taken without a reference wire, this information is often more reliable at the higher frequencies. The errors shown in Appendix B refer to one standard deviation of the observed data. These are accurate representations of the true error if the sources of noise are random. Unfortunately, most noise sources observed are not random, especially above 30 Hz, so the noise estimate given in Appendix B is probably somewhat low at higher frequencies where nonrandom noise sources are greatest.

Data Interpretation

All EM soundings were interpreted individually using a layered-earth least-squares inversion program (Inman, 1975). The program finds a layered model whose EM response fits the weighted observed data. It also estimates parameter resolution and data point-parameter sensitivity. Layered model fits, model parameters, and estimated resolutions of the parameters are given in Appendix C. As it is difficult to estimate the true errors, and because, for some soundings, a one-dimensional model may not be appropriate, the errors for parameters resolution in Appendix C may be somewhat low.

Points with high errors and points that do not fall on a layered model curve were deleted from the inversions. Such data often were vertical magnetic field components because the vertical component is sensitive to, and will be distorted by, lateral inhomogeneities (Ward, 1976; Wilt et al., 1979).

Discussion

Figures 5 and 6 are resistivity cross sections along orthogonal lines over the Panther Canyon thermal anomaly. Each figure gives a comparison between dipole-dipole resistivity and EM-60 Electromagnetic interpretations. The resistivity data and the 2-D interpretation are from Beyer (1977). An example of observed dipole-dipole data, the two-dimensional and the fit of calculated-to-observed data, is given in Figure 7. The EM-60 cross sections are made from one dimensional interpretations given in Appendix C.

Along the north-south line (Figure 5), the EM and dipole-dipole interpretations are remarkably similar. Both cross sections indicate resistive surface material overlying an irregular southward-dipping conductive body. Depth to resistive basement (which may be the Havallah formation) is shown to vary between 250 and 800 m below the surface. The depth to, and lateral extent of, the conductive body, which may be associated with the thermal anomaly, is well resolved by both methods. The two profiles disagree somewhat on the depth to resistive basement beneath the conductor. Because the EM method is less sensitive to resistive formations, and because the transmitter-receiver separations were more than five times greater with the dipole-dipole data, the conventional resistivity section is probably more accurate in determining this parameter.

Figure 6 shows results for an east-west line over the central portion of the thermal anomaly. For this cross section, the EM and dc resistivity interpretations disagree somewhat. Both cross sections indicate the presence of an irregularly shaped conductive body near the central portion of the thermal anomaly. The EM data place the thickest portion slightly west of the thermal maximum, whereas the dc data place it directly beneath the maximum. The dc resistivity data indicate that basement dips steeply westward from 250 to about 800 m adjacent to the edge of the Tobin Range; the EM induction data show a similar behavior, but with fewer points and larger uncertainty.

Although the interpreted sections in both cases are similar, the EM results show a smoother variation, a consequence of one-dimensional interpretation. However, there are other differences between the EM and dc resistivity surveys that are not apparent in the data and interpretations. The dipole-dipole sections required a crew of four working for about 20 field days; whereas the same size crew collected the EM data in six field days.

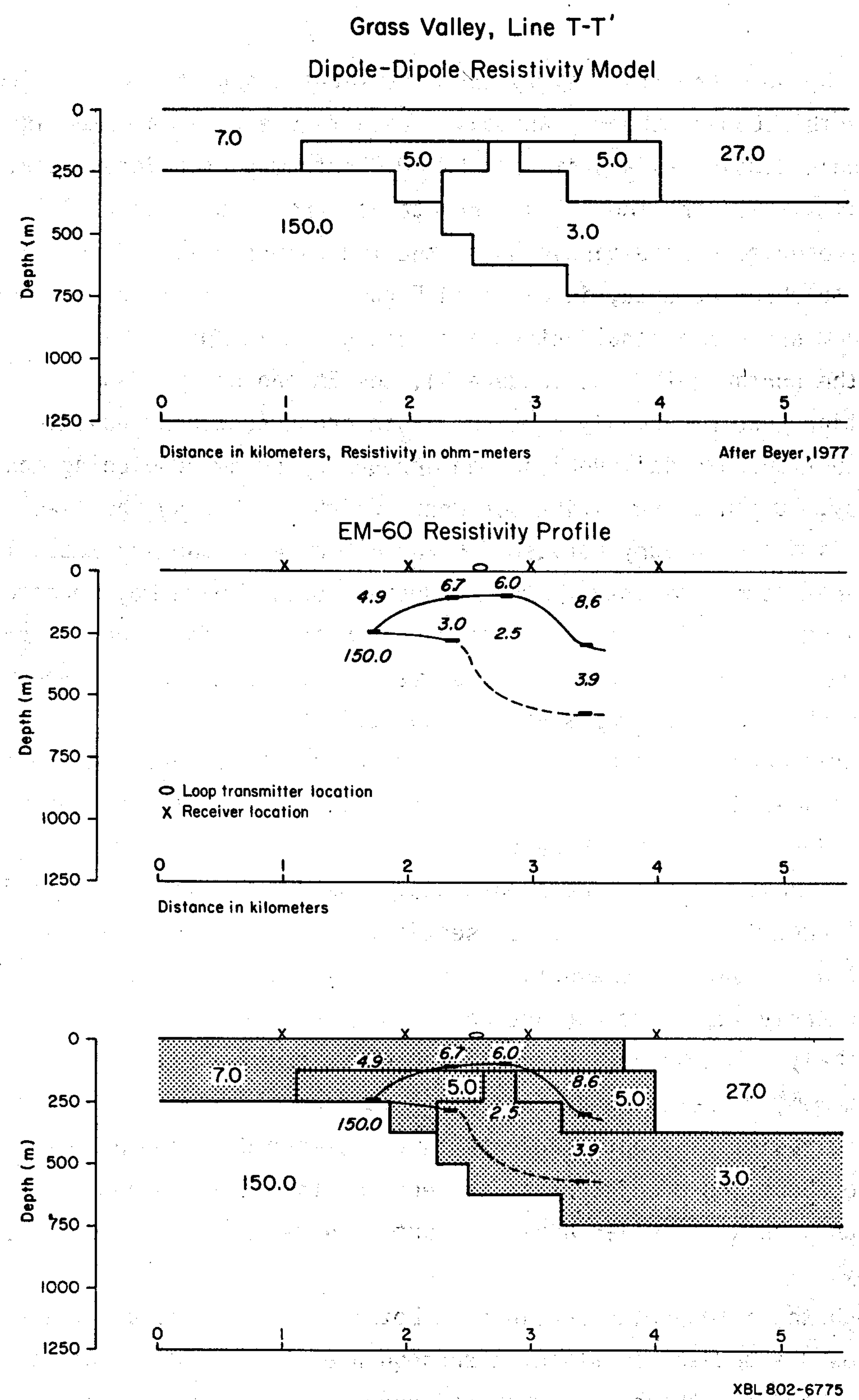

Figure 5. Resistivity cross section over line in Panther Canyon: (a) two-dimensional dipole-dipole resistivity model; (b) profile of one-dimensional EM-60 electromagnetic soundings; (c) comparison of parts (a) and (b).

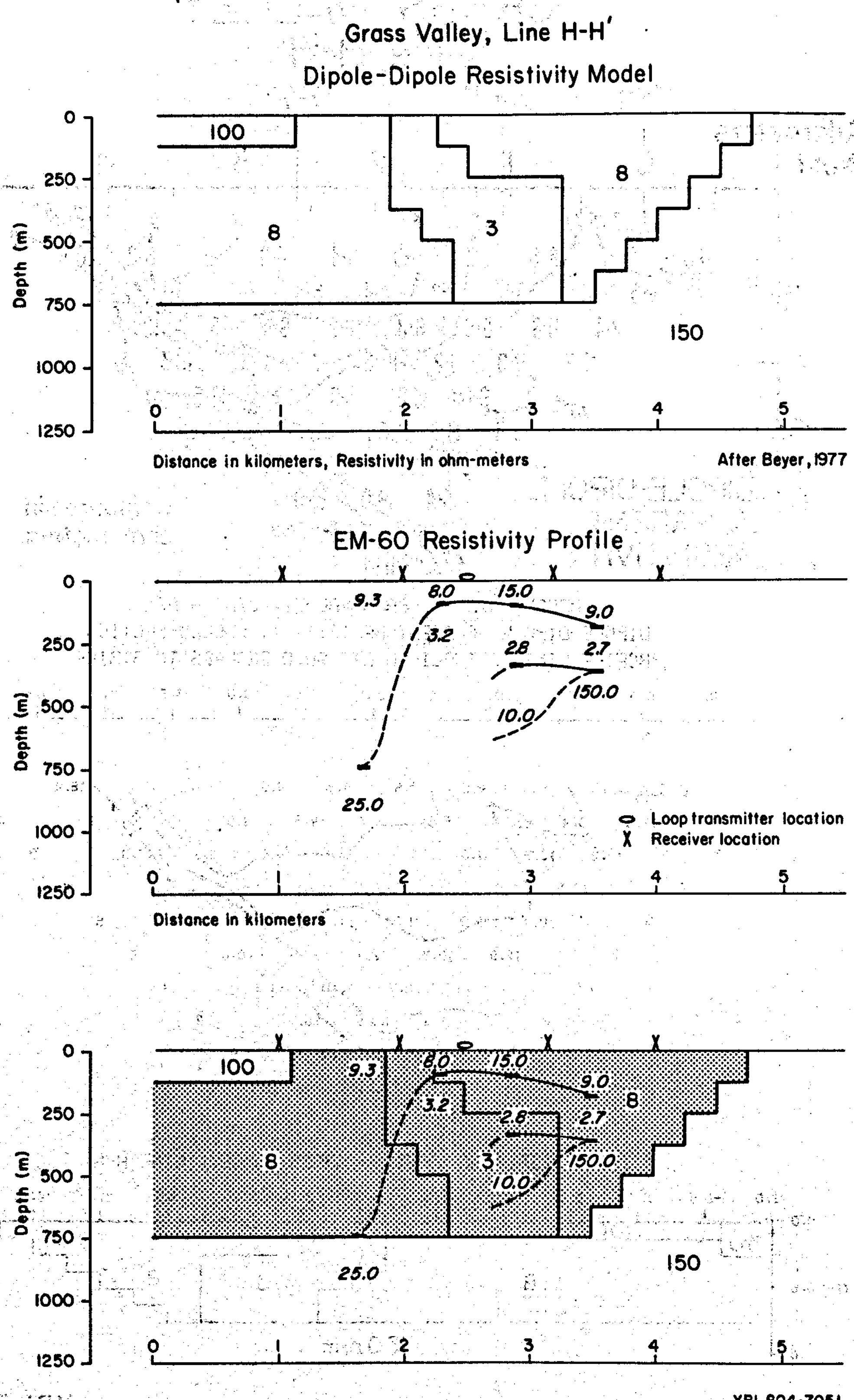

Figure 6. Resistivity cross section over line H-H' in Panther Canyon: (a) two-dimensional dipole-dipole resistivity model; (b) profile of one-dimensional EM-60 electromagnetic soundings; (c) comparison of parts (a) and (b).

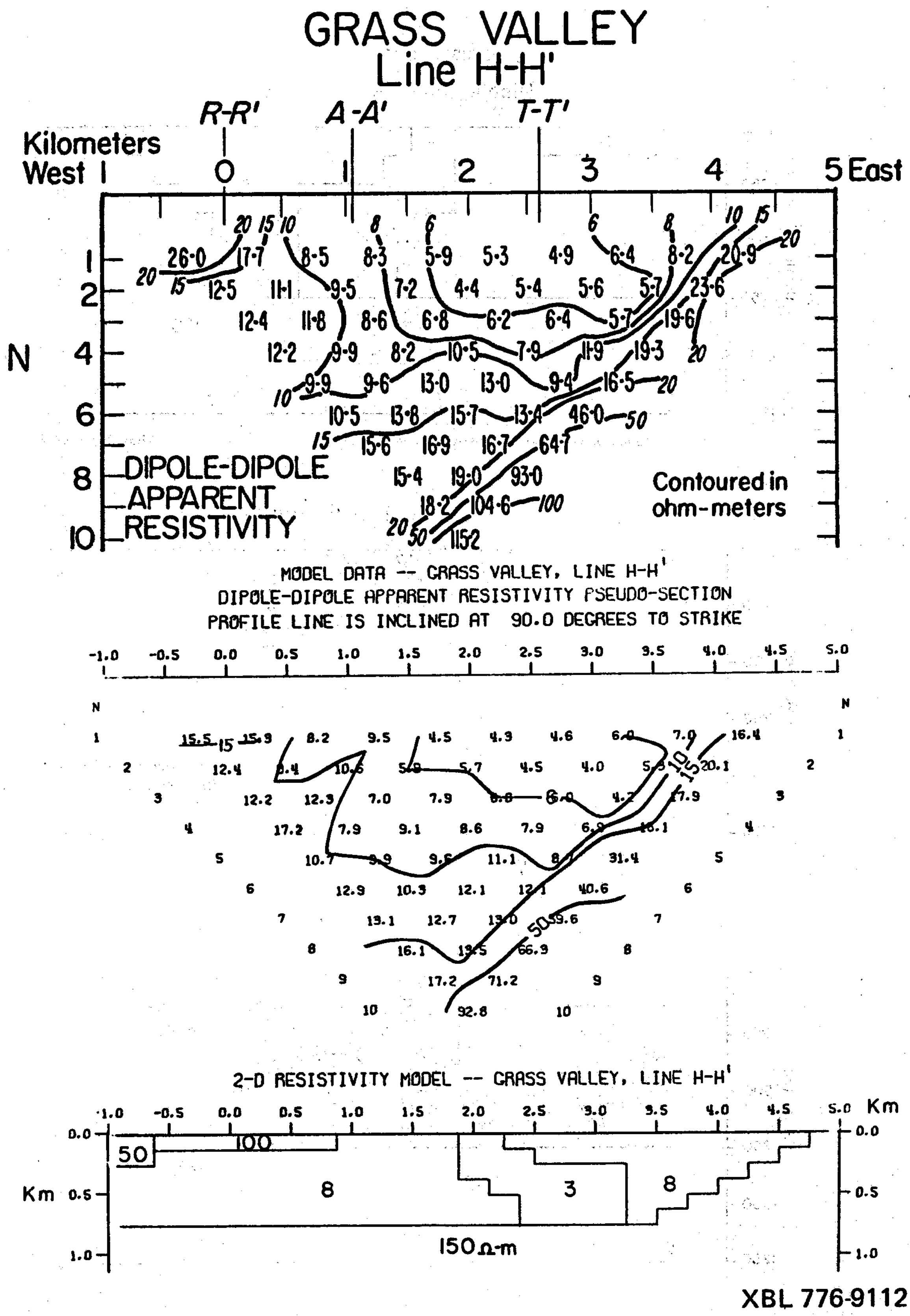

Figure 7. Dipole-dipole apparent resistivity pseudosection for 1 km dipoles along line H-H': field data, model generated data, and two-dimensional model.

The dc resistivity data cover an area about 50% larger, but far more labor was required to achieve coverage comparable to that of the EM survey. Interpretation of dipole-dipole data is presently better able to handle complex geology, and the data is better able to resolve resistive bedrock. However, deep EM interpretations required much shorter transmitter-receiver separations, thus reducing the effects of lateral inhomogeneities on interpretations. The two cross sections suggest that, even in regions of two, and three-dimensional geology, EM data will adequately resolve major features without severe distortion.

Acknowledgment

This work was supported by the Division of Geothermal Energy of the U. S. Department of Energy under Contract No. W-7405-ENG-48.

References

Beyer, J. H., Dey, A., Liaw, A., Majer, E., McEvilly, T. V., Morrison, H. F., and Wollenberg, H. A., 1976. Preliminary Open File Report. Geological and geophysical studies in Grass Valley, Nevada. Lawrence Berkeley Laboratory, LBL-5262.

Beyer, J. H., 1977. Telluric and d.c. resistivity techniques applied to the geophysical investigation of basin and range geothermal systems, Part III: The analysis of data from Grass Valley, Nevada. Lawrence Berkeley Laboratory, LBL-6325, March 3, 115 p.

Goldstein, N. E., and Paulsson, B., 1977. Interpretation of gravity surveys in Grass and Buena Vista Valleys, Nevada. Lawrence Berkeley Laboratory, LBL-7013.

Inman, J. R., 1975. Resistivity inversion with Ridge regression. Geophysics, 40, pp. 798-817.

Majer, E., 1978. Seismological investigations in geothermal areas. Ph. D. dissertation, Department of Geology and Geophysics, University of California Berkeley, LBL-7054.

Morrison, H. F., Goldstein N. E. Hoversten, N., Opplinger, G., and Riveros, C., 1978. Description, field test and data analysis of controlled-source EM system EM-60, Lawrence Berkeley Laboratory, LBL-7088.

Nichols, K. M., 1972. Triassic depositional history of China Mountain and vicinity, north-central Nevada. Ph. D. dissertation, Stanford University.

Noble, D. C., 1975. Geologic history and geothermal potential of the Leach Hot Springs area, Pershing County, Nevada. Preliminary report to Lawrence Berkeley Laboratory.

Olmsted, F. H., Glancy, P. A., Harrill, J. R., Rush, F. E., Van Denburgh, A. S., 1975. Preliminary hydrologic appraisal of selected hydrothermal systems in northern and central Nevada. USGS Open File Report 75-56.

Sass, J. H., Siagos, J. P.. Wollenberg, H. A., Munroe, R. J., DiSomma, D., and Lachenbruch, A. H., 1977. Application of heat flow techniques to geothermal energy exploration, Leach Hot Springs, Grass Valley, Nevada. Lawrence Berkeley Laboratory, LBL-6809, USGS Open File Report (in preparation).

Sass, J. H., Lachenbruch, A. H., Munroe, R. G., Greene, G. W., and Moses, T. H., Jr., 1971. Heat flow in the western United States. J. Geophys. Res. 76, 6376.

Silberling, N. J., 1975. Age relationships of the Golconda thrust fault, Sonoma Range, north-central Nevada. Geol. Soc. America, Special Paper 163.

Ward, S. H., 1967. Mining geophysics, vol. 2, Society of Exploration Geophysicists, Tulsa, Oklahoma,

Wilt, M., Goldstein, N. E., Hoversten, M. and Morrison, H. F., 1979. Controlled-source EM experiment at Mt. Hood, Oregon, Lawrence Berkeley Laboratory, LBL-9399.

APPENDIX A

EM-60 Electromagnetic System

In 1976 the Lawrence Berkeley Laboratory (LBL), in conjunction with the University of California at Berkeley, made preliminary measurements with a prototype large-moment, horizontal-loop electromagnetic prospecting system (Jain, 1978) in a geothermal area in Nevada. Encouraging results from this work led to the development of the EM-60 horizontal-loop system (Morrison et al., 1978) which has now been operated for more than 500 hr at various geothermal sites in Nevada and Oregon.

The EM method may be a significant improvement over existing techniques, i.e., dc resistivity and magnetotellurics in geothermal exploration, for three reasons:

1. The maximum depth of exploration with EM is approximately equal to the distance between the transmitter and receiver; this compares to almost five times the source receiver separation for dc resistivity.

2. The EM method is faster and less expensive than the dc resistivity or Magnetotelluric method (MT).

3. Distant lateral inhomogeneities, which often affect MT data, have relatively minor significance for EM because the strength of the fields strongly decreases with increasing distance from the transmitter.

System Description

The system, as shown schematically in Figure A-1 consists of two sections:

(a) a transmitter section consisting of the power source, control electronics, timing, and a transistorized switch capable of handling large current; and

(b) a receiver section consisting of magnetic, or a combination of magnetic and electric, field detectors, signal conditioning amplifiers, and antialias filters, and a multichannel programmable receiver (spectrum analyzer).

Transmitter System

The EM-60 transmitter is powered by a Hercules gasoline engine linked to an aircraft 60-kW 400-Hz, 3ϕ alternator. These two components are mounted in the bed of a one-ton, four-wheel-drive truck. The output is full-wave rectified and capable of providing ±150 V at up to 400 A to the horizontal

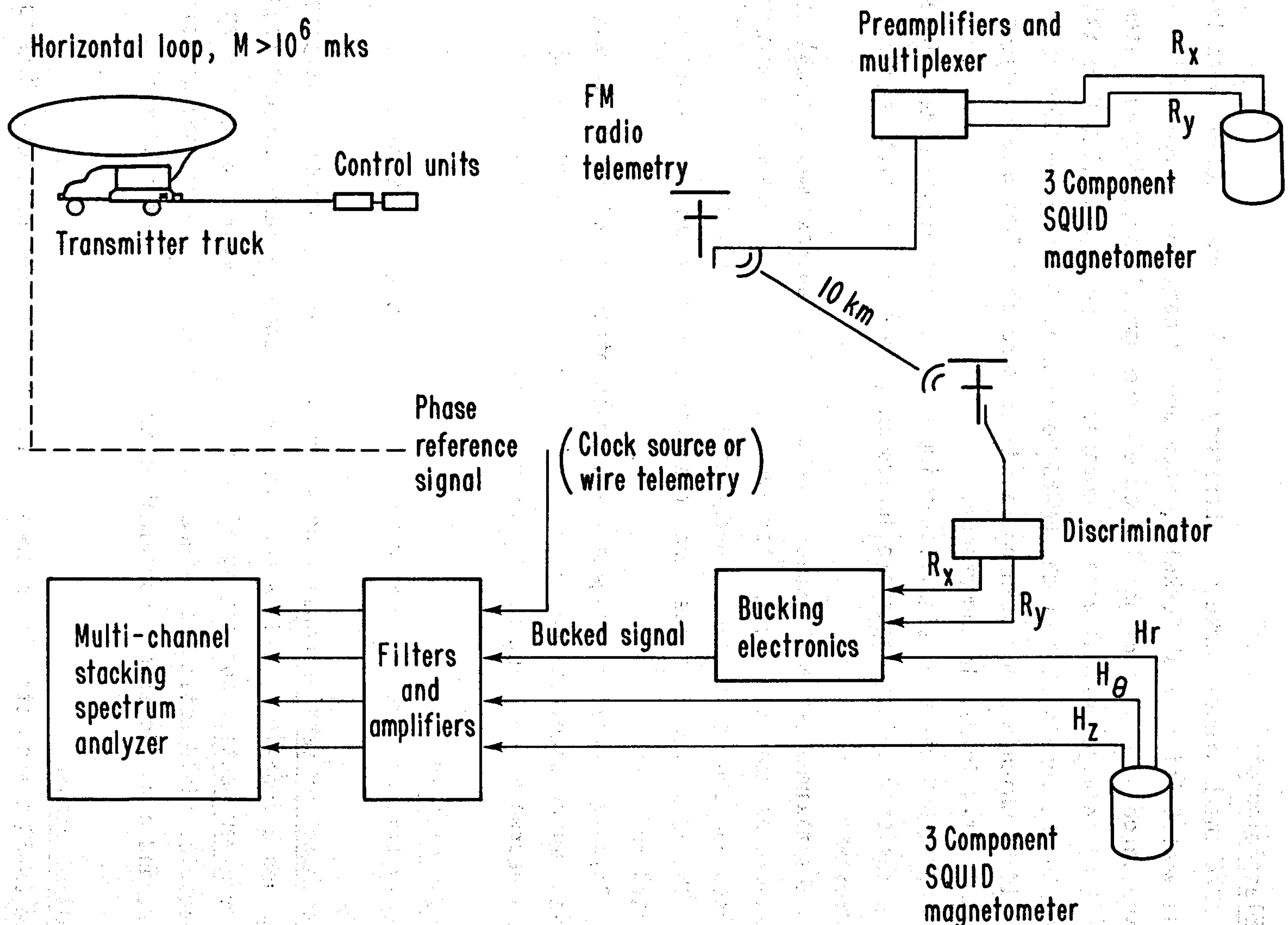

Figure A-1. Schematic diagram of the EM-60 horizontal loop electromagnetic prospecting system as used in Nevada in 1979.

coil. The square wave current pulses are created by means of a transistorized switch, which consists of two parallel arrays of from 6 to 60 transistors in interchangeable modules within the "crate" (the lower outward pivoting box in Figure A-2). The upper unit contains array-driving electronics and timing circuitry. The transmitter is operated by one man who controls the frequency of the primary magnetic field over the range of 10^{-3} to 10^{3} Hz by means of switches on a remote control box which contains a crystal-controlled oscillator and dividers (Morrison et al., 1978).

The dipole moment, which is a measure of the strength of the signal, is determined by the resistance and inductance of the loop. At frequencies below 50 Hz, inductive reactance is negligible and the dipole moment is governed by the load resistance. Four turns of No. 6 wire in a square or circular loop, 50 m in radius, will yield a dipole moment of about 3×10^{6} mks. This provides adequate signal for soundings where transmitter-receiver separations are less than about 5 km, which corresponds to a maximum depth of exploration of about 5 km. At frequencies above about 100 Hz, the inductance causes the moment to decrease and the current waveform to become quasisinusoidal. High frequency information is thus more difficult to obtain at large transmitter-receiver separations.

Receiver Section

The fields are detected at a point up to 5 km distant from the transmitter by means of a three-component SQUID magnetometer oriented to measure the vertical, radial, and tangential components with respect to the loop. Signals are amplified, antialias filtered, and inputted to a six-channel, programmable, multifrequency phase-sensitive receiver (Figure 1). Through the receiver key-pad, the operator sets parameters controlling signal processing: (a) fundamental period of the waveform to be processed; (b) maximum number of harmonics to be analyzed, up to 15; (c) number of cycles in increments of 2^{N}, to be stacked prior to Fourier decomposition; and (d) number of input channels of data to be processed. Signal processing results in a raw amplitude estimate for each component and a phase estimate relative to the phase of the current in the loop. Phase referencing is maintained with a hard-wire link between a shunt on the loop and the receiver. This reference voltage is applied directly to channel 1 of the receiver for phase comparison.

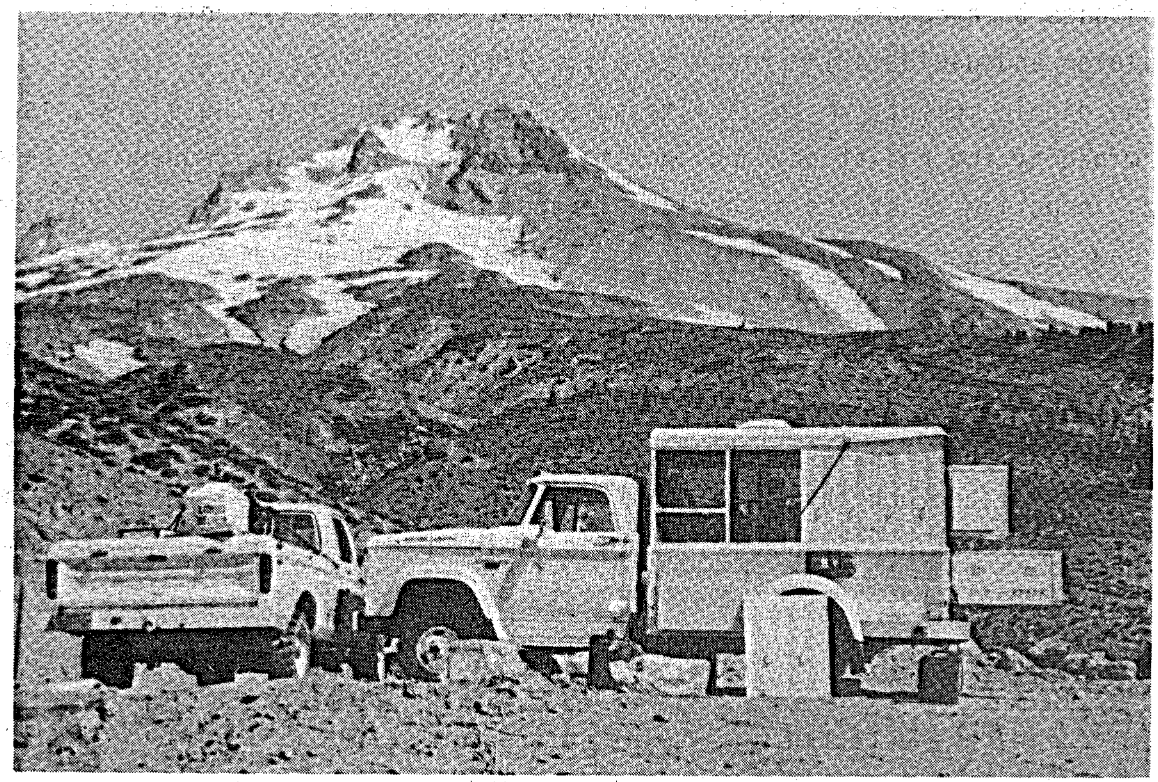

XBC 789-12736

Figure A-2. The EM-60 transmitter in field operation.

Raw amplitude estimates must be later corrected for dipole moment and distance between loop and magnetometer.

In practice, the hard-wire link was found to be a source of noise, particularly above 50 Hz. This has required the elimination of the absolute phase reference at high frequencies in favor of relative phase measurements between vertical and radial components. With relative phase measurements, interpretation is based on the ellipticity and tilt angle of the magnetic field rather than the amplitude-phase of the vertical and radial fields. At low frequencies ($\leq$0.1 Hz), natural geomagnetic signal amplitude increases roughly as 1/f while the signal sought decreases as 1/f. The net result is an effective signal-to-noise ratio that decreases as $1/f^2$, making noise cancellation imperative for recovery of low frequency information. To cancel geomagnetic noise, a reference magnetometer is placed far enough from the transmitter loop (10-12 km) so that the observed fields will consist only of the geomagnetic fluctuations. Once installed, the reference magnetometer can often remain fixed over the course of a survey. The remote signals are transmitted to the mobile receiver station from the transmitter via FM radio telemetry. Before the loop is energized, the remote signals are inverted, adjusted in amplitude, and then added to the base station geomagnetic signal to produce essentially a null signal. A good example of this simple noise cancellation scheme is shown in Figure A-3. The resulting signal-to-noise improvement of roughly 20 dB has allowed us to obtain reliable data to 0.05 Hz, a gain of three or four important data points on the sounding curve. These points are invaluable for resolving deeper horizons.

Data Interpretation

Basic data interpretation is accomplished by direct inversion of observed data to fit one-dimensional models. The program used fits amplitude-phase and/or ellipse polarization parameters jointly or separately, to fit arbitrarily layered models. This program allows the use of ellipse polarization parameters to separately fit high frequency points, where absolute phase data is much noisier, while simultaneously using absolute phase data at the lower frequencies, where the phase reference may allow for better parameter resolution. Two-dimensional modeling, although possible, is currently cumbersome and prohibitively expensive (Lee, 1979).

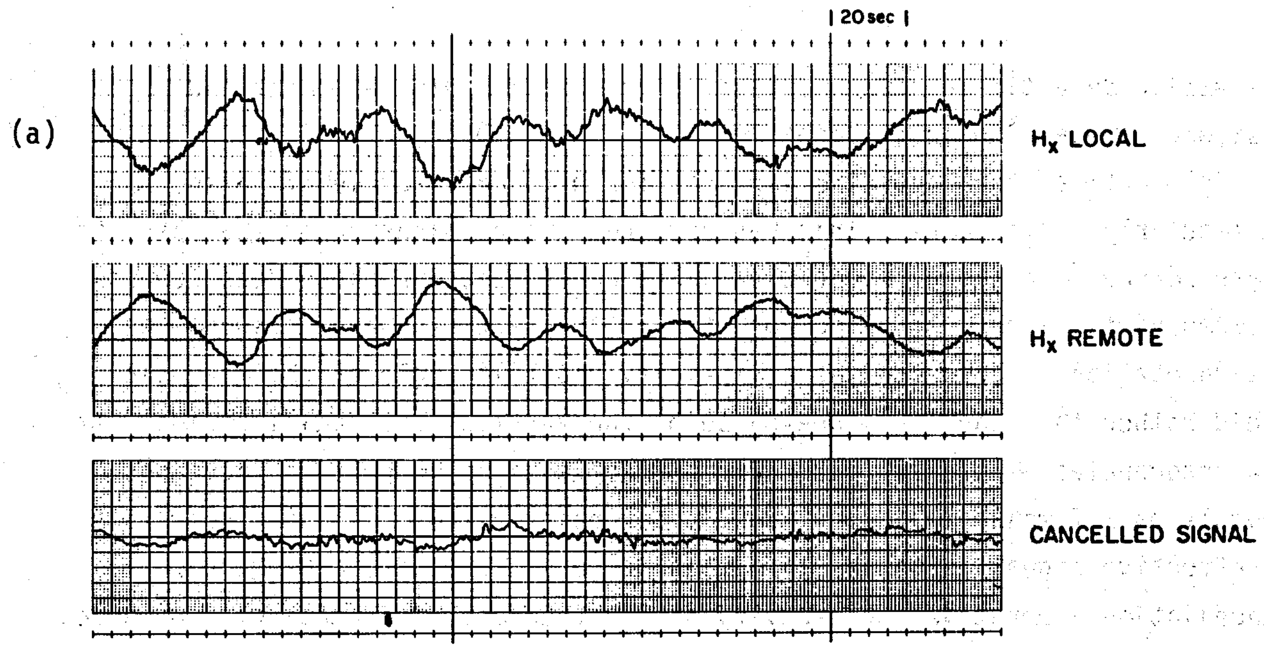

NATURAL MAGNETIC FIELD CANCELLATION

XBL 7911-13079

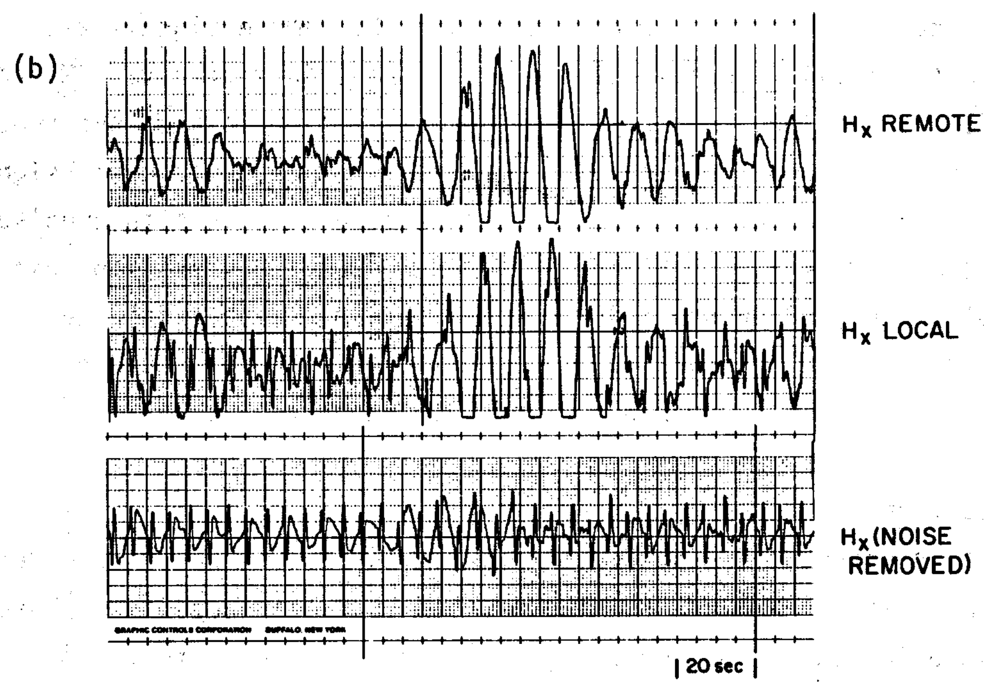

SAMPLE FIELD RECORD
TRANSMITTER FREQUENCY = 0.1 Hz

XBL 7911-13078

Figure A-3. Example of data improvement using the telluric noise cancellation scheme. (a) Natural geomagnetic signal and initial cancelling at the receiver site with transmitter off; (b) same system, but with transmitter on.

Samples of EM-60 amplitude-phase spectra soundings are given in Figures A-4 and A-5; the error bars signify one standard deviation. The fit to a three-layer model is fairly good, but data were interpreted only to 50 Hz, because high noise due to the use of the reference wire prohibited obtaining higher frequency amplitude-phase data. Ellipticity data, however, could be intepreted to 500 Hz.

References

Jain, B., 1978. A low frequency electromagnetic prospecting system, Ph. D. dissertation, Department of Engineering Geosciences, University of California. Berkeley, Lawrence Berkeley Laboratory, LBL-7042.

Morrison, H. F., Goldstein, N. E., Hoversten, N., Oppliger, G., and Riveros, C., 1978. Description, field test and data analysis of a controlled-source EM system EM-60. Lawrence Berkeley Laboratory, LBL-7088.

Lee, K. H., 1978. Electromagnetic scattering by a two-dimensional inhomogeneity due to an oscillating magnetic dipole. Ph. D. dissertation, Department of Engineering Geosciences, University of California, Berkeley. Lawrence Berkeley Laboratory, LBL-8275.

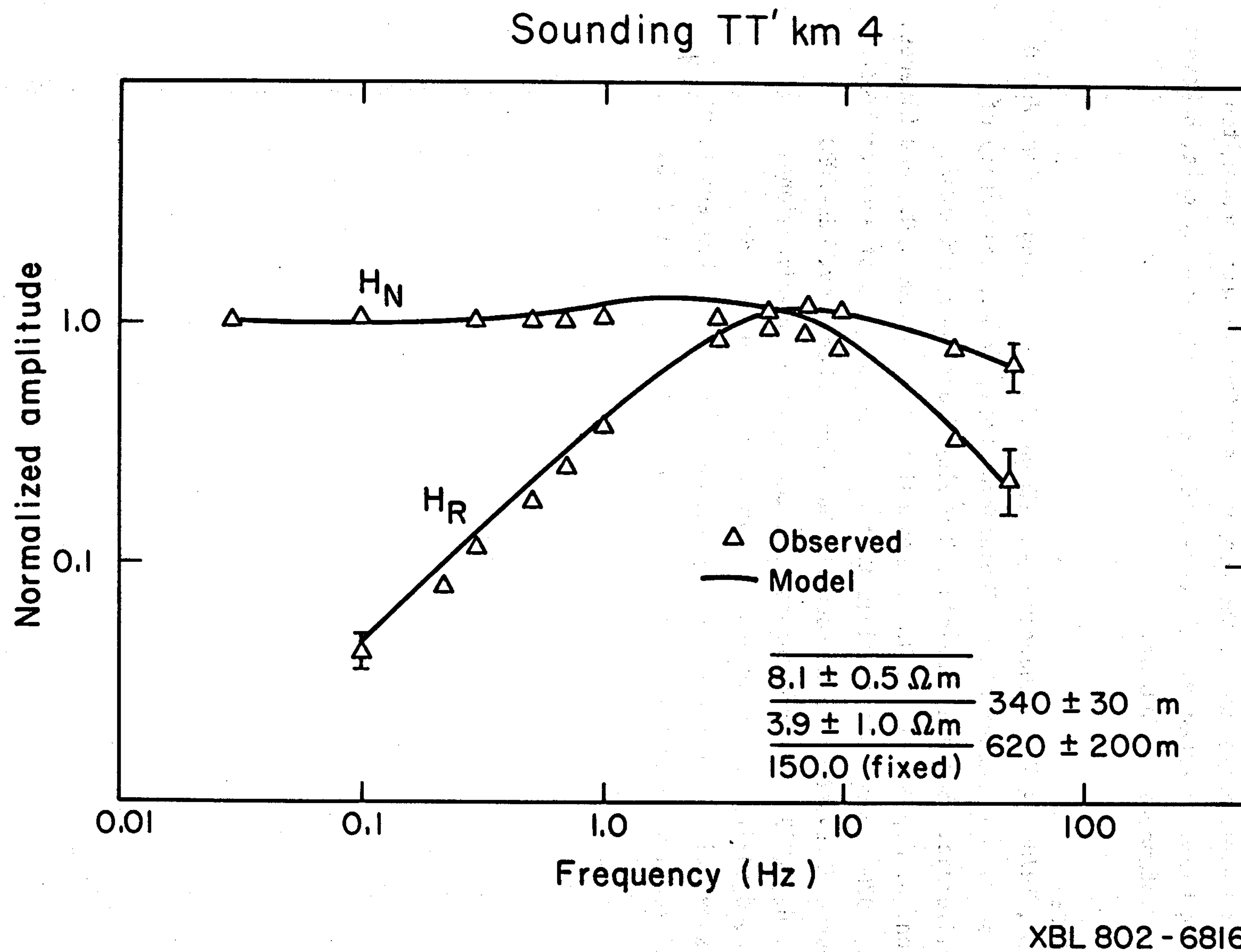

Figure A-4. Normalized magnetic field amplitude spectra normal and radial fields sounding T-T' Km 4 Panther Canyon.

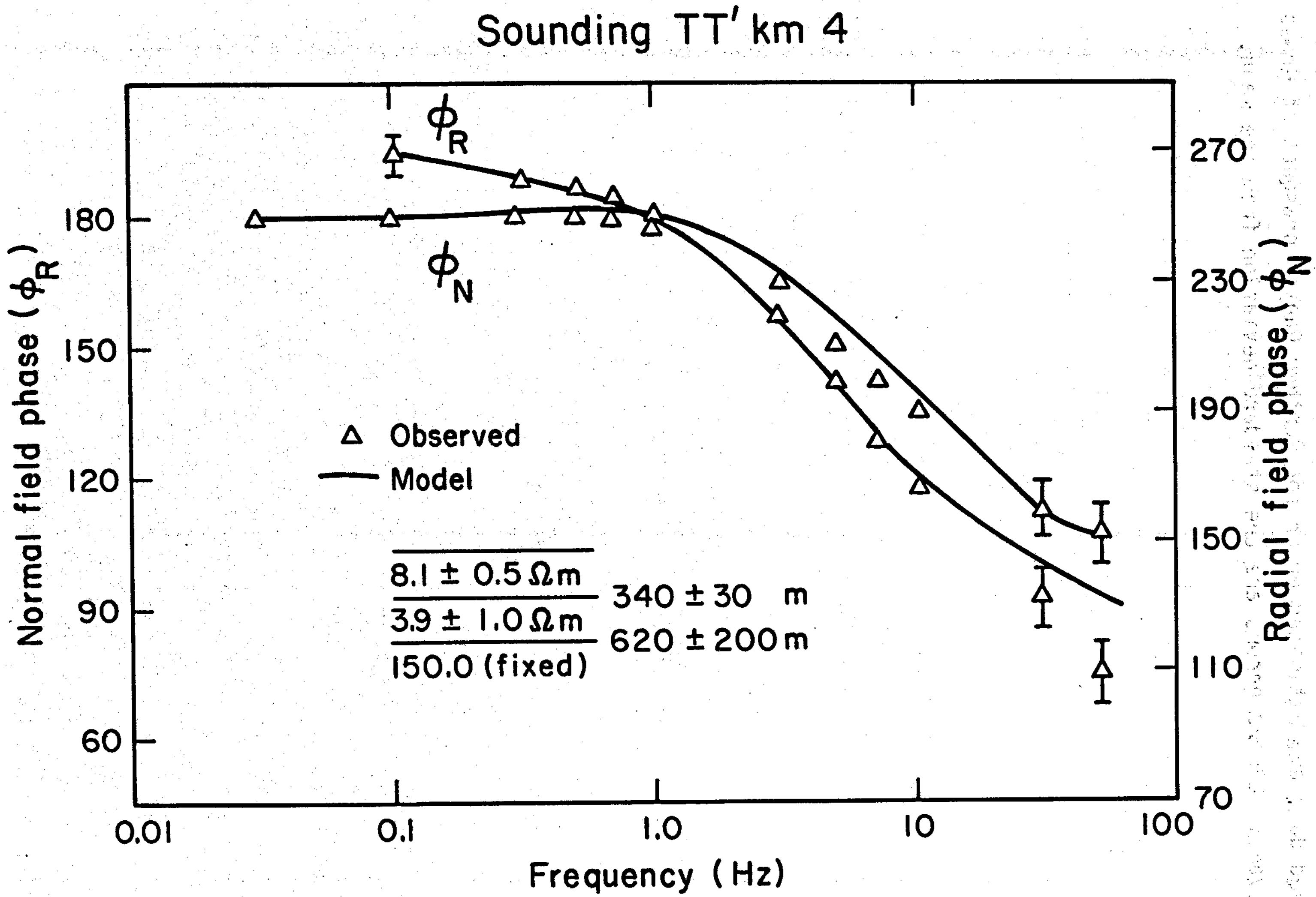

XBL 802-6815

Figure A-5. Normalized magnetic field phase spectra normal and radial fields sounding T-T' Km 4 Panther Canyon.

APPENDIX B

Observed data and estimated error for Panther Canyon prospect at Grass Valley, Nevada. Listed errors are one standard-deviation from the mean.

station: t-t 1.5 km north   seperation=1548 meters
number of turns=4   loop radius=50 meters
hr mag const=7.936   hz mag const=7.092

frequency	hr amp	amp err	hr phase	phase err
0.100	0.042	0.001	302.500	0.500
0.300	0.106	0.001	278.500	0.500
0.500	0.173	0.001	266.500	0.500
0.700	0.226	0.001	264.500	0.500
1.000	0.335	0.001	259.500	0.500
3.000	0.856	0.004	229.500	0.500
5.000	1.146	0.001	208.500	0.500
7.000	1.281	0.001	192.500	0.500
10.000	1.386	0.001	174.500	0.500
30.000	0.755	0.001	126.500	0.500
50.000	0.622	0.001	121.500	0.500
100.000	0.368	0.001	127.500	0.500

frequency	hz amp	amp err	hz phase	phase err
0.100	1.028	0.001	181.250	0.250
0.300	1.007	0.001	178.500	0.500
0.500	0.998	0.001	178.000	0.000
0.700	0.996	0.001	177.500	0.500
1.000	0.975	0.001	177.500	0.500
3.000	1.021	0.009	166.500	0.500
5.000	1.010	0.001	153.500	0.500
7.000	0.956	0.001	141.500	0.500
10.000	0.862	0.001	126.500	0.500
30.000	0.265	0.002	81.750	0.250
50.000	0.191	0.001	82.500	0.500
100.000	0.094	0.002	65.500	0.500

frequency	ellipticity	ellip err	tilt angle	tilt err
0.100	-0.035	0.001	91.217	0.054
0.300	-0.104	0.001	91.064	0.009
0.500	-0.173	0.001	89.731	0.091
0.700	-0.226	0.001	89.284	0.003
1.000	-0.339	0.001	86.905	0.008
3.000	-0.593	0.001	55.696	0.221
5.000	-0.513	0.000	38.781	0.001
7.000	-0.447	0.000	32.380	0.006
10.000	-0.382	0.000	26.792	0.010
30.000	-0.232	0.002	14.831	0.030
50.000	-0.183	0.000	13.901	0.043
100.000	-0.223	0.003	7.213	0.125

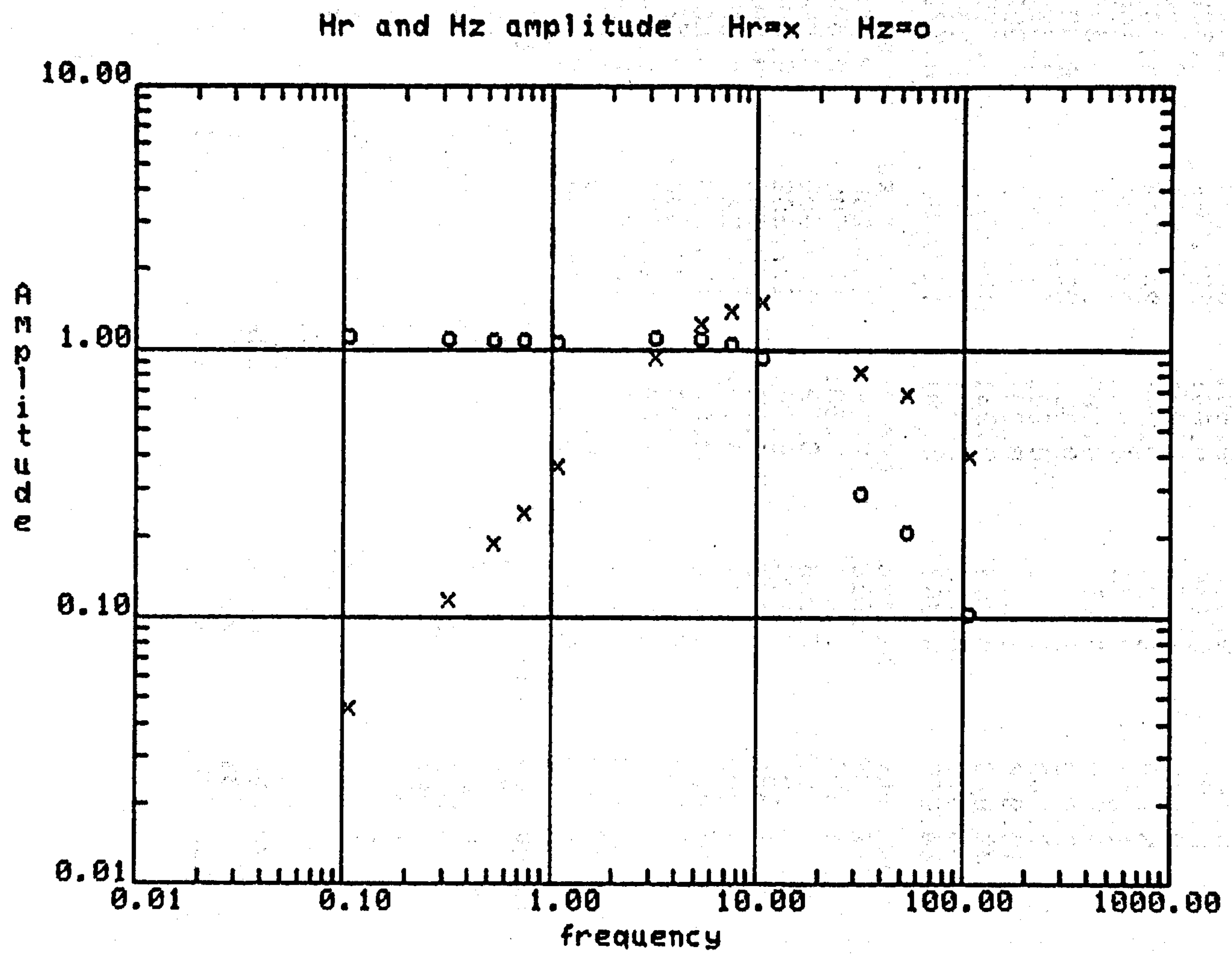

station: t-t 1.5 km north
separation=1548 meters

XBL 806-9812

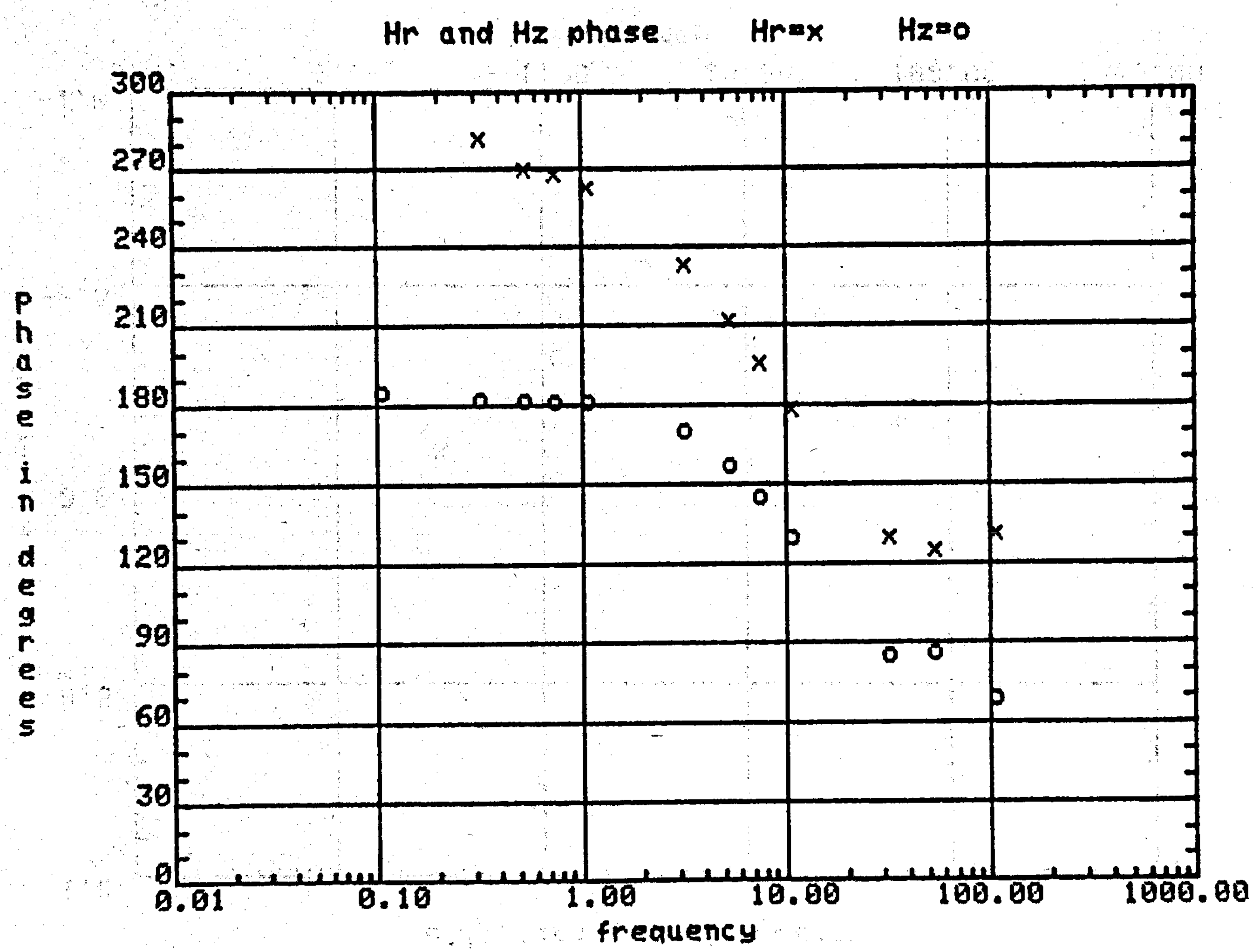

station: t-t 1.5 km north
separation=1548 meters

XBL 806-9811

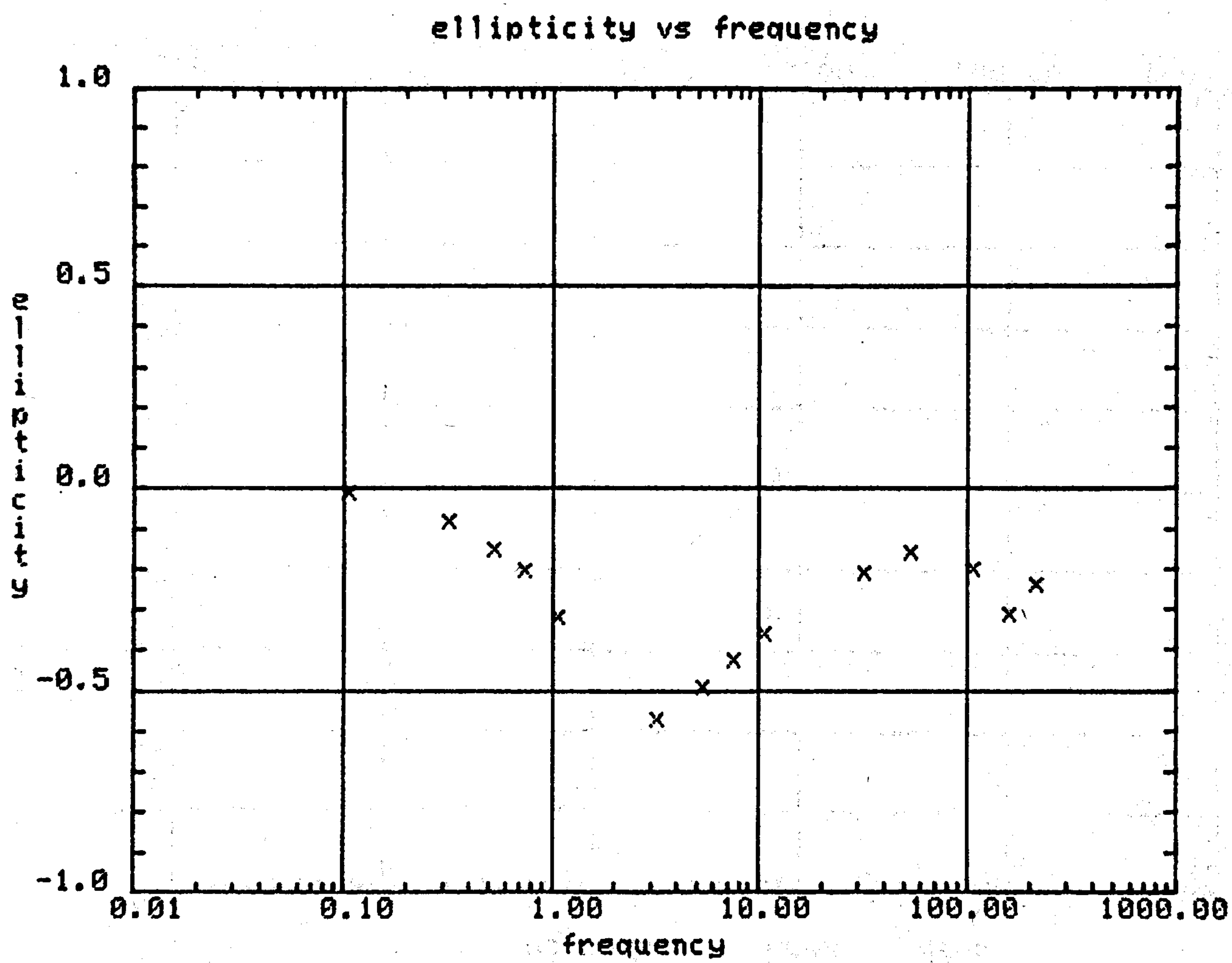

station: t-t 1.5 km north
separation=1548 meters

XBL 806-9814

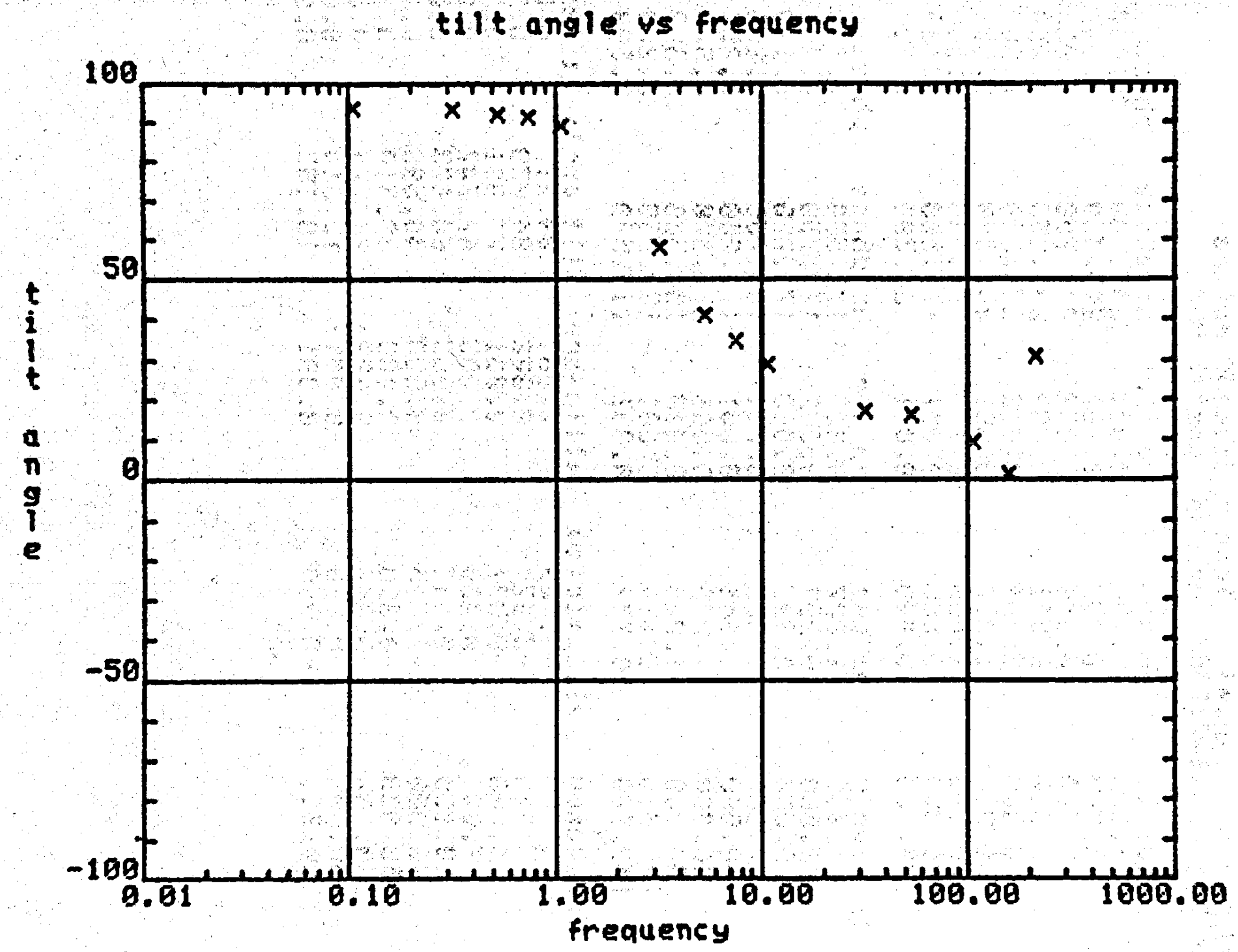

station: t-t 1.5 km north
separation=1548 meters

XBL 806-9813

station: t-t .5km north seperation=562 meters
number of turns=4 loop radius=50 meters
hr mag const=7.936 hz mag const=7.092

frequency	hr amp	amp err	hr phase	phase err
1.000	0.106	0.001	255.000	0.000
3.000	0.292	0.001	249.500	0.500
5.000	0.446	0.002	241.750	0.250
7.000	0.571	0.002	235.250	0.250
10.000	0.794	0.002	230.500	0.500
30.000	1.237	0.001	205.500	0.500
50.000	1.409	0.003	198.500	0.500
100.000	0.855	0.001	175.500	0.500
150.000	0.649	0.001	164.500	0.500

frequency	hz amp	amp err	hz phase	phase err
1.000	1.027	0.004	172.500	0.500
3.000	0.999	0.002	178.750	0.250
5.000	0.993	0.003	179.700	0.100
7.000	1.000	0.001	180.750	0.250
10.000	1.144	0.001	178.250	0.250
30.000	1.295	0.006	171.500	0.500
50.000	1.220	0.003	154.500	0.500
100.000	0.489	0.001	129.250	0.250
150.000	0.257	0.001	115.500	0.500

frequency	ellipticity	ellip err	tilt angle	tilt err
1.000	-0.103	0.001	89.217	0.060
3.000	-0.274	0.002	84.038	0.203
5.000	-0.377	0.001	76.091	0.270
7.000	-0.409	0.003	67.747	0.236
10.000	-0.443	0.003	60.673	0.049
30.000	-0.305	0.000	46.598	0.183
50.000	-0.398	0.000	39.310	0.020
100.000	-0.349	0.002	24.774	0.053
150.000	-0.278	0.001	15.814	0.059
200.000	-0.299	0.001	10.153	0.077

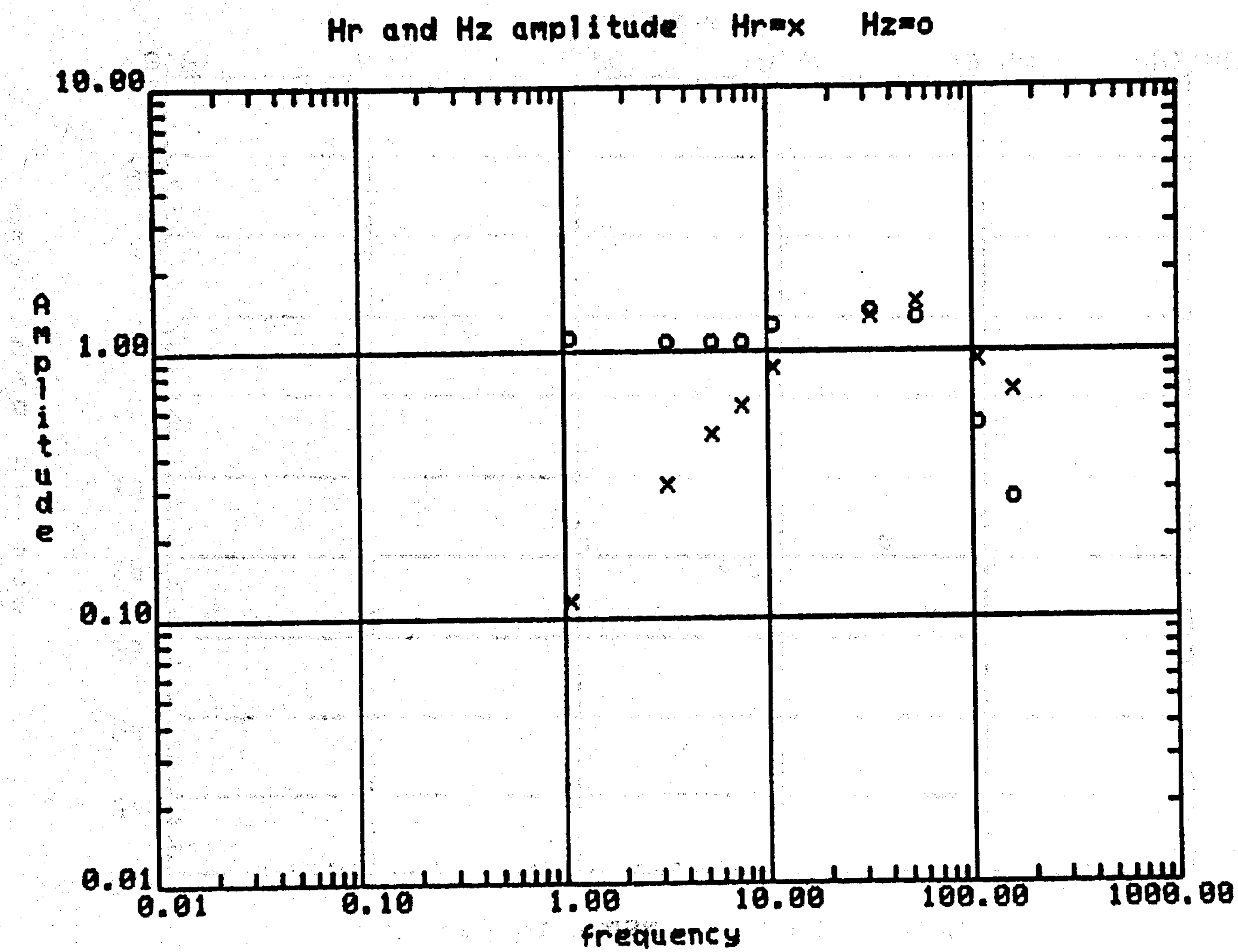

station: t-t .5km north
separation=562 meters

XBL 806-9808

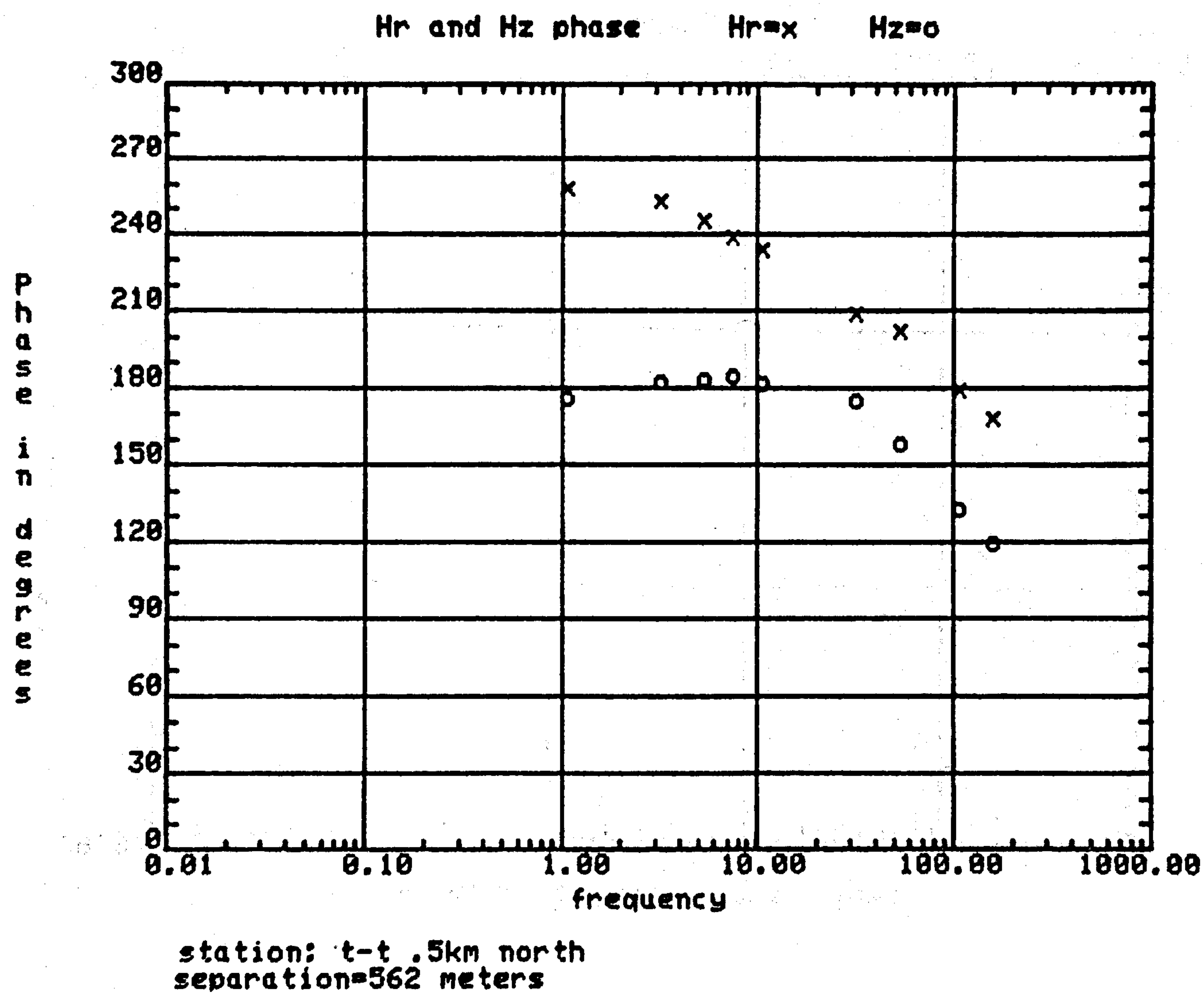

Hr and Hz phase Hr=x Hz=o
300
270
240
210
180
150
120
90
60
30
0
0.01
0.10
1.00
10.00
100.00
1000.00
frequency
phase in degrees
station: t-t .5km north
separation=562 meters

XBL 806-9809

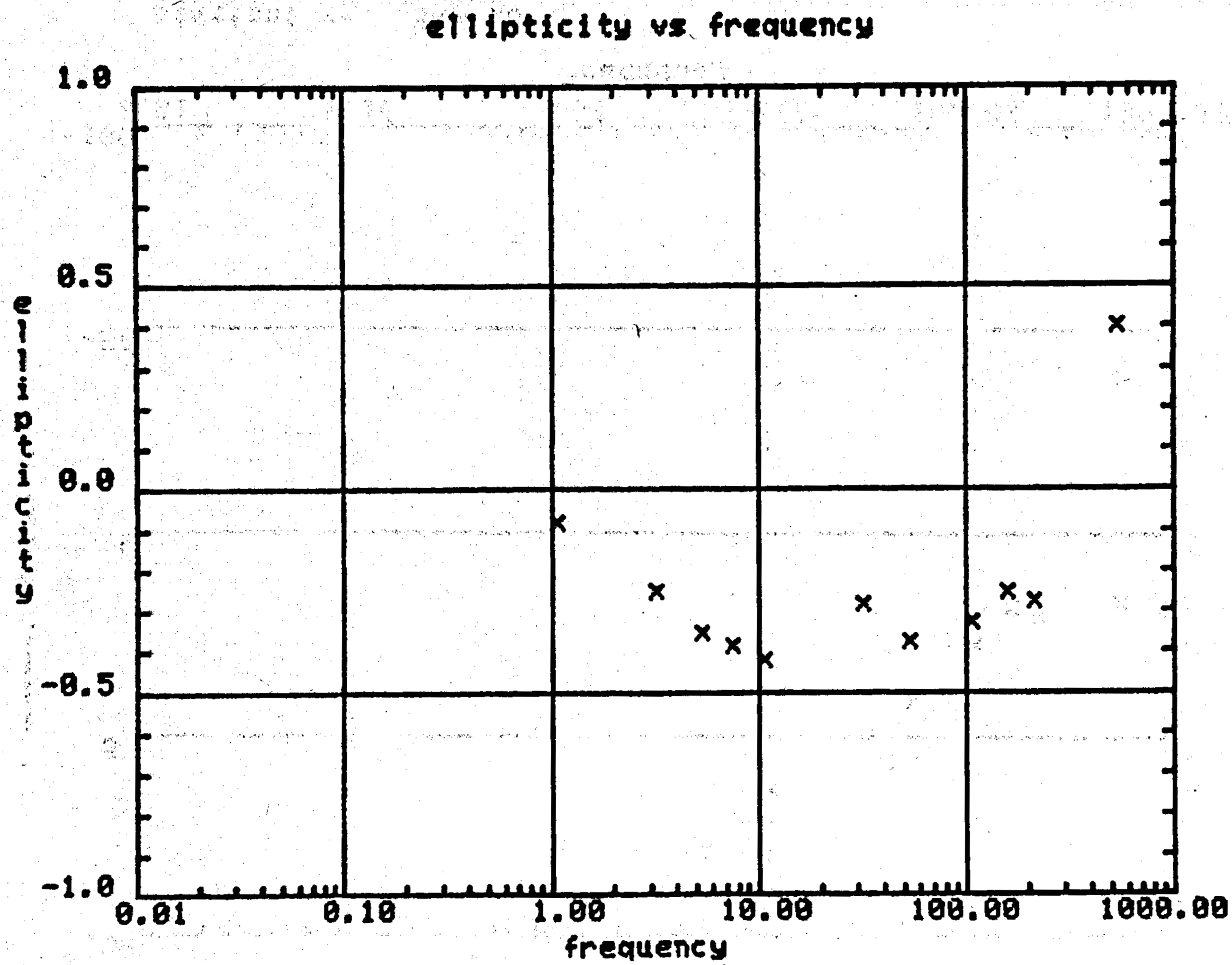

station: t-t .5km north
separation=562 meters

XBL 806-9810

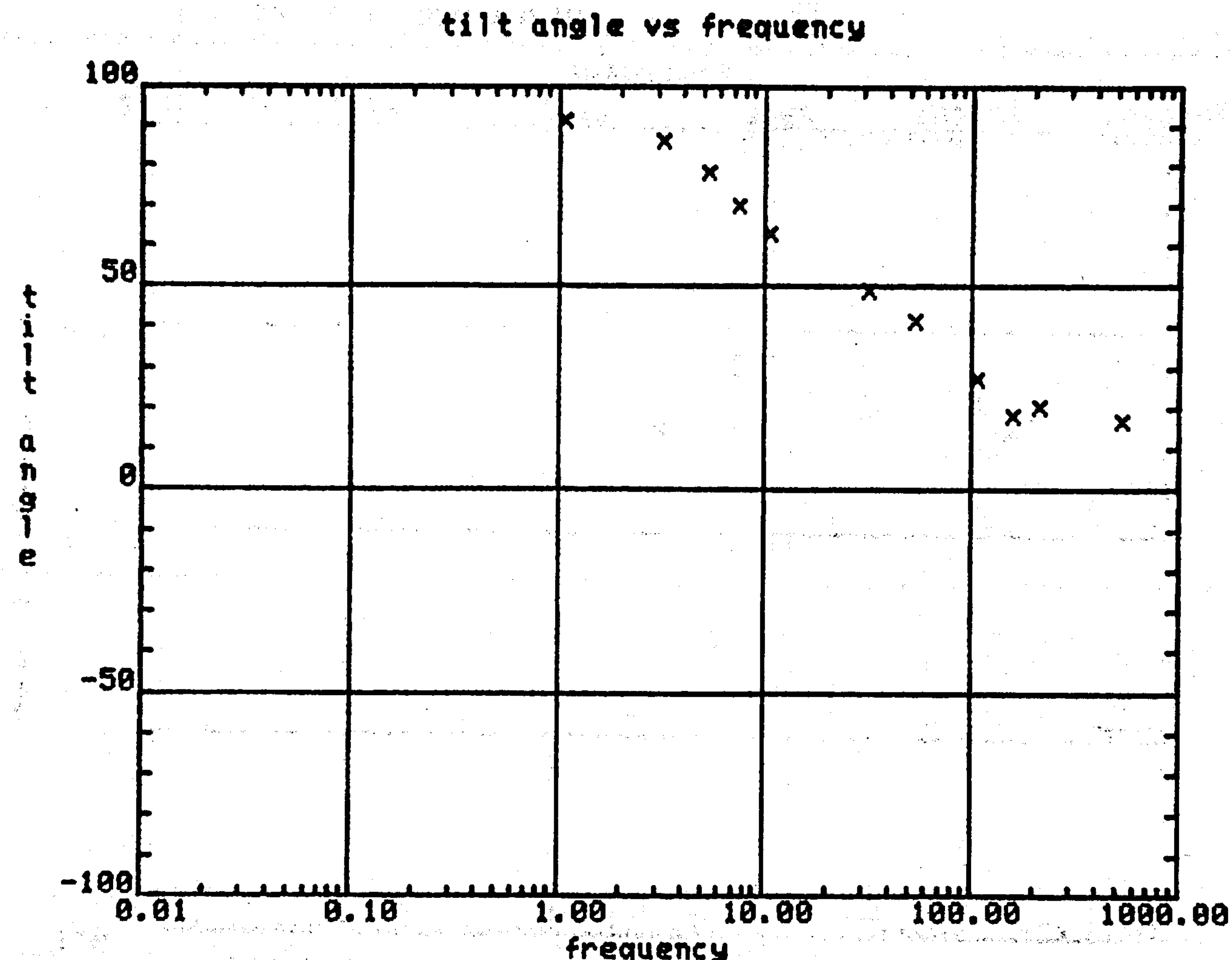

station: t-t .5km north
separation=562 meters

XBL 806-9807

station: t-t .5km south   seperation=451 meters
number of turns=4   loop radius=50 meters
hr mag const=7.936   hz mag const=7.092

frequency	hr amp	amp err	hr phase	phase err
1.000	0.107	0.000	257.533	0.089
3.000	0.306	0.000	250.840	0.062
5.000	0.476	0.003	241.683	0.041
7.000	0.602	0.001	234.360	0.090
10.000	0.847	0.005	228.603	0.009
30.000	0.998	0.009	202.253	0.095
50.000	0.720	0.023	208.460	0.670
100.000	0.611	0.001	185.235	0.179
200.000	0.380	0.003	165.722	0.455

frequency	hz amp	amp err	hz phase	phase err
1.000	1.014	0.005	171.163	0.027
3.000	1.003	0.005	177.817	0.009
5.000	1.009	0.001	179.360	0.021
7.000	1.002	0.005	180.973	0.027
10.000	1.125	0.007	180.320	0.610
30.000	1.326	0.012	180.806	0.071
50.000	0.662	0.021	168.437	0.682
100.000	0.358	0.000	143.378	0.156
200.000	0.258	0.002	125.720	0.461

frequency	ellipticity	ellip err	tilt angle	tilt err
1.000	-0.105	0.000	89.613	0.009
3.000	-0.289	0.001	84.441	0.040
5.000	-0.395	0.002	75.293	0.112
7.000	-0.415	0.000	65.885	0.132
10.000	-0.423	0.006	56.672	0.129
30.000	-0.181	0.000	53.617	0.044
50.000	-0.362	0.000	41.821	0.002
100.000	-0.321	0.000	26.516	0.031
200.000	-0.315	0.006	27.723	0.967
500.000	-0.231	0.002	19.822	0.057

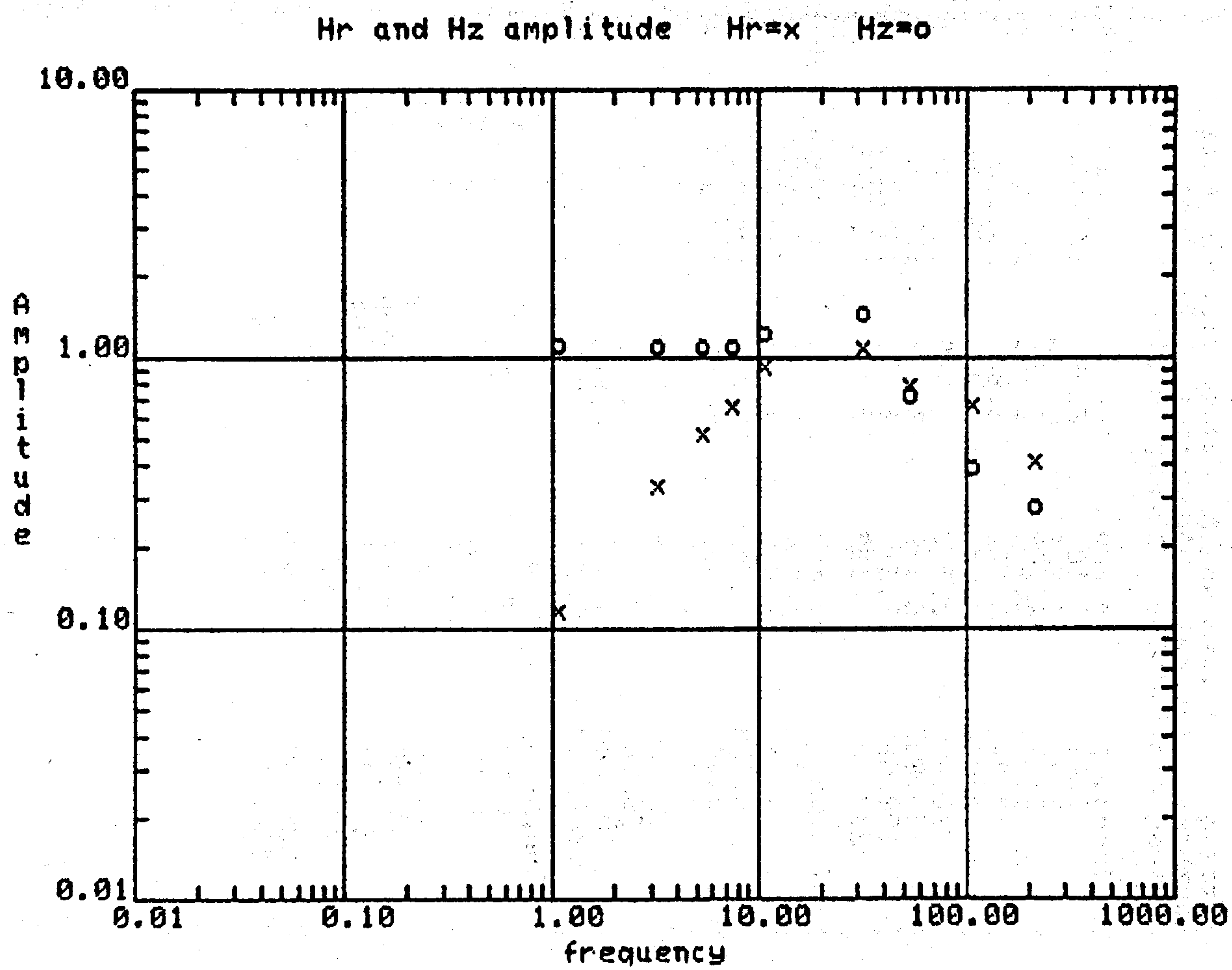

station: t-t .5km south
separation=451 meters

XBL 806-9820

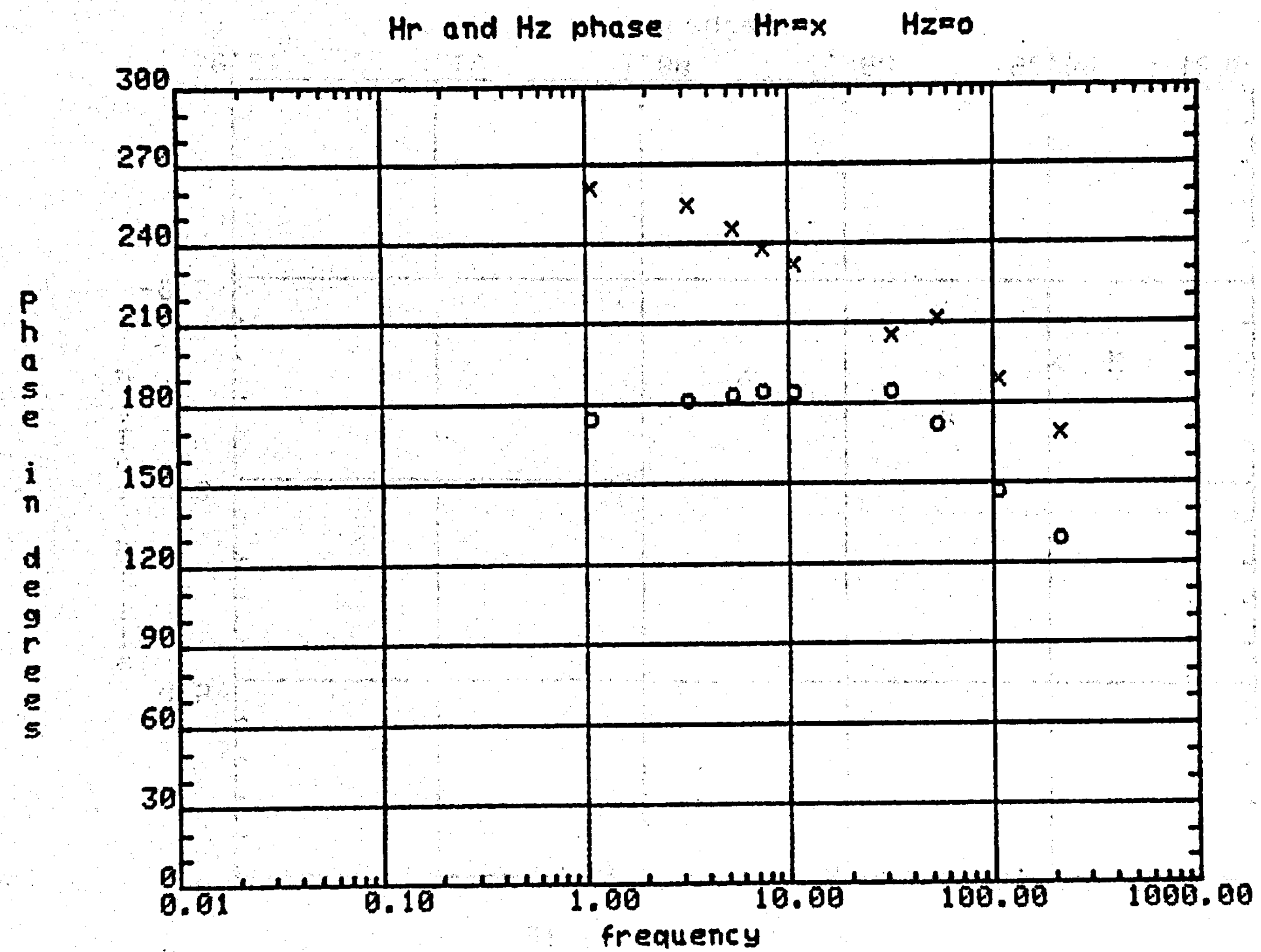

station: t-t .5km south
separation=451 meters

XBL 806-9819

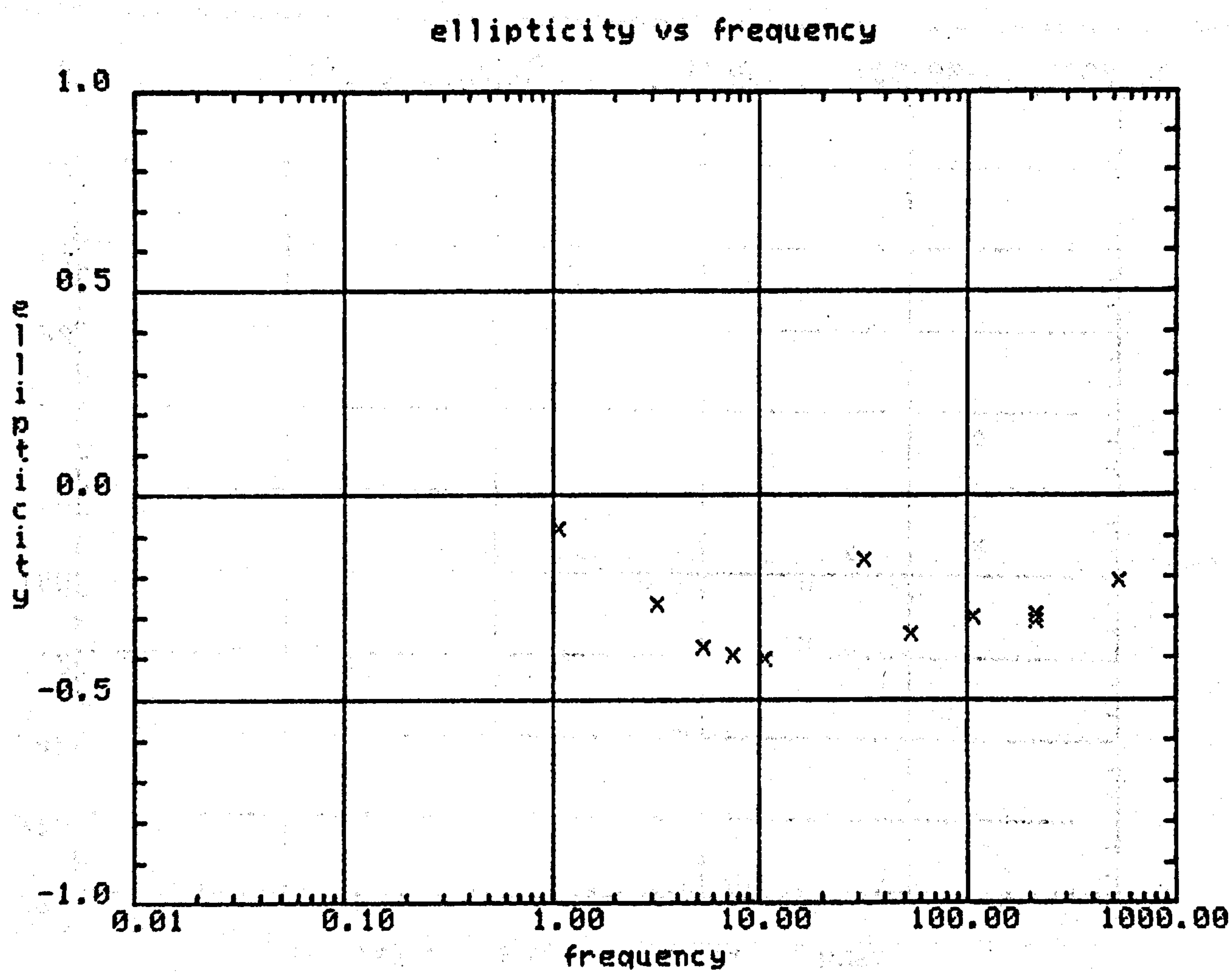

station: t-t .5km south
separation=451 meters

XBL 806-9822

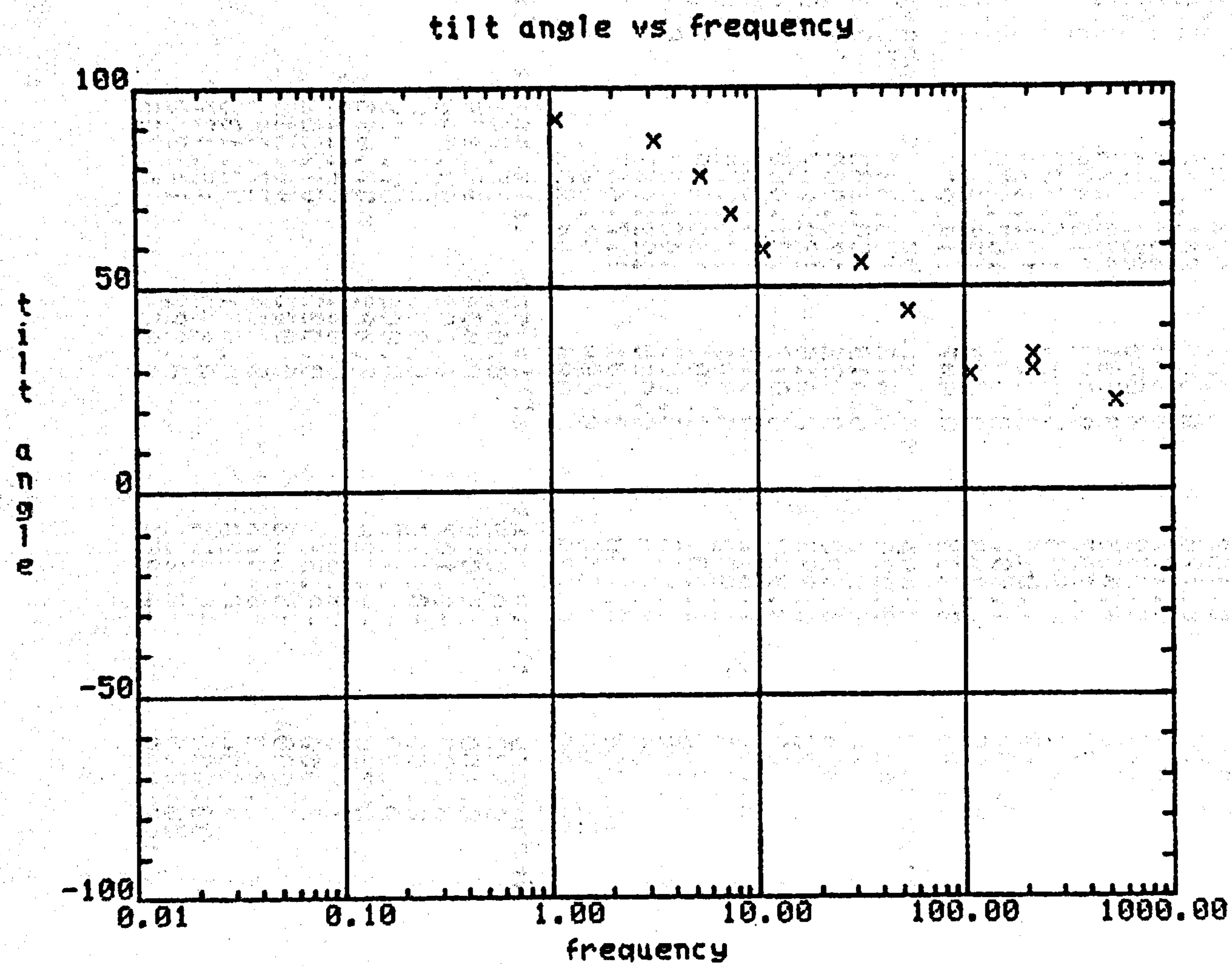

station: t-t .5km south
separation=451 meters

XBL 806-9821

station: t-t 1.5km south   seperation=1451 meters
number of turns=4   loop radius=50 meters
hr mag const=7.936   hz mag const=7.092

frequency	hr amp	amp err	hr phase	phase err
0.033	0.033	0.017	210.667	31.756
0.100	0.040	0.004	274.467	13.593
0.300	0.107	0.001	264.433	0.296
0.500	0.178	0.005	261.300	0.907
0.500	0.177	0.008	260.450	0.550
0.700	0.238	0.005	257.400	0.306
1.000	0.335	0.001	250.575	0.229
3.000	0.797	0.002	219.470	0.058
5.000	0.983	0.004	196.633	0.120
7.000	1.015	0.006	181.133	0.441
10.000	1.097	0.001	167.856	0.034
30.000	0.795	0.003	135.219	0.291
50.000	0.695	0.007	110.279	[illegible]

frequency	hz amp	amp err	hz phase	phase err
0.033	0.886	0.013	133.333	55.360
0.100	0.997	0.019	180.133	0.882
0.300	0.998	0.022	179.000	0.577
0.500	0.992	0.016	180.267	0.819
0.500	0.980	0.019	181.400	0.400
0.700	1.017	0.011	179.367	1.567
1.000	1.032	0.001	176.775	0.025
3.000	1.101	0.001	160.670	0.000
5.000	1.015	0.003	143.167	0.176
7.000	0.870	0.000	129.667	0.120
10.000	0.768	0.001	117.467	0.033
30.000	0.344	0.000	94.367	0.176
50.000	0.239	0.004	64.833	0.353

frequency	ellipticity	ellip err	tilt angle	tilt err
0.033	-0.020	0.005	88.741	1.440
0.100	-0.038	0.004	90.176	0.454
0.300	-0.107	0.002	89.506	0.041
0.500	-0.177	0.003	88.348	0.299
0.500	-0.177	0.006	87.979	0.112
0.700	-0.228	0.008	87.095	0.255
1.000	-0.309	0.001	84.272	0.096
3.000	-0.513	0.000	61.202	0.096
5.000	-0.503	0.003	46.518	0.276
7.000	-0.473	0.004	37.989	0.291
10.000	-0.428	0.001	30.135	0.016
30.000	-0.254	0.002	19.437	0.097
50.000	-0.231	0.002	14.342	0.233
100.000	-0.254	0.004	5.368	0.340

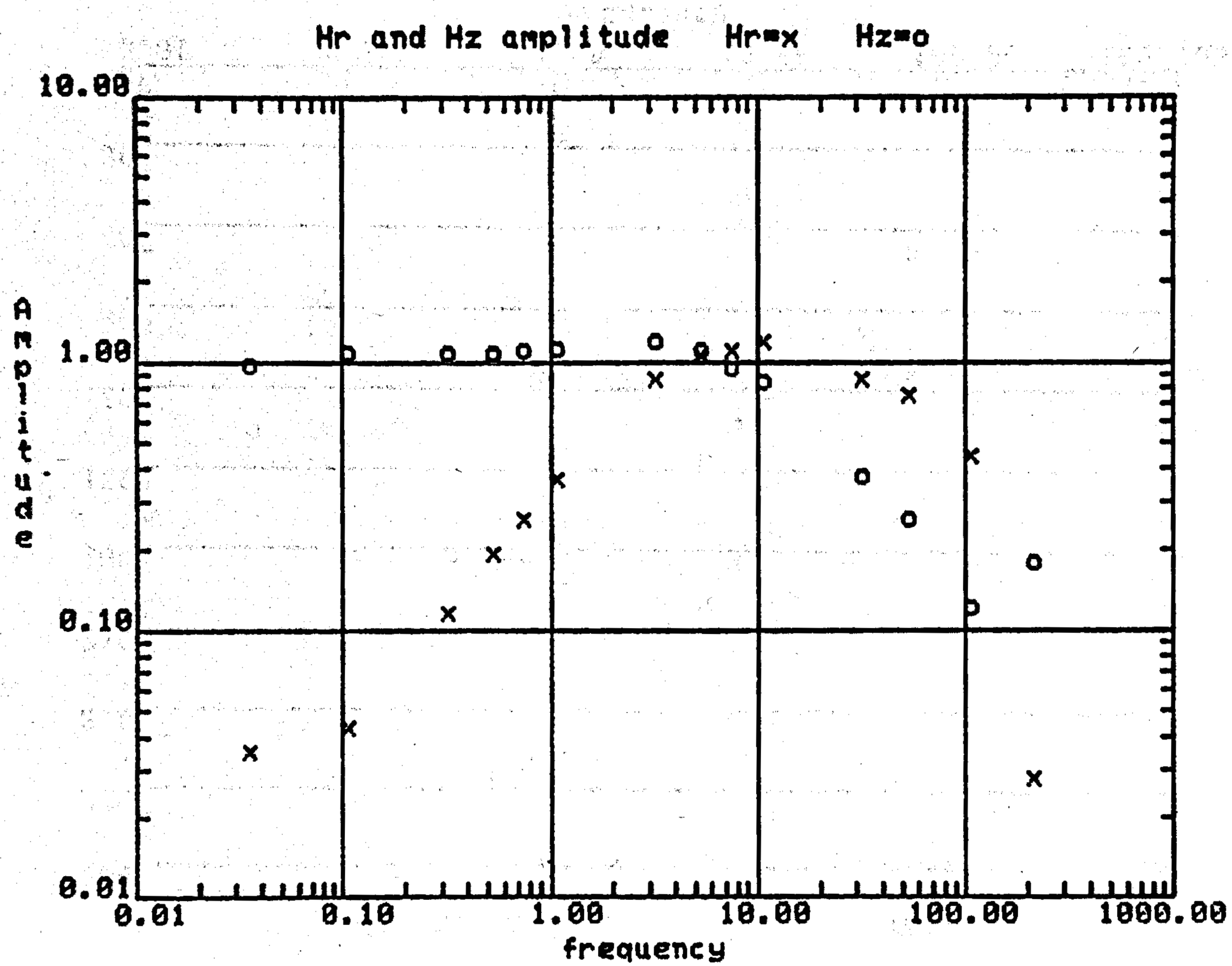

station: t-t 1.5km south
separation=1451 meters

XBL 806-9816

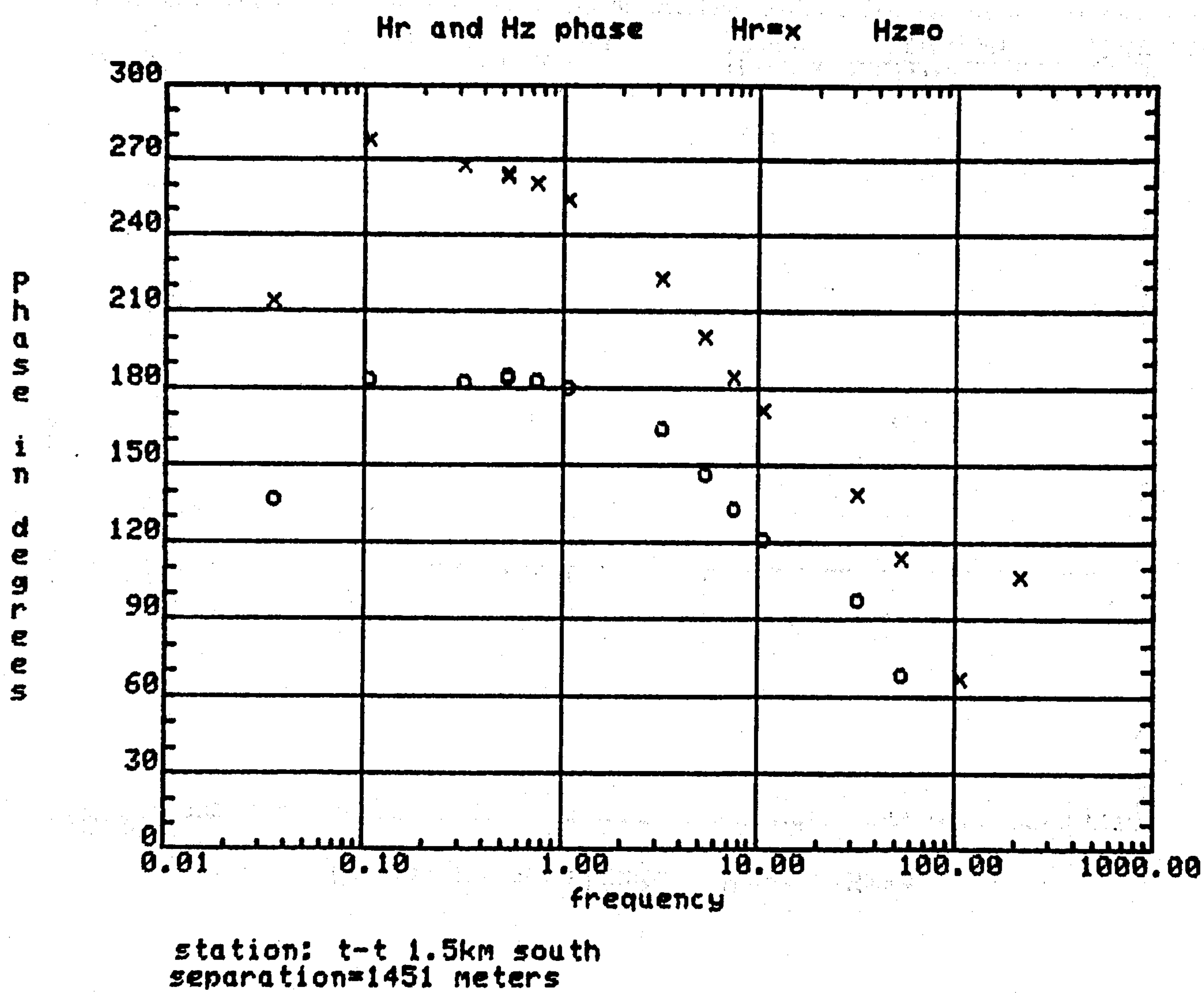
Hr and Hz phase Hr=x Hz=o
300
270
240
210
180
150
120
90
60
30
0
phase in degrees
0.01
0.10
1.00
10.00
100.00
1000.00
frequency
station: t-t 1.5km south
separation=1451 meters

XBL 806-9815

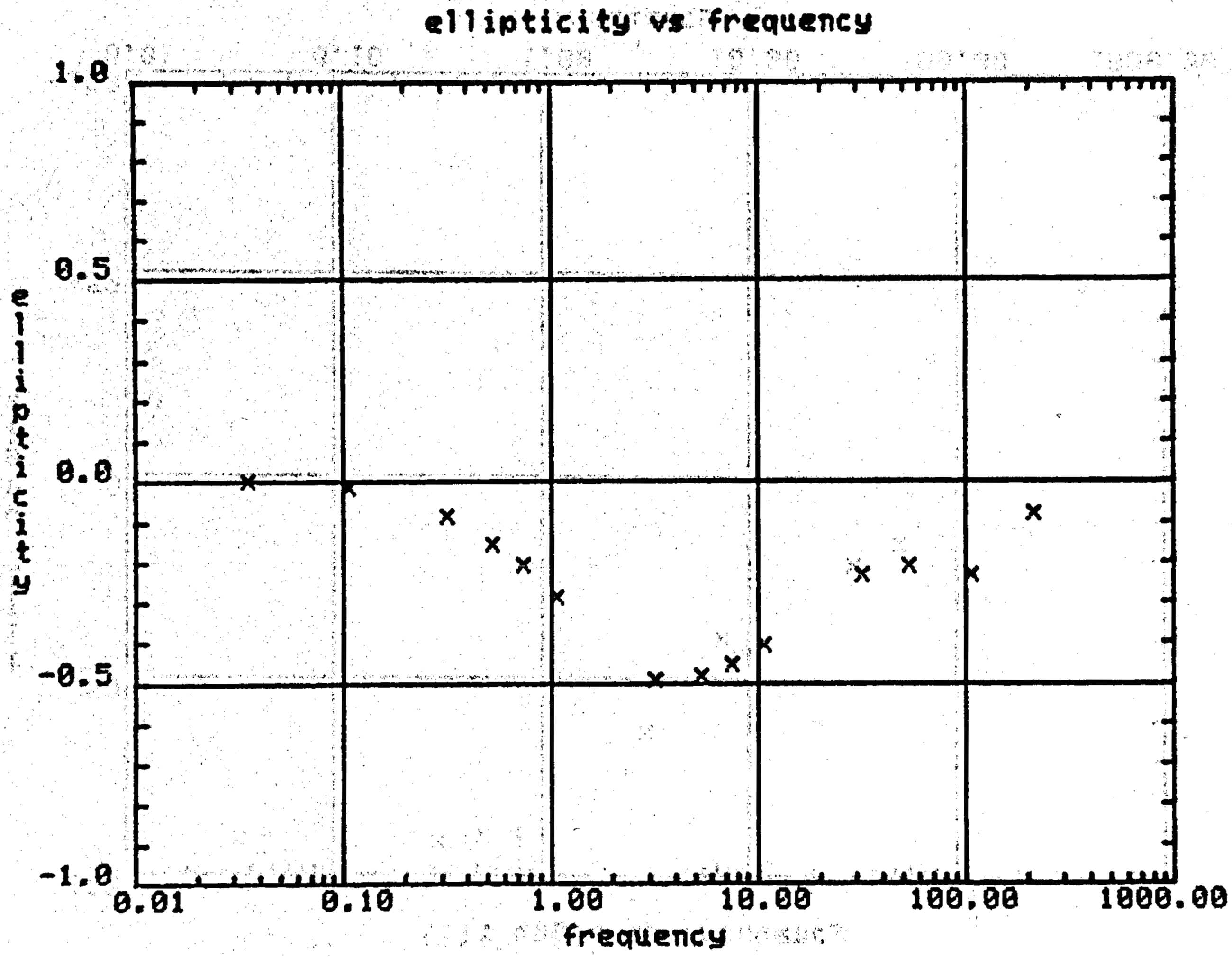

station: t-t 1.5km south
separation=1451 meters

XBL 806-9818

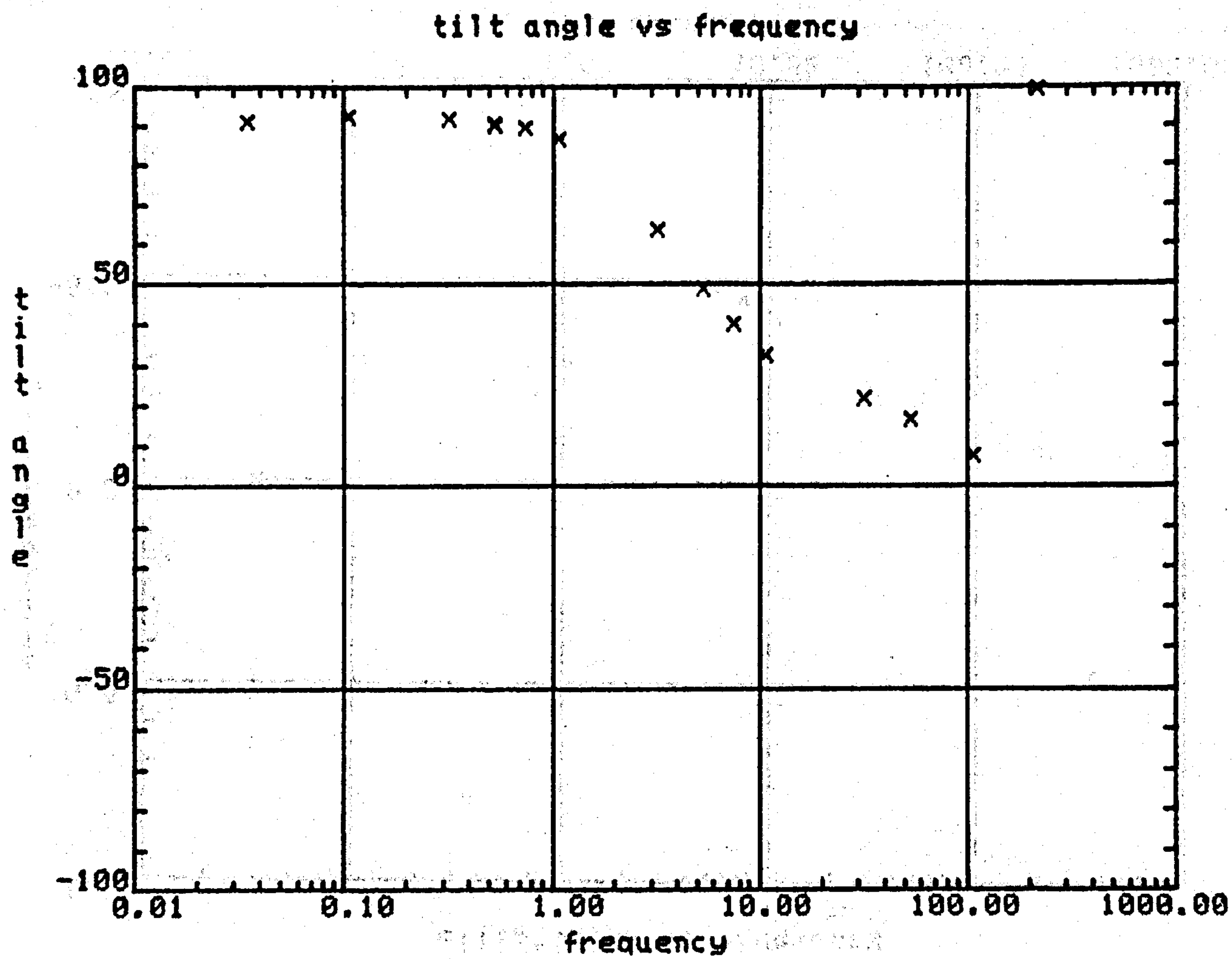

station: t-t 1.5km south
separation=1451 meters

XBL 806-9817

station: h-h 1.5km east   seperation=1438 meters
number of turns=4   loop radius=50 meters
hr mag const=7.936   hz mag const=7.092

frequency	hr amp	amp err	hr phase	phase err
0.100	0.062	0.000	265.829	0.650
0.300	0.105	0.000	274.526	0.574
0.500	0.164	0.001	258.282	0.546
0.700	0.244	0.001	259.145	0.458
1.000	0.320	0.000	254.206	0.506
3.000	0.837	0.003	224.968	0.491
5.000	1.115	0.014	205.785	0.507
7.000	1.200	0.002	191.233	0.154
10.000	1.438	0.006	177.359	0.490
30.000	1.011	0.003	137.969	0.495
50.000	0.895	0.006	133.213	0.249
100.000	0.469	0.003	109.635	0.019

frequency	hz amp	amp err	hz phase	phase err
0.100	1.065	0.000	175.617	0.250
0.300	1.007	0.003	177.261	0.001
0.500	1.006	0.003	177.530	0.099
0.700	0.988	0.000	175.937	0.498
1.000	1.012	0.000	174.787	0.499
3.000	1.007	0.003	161.310	0.008
5.000	0.996	0.003	150.947	0.034
7.000	0.939	0.001	130.150	0.688
10.000	0.937	0.012	120.965	0.524
30.000	0.332	0.002	93.881	0.226
50.000	0.229	0.002	67.869	0.548
100.000	0.070	0.005	38.202	0.691

frequency	ellipticity	ellip err	tilt angle	tilt err
0.100	-0.058	0.000	90.012	0.023
0.300	-0.104	0.000	90.766	0.059
0.500	-0.161	0.001	88.461	0.070
0.700	-0.245	0.001	88.220	0.259
1.000	-0.309	0.000	86.329	0.001
3.000	-0.598	0.006	56.334	0.161
5.000	-0.513	0.005	39.417	0.552
7.000	-0.556	0.009	31.440	0.298
10.000	-0.396	0.002	28.191	0.308
30.000	-0.216	0.002	13.945	0.195
50.000	-0.230	0.000	6.429	0.095
100.000	-0.158	0.008	3.127	0.299

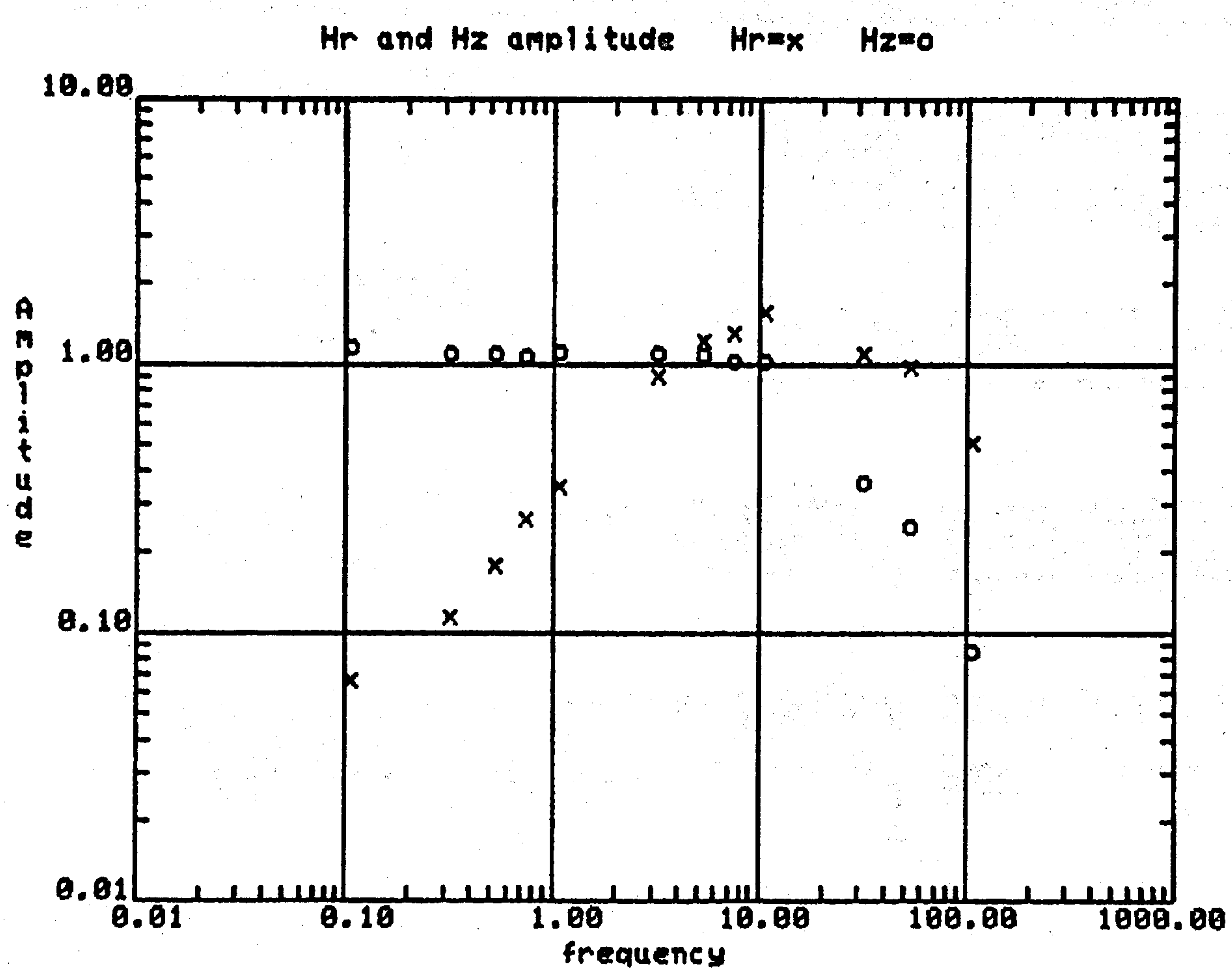

station: h-h 1.5km east
separation=1438 meters

XBL 806-9797

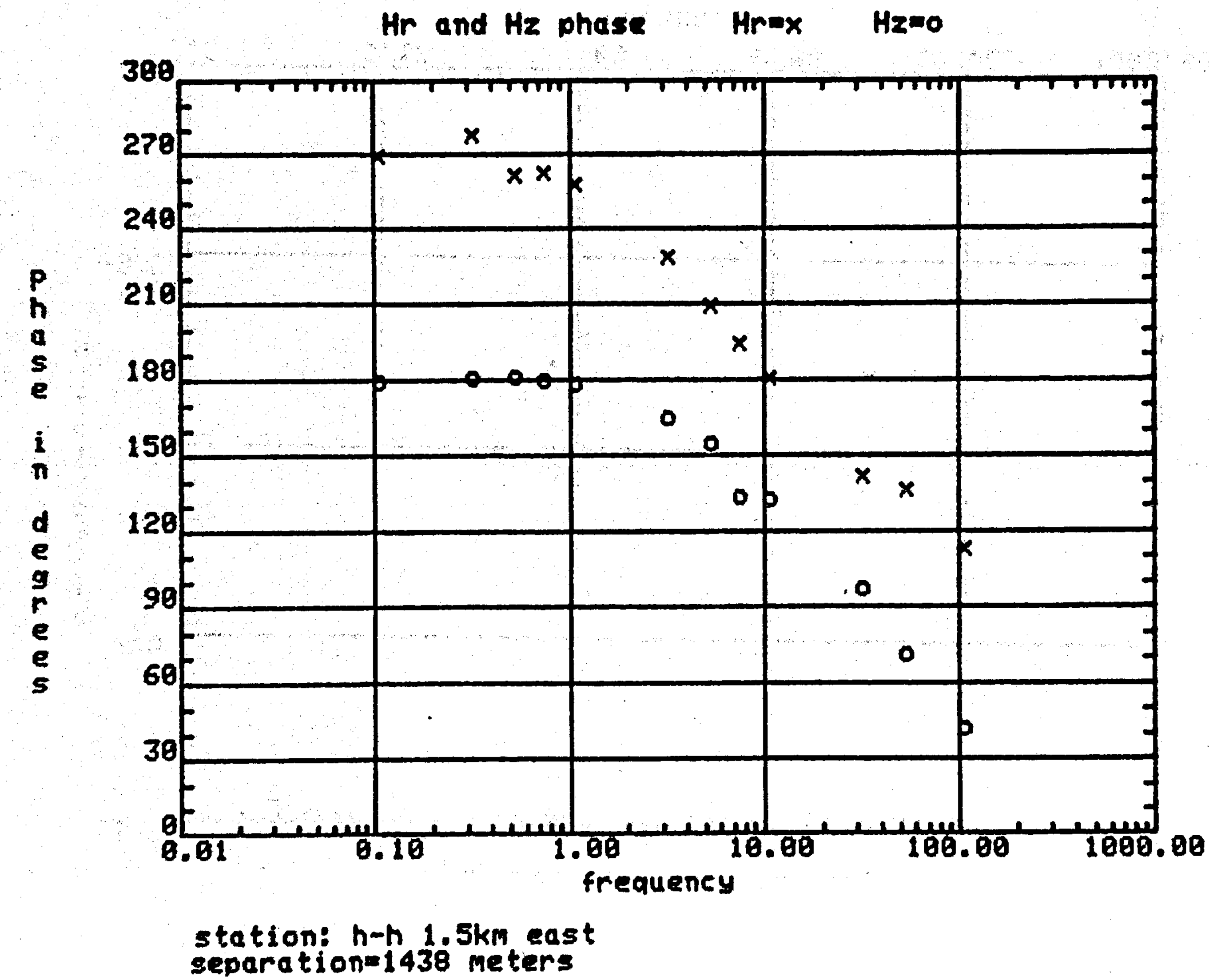
Hr and Hz phase Hr=x Hz=o
300
270
240
210
180
150
120
90
60
30
0
phase in degrees
0.01
0.10
1.00
10.00
100.00
1000.00
frequency
station: h-h 1.5km east
separation=1438 meters

XBL 806-9796

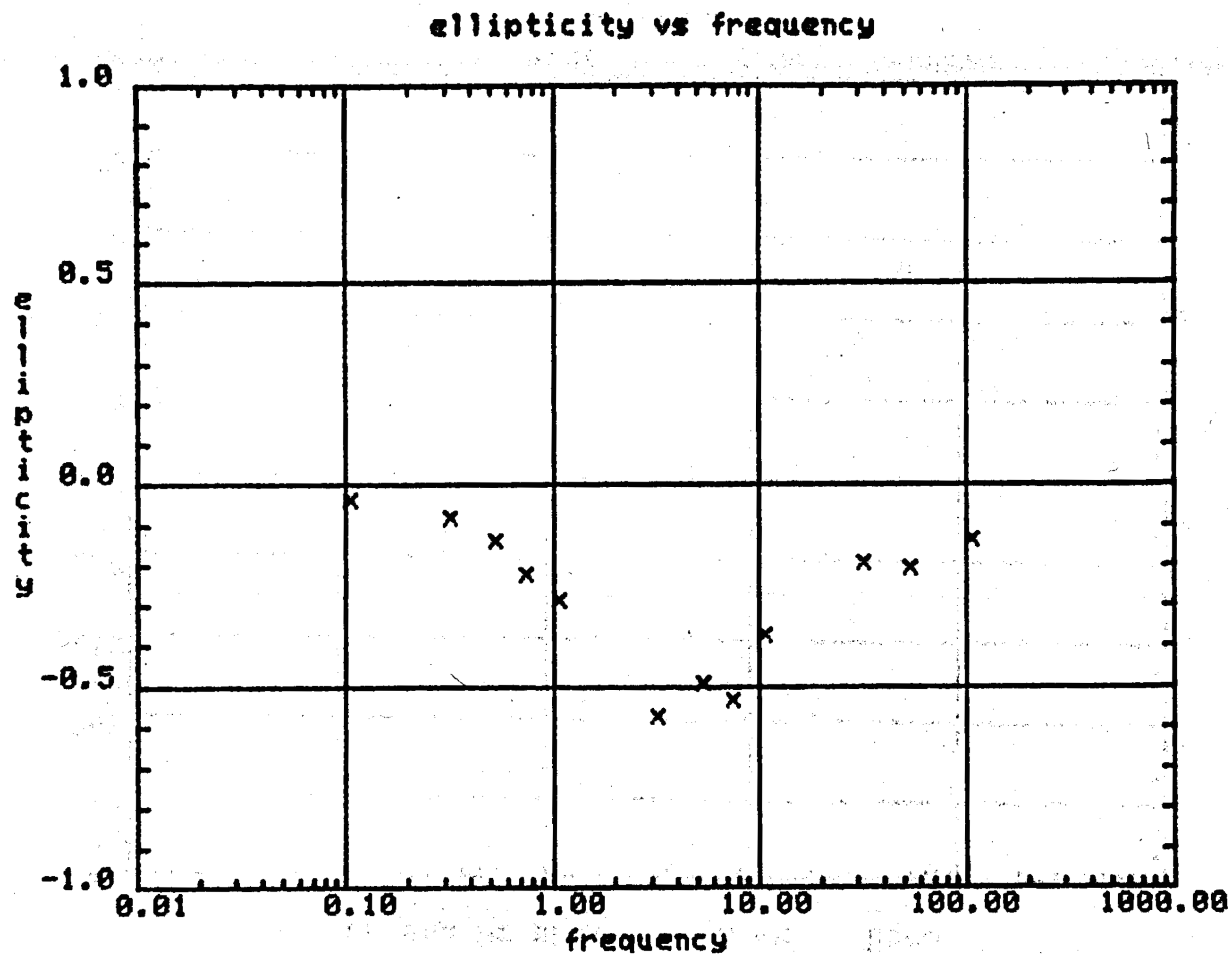

station: h-h 1.5km east
separation=1438 meters

XBL 806-9795

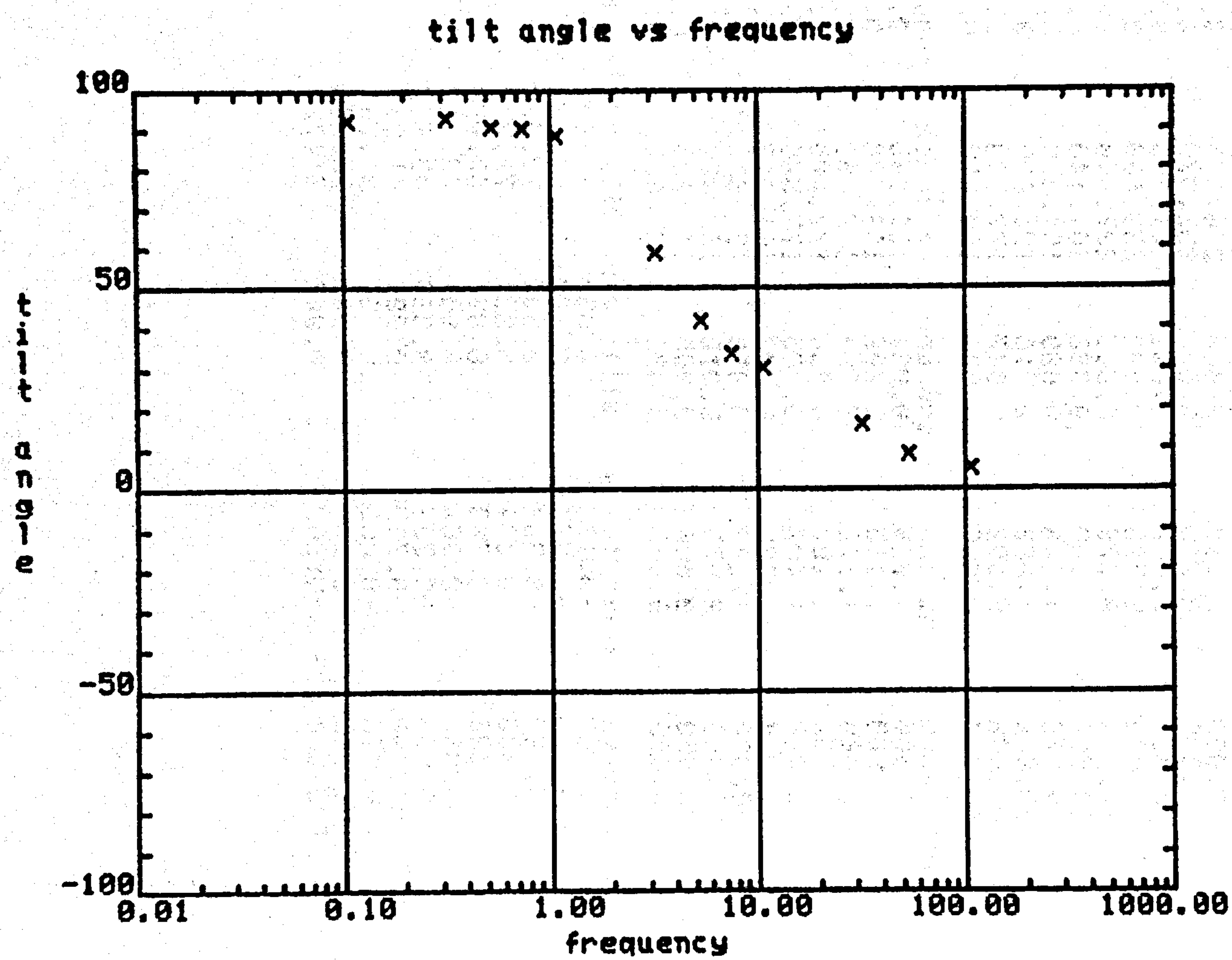

station: h-h 1.5km east
separation=1438 meters

XBL 806-9798

station: h-h .5km east   separation=646 meters
number of turns=4   loop radius=50 meters
hr mag const=7.936   hz mag const=7.092

frequency	hr amp	amp err	hr phase	phase err
1.000	0.119	0.000	278.825	0.085
3.000	0.315	0.000	253.970	0.200
5.000	0.467	0.001	241.600	0.000
7.000	0.580	0.002	233.500	0.000
10.000	0.779	0.003	227.440	0.103
30.000	1.100	0.038	201.140	0.024
50.000	1.246	0.009	194.550	0.250
50.000	1.062	0.010	195.600	0.200
100.000	0.692	0.007	177.700	0.238
150.000	0.669	0.032	160.800	0.850

frequency	hz amp	amp err	hz phase	phase err
1.000	1.046	0.001	181.263	0.152
3.000	1.115	0.002	182.670	0.058
5.000	1.170	0.004	179.600	0.000
7.000	1.187	0.004	177.225	0.243
10.000	1.407	0.005	177.500	0.210
30.000	1.222	0.043	161.213	0.091
50.000	1.182	0.008	154.550	0.250
50.000	0.973	0.010	159.480	0.185
100.000	0.508	0.005	144.725	0.243
150.000	0.469	0.023	127.650	0.858

frequency	ellipticity	ellip err	tilt angle	tilt err
1.000	-0.113	0.000	90.872	0.026
3.000	-0.265	0.000	84.432	0.073
5.000	-0.339	0.001	77.979	0.042
7.000	-0.374	0.001	72.242	0.111
10.000	-0.368	0.001	67.098	0.046
30.000	-0.361	0.001	48.917	0.026
50.000	-0.363	0.000	43.028	0.030
50.000	-0.325	0.001	41.930	0.008
100.000	-0.280	0.000	34.734	0.012
150.000	-0.277	0.002	33.288	0.088
200.000	-0.269	0.007	34.788	0.082

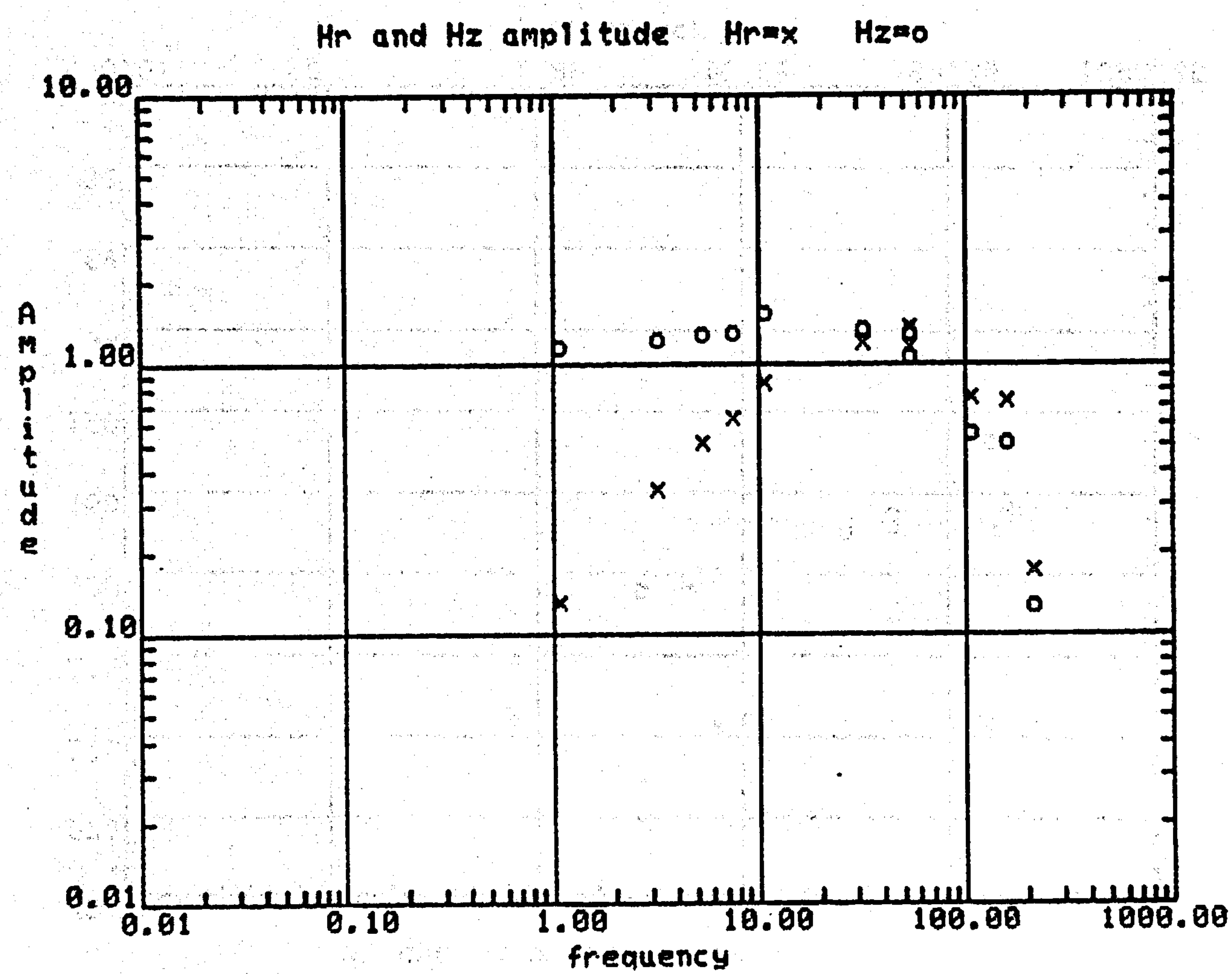

station: h-h .5km east
separation=646 meters

XBL 806-9791

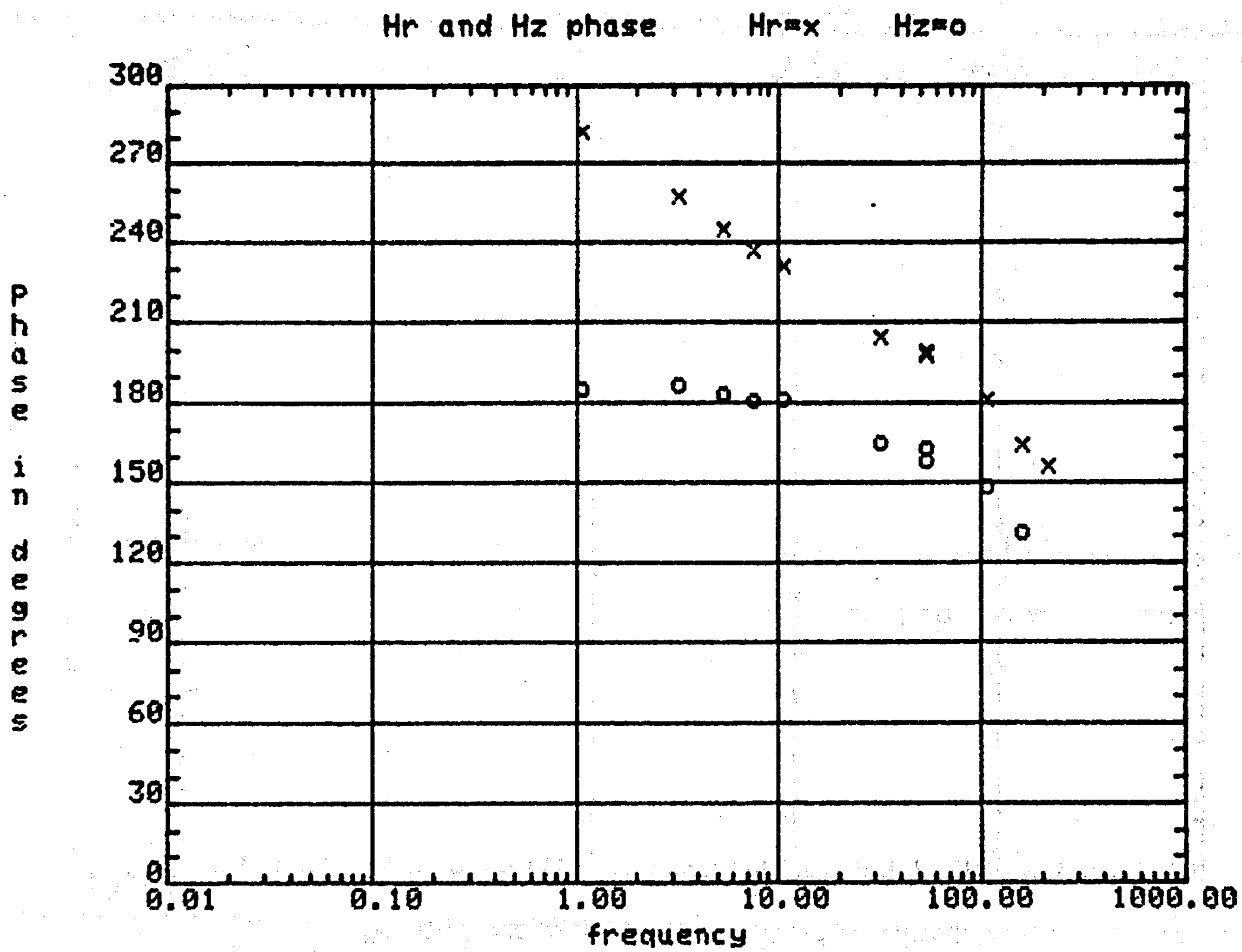

station: h-h .5km east
separation=646 meters

XBL 806-9792

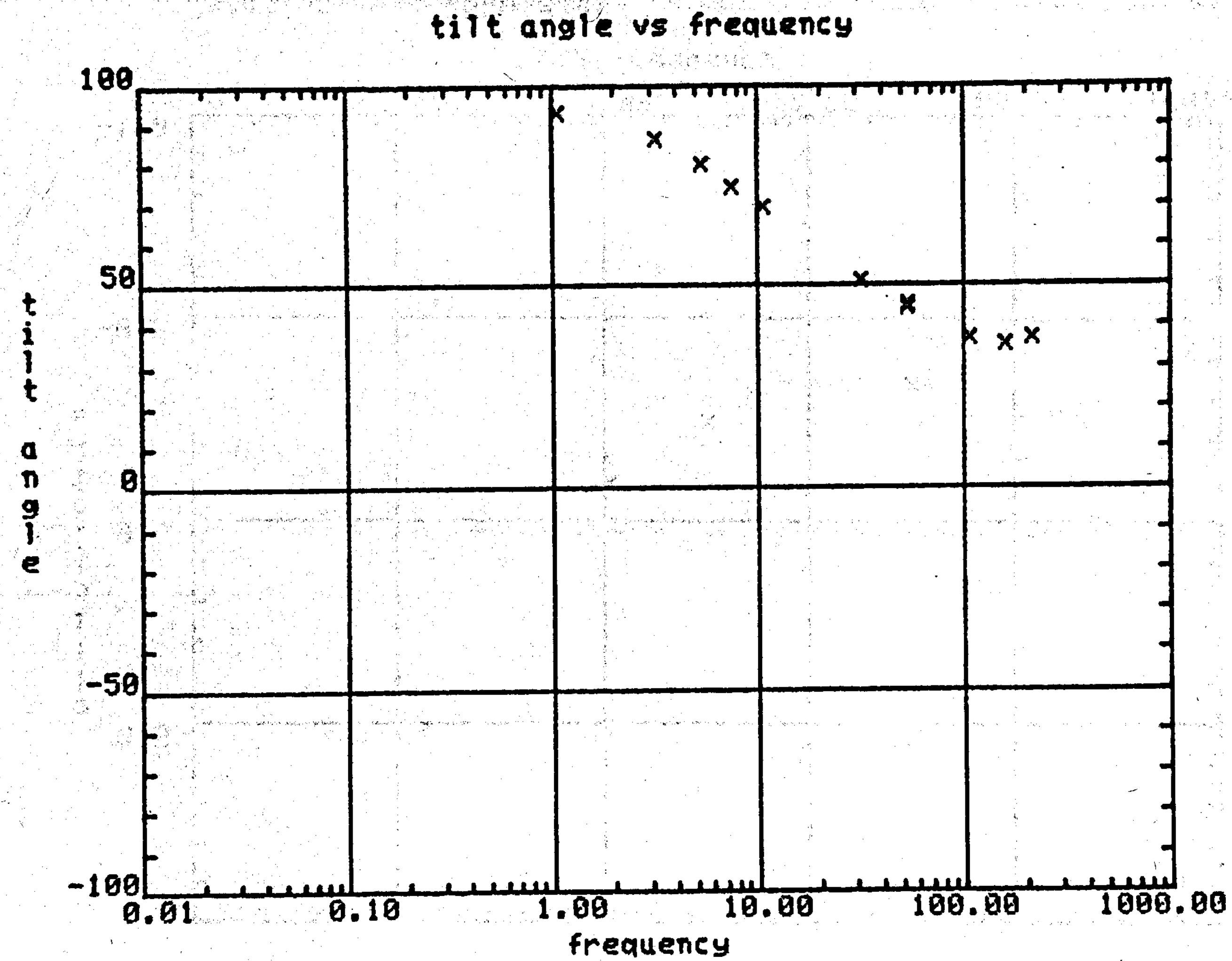

station: h-h .5km east
separation=646 meters

XBL 806-9793

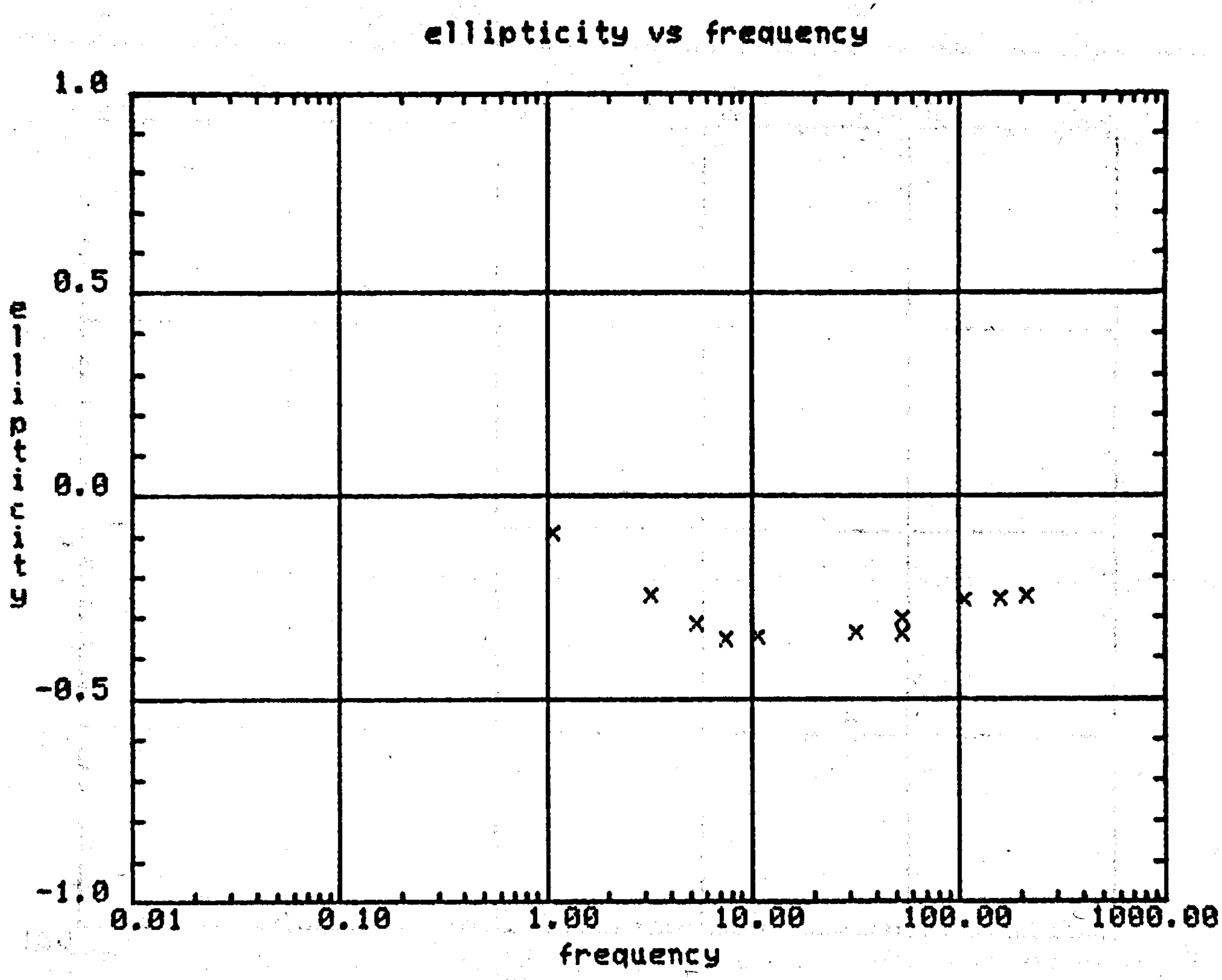

station: h-h .5km east
separation=646 meters

XBL 806-9794

station: h-h.5km west seperation=548 meters
number of turns=4 loop radius=50 meters
hr mag const=7.936 hz mag const=7.092

frequency	hr amp	amp err	hr phase	phase err
0.100	0.019	0.002	218.800	3.512
0.300	0.035	0.001	241.000	1.080
0.500	0.055	0.000	248.750	0.479
0.700	0.075	0.000	252.133	0.333
1.000	0.108	0.000	254.763	0.137
3.000	0.300	0.000	247.870	0.100
5.000	0.457	0.001	239.600	0.000
7.000	0.580	0.001	232.833	0.333
10.000	0.793	0.006	226.667	0.333
30.000	1.124	0.010	200.200	0.000
50.000	1.060	0.019	193.467	0.333
100.000	0.624	0.007	174.020	0.058

frequency	hz amp	amp err	hz phase	phase err
0.100	0.948	0.002	174.800	0.000
0.300	0.781	0.005	164.750	0.750
0.500	0.562	0.003	156.750	0.250
0.700	0.359	0.003	155.800	0.000
1.000	1.070	0.002	174.873	0.077
3.000	0.976	0.000	178.770	0.000
5.000	0.998	0.001	178.600	0.000
7.000	1.003	0.002	179.167	0.333
10.000	1.224	0.009	176.000	0.000
30.000	1.334	0.009	166.200	0.000
50.000	1.407	0.018	148.800	0.000

frequency	ellipticity	ellip err	tilt angle	tilt err
0.100	-0.013	0.001	89.186	0.126
0.300	-0.044	0.002	89.386	0.045
0.500	-0.098	0.001	90.200	0.058
0.700	-0.209	0.001	91.389	0.066
1.000	-0.099	0.000	88.974	0.009
3.000	-0.283	0.000	83.194	0.028
5.000	-0.378	0.001	75.345	0.037
7.000	-0.407	0.003	67.095	0.088
10.000	-0.413	0.003	62.610	0.072
30.000	-0.300	0.000	50.879	0.111
50.000	-0.389	0.003	55.989	0.171
100.000	-0.361	0.000	28.090	0.007
200.000	-0.302	0.002	18.636	0.086
500.000	-0.196	0.001	12.700	0.050

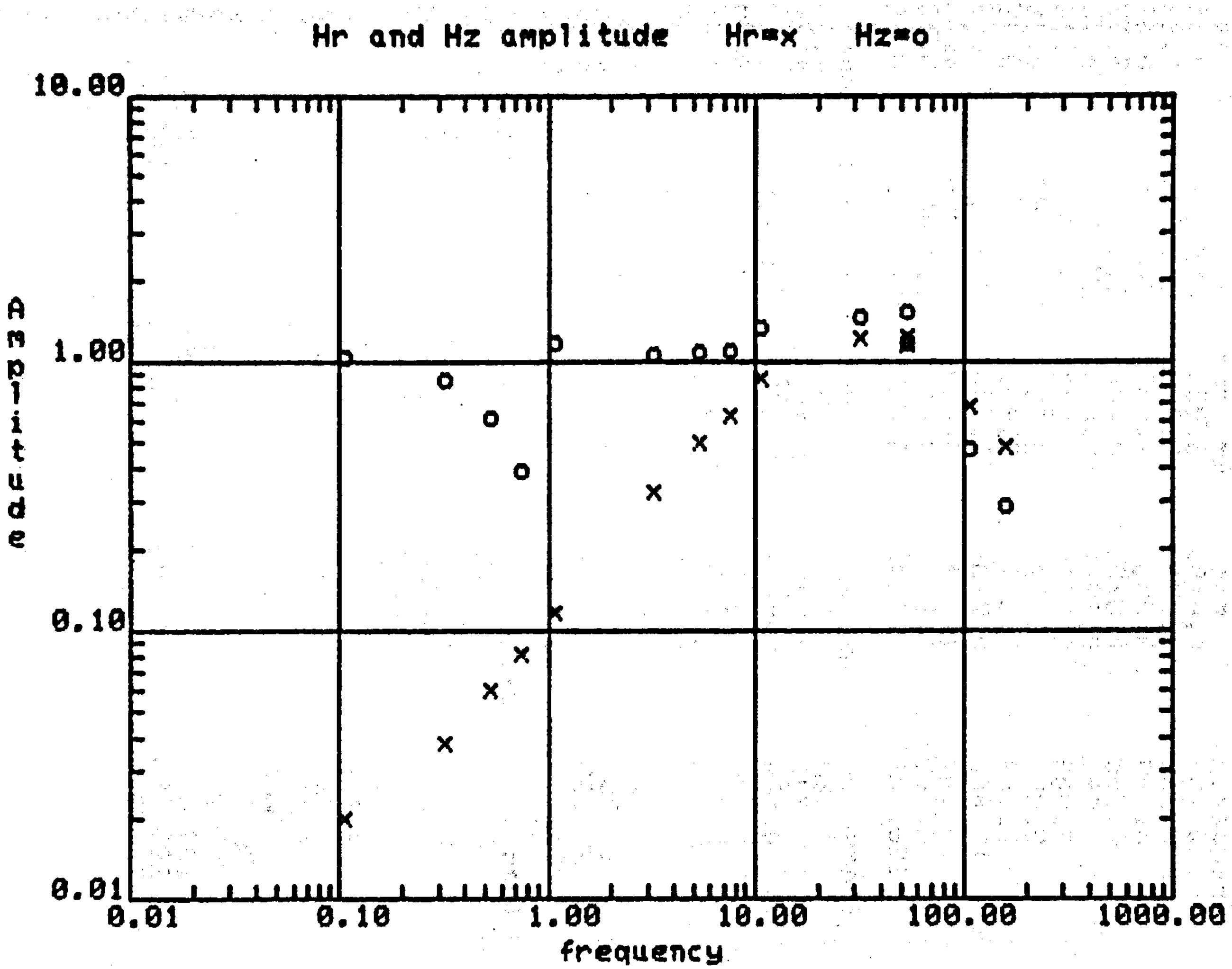

station: h-h.5km west
separation=548 meters

XBL 806-9800

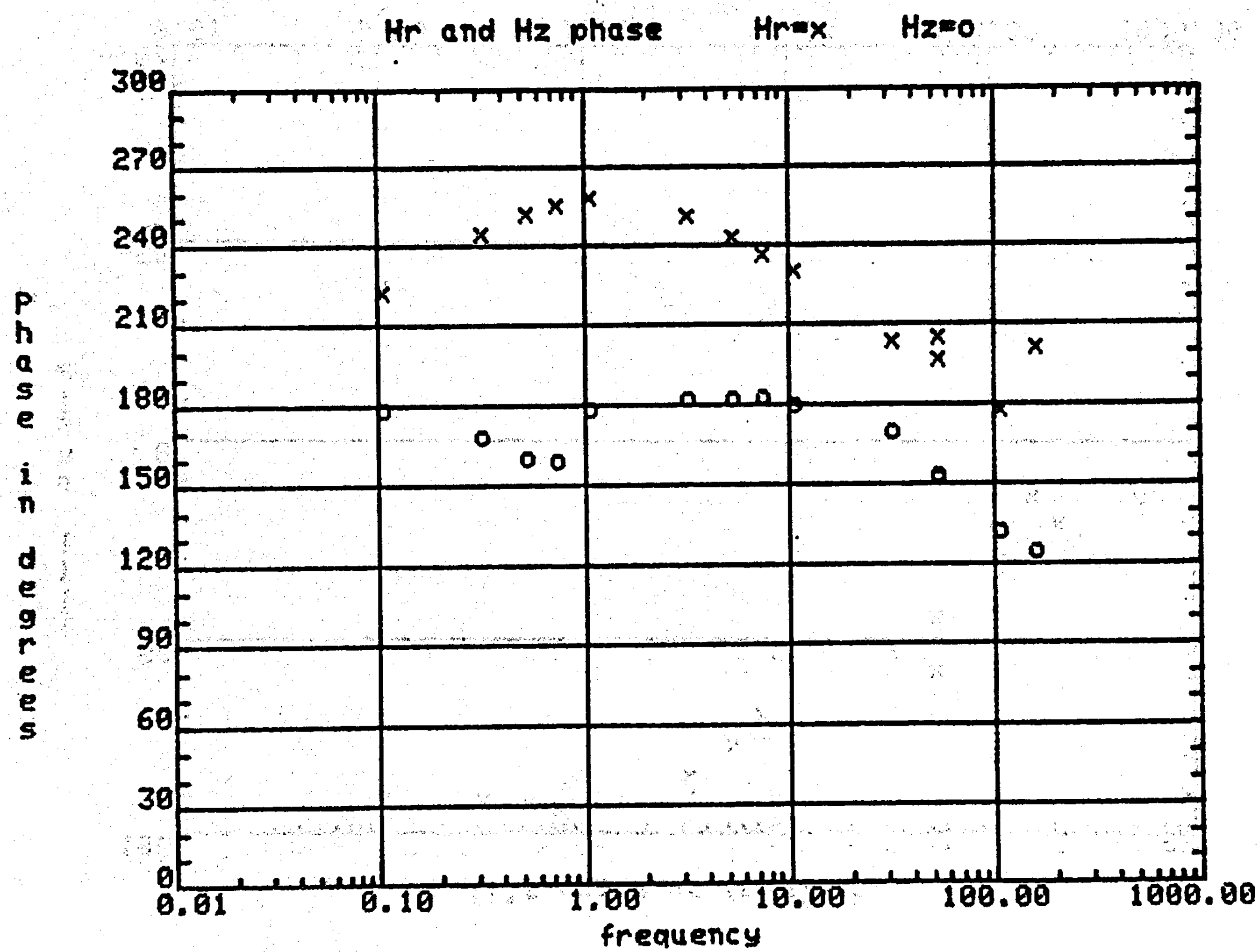

station: h-h.5km west
separation=548 meters

XBL 806-9799

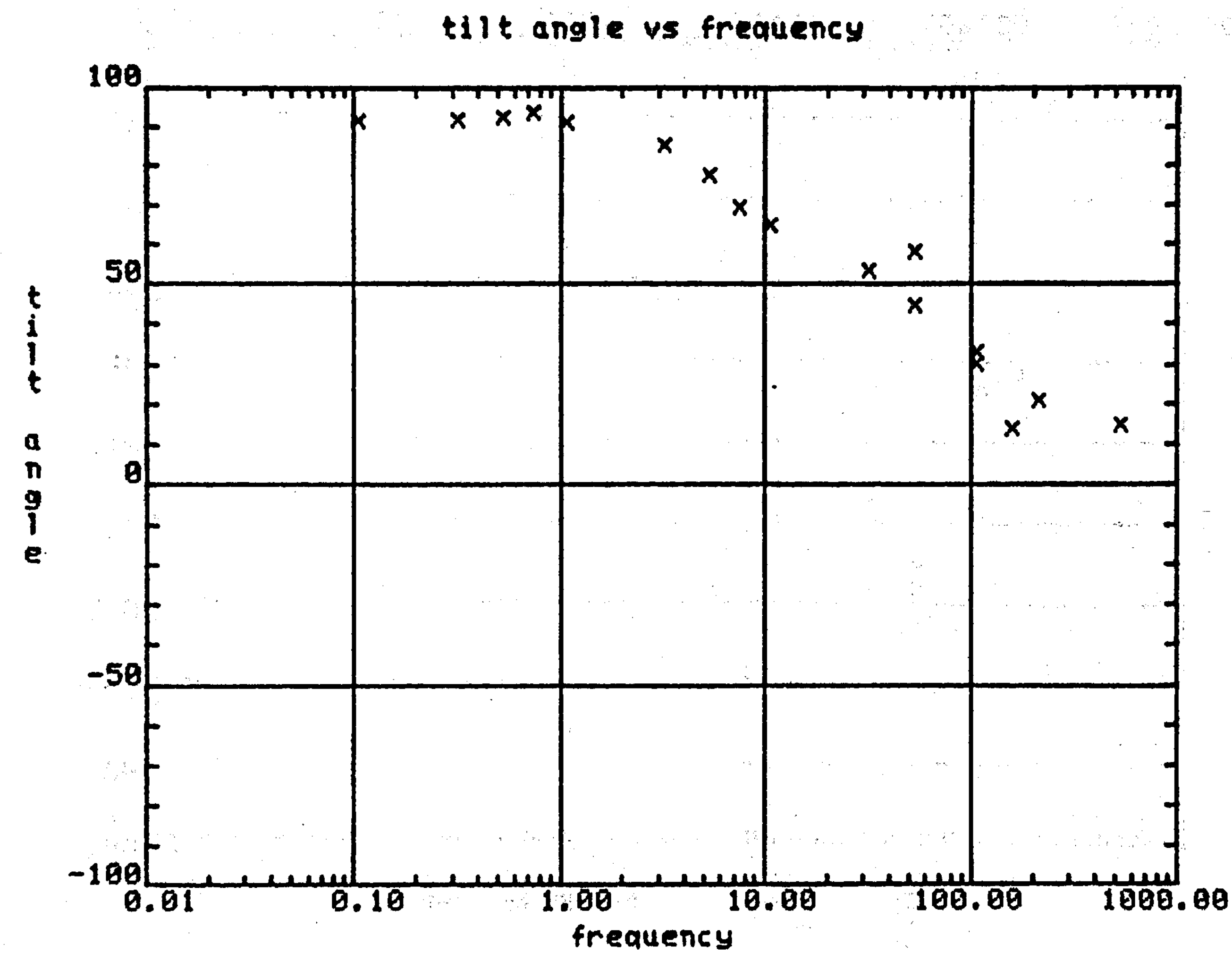

station: h-h.5km west
separation=548 meters

XBL 806-9801

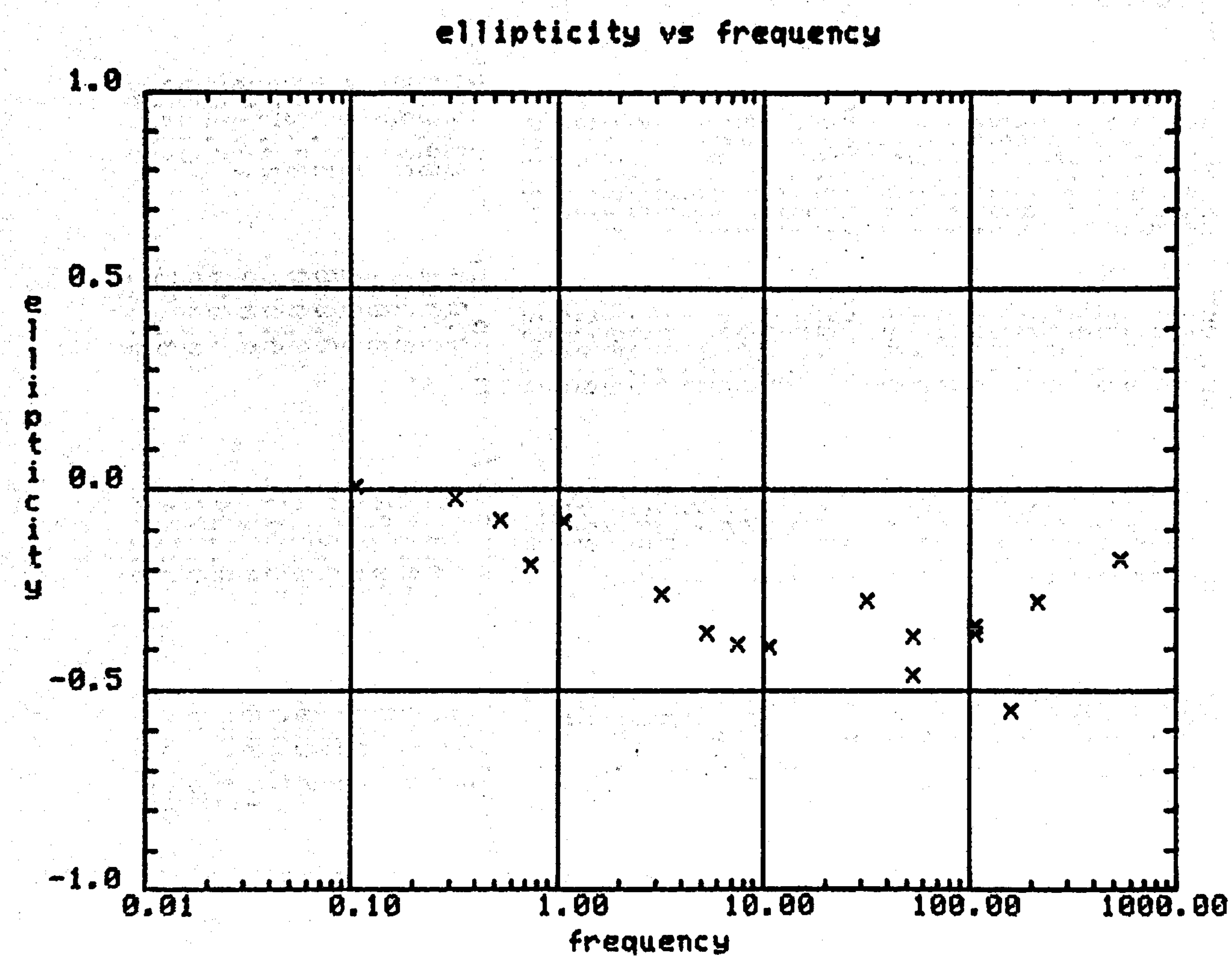

station: h-h.5km west
separation=548 meters

XBL 806-9802

station: h-h 1.5 km west   seperation=1562 meters
number of turns=4   loop radius=50 meters
hr mag const=7.936   hz mag const=7.092

frequency	hr amp	amp err	hr phase	phase err
0.100	0.042	0.001	268.616	0.229
0.300	0.147	0.002	261.033	0.332
0.500	0.215	0.001	256.408	0.075
0.700	0.323	0.001	256.737	0.482
1.000	0.412	0.001	251.091	0.506
3.000	0.984	0.002	221.706	0.493
5.000	1.254	0.001	201.067	0.502
7.000	1.323	0.001	185.772	0.500
10.000	1.641	0.011	172.332	0.496
30.000	1.087	0.003	171.135	0.524
50.000	0.770	0.001	134.891	0.499
150.000	0.495	0.002	168.818	0.507

frequency	hz amp	amp err	hz phase	phase err
0.100	1.000	0.005	179.093	0.002
0.300	1.108	0.004	177.790	0.503
0.500	1.096	0.001	176.924	0.501
0.700	1.101	0.001	175.140	0.502
1.000	1.099	0.002	173.806	0.003
3.000	1.115	0.001	157.279	0.505
5.000	1.025	0.002	138.933	0.497
7.000	0.882	0.001	124.475	0.499
10.000	0.720	0.001	112.044	0.522
30.000	0.274	0.015	119.246	0.117
50.000	0.160	0.000	75.483	0.513
150.000	0.073	0.002	92.000	0.297

frequency	ellipticity	ellip err	tilt angle	tilt err
0.100	-0.042	0.001	89.980	0.010
0.300	-0.132	0.001	89.089	0.033
0.500	-0.192	0.001	87.876	0.095
0.700	-0.290	0.001	87.317	0.014
1.000	-0.362	0.002	84.576	0.193
3.000	-0.619	0.000	53.051	0.191
5.000	-0.578	0.000	33.250	0.055
7.000	-0.510	0.000	24.537	0.011
10.000	-0.361	0.002	14.159	0.078
30.000	-0.194	0.010	9.206	0.417
50.000	-0.177	0.000	6.220	0.006
150.000	-0.144	0.003	1.977	0.079
200.000	-0.140	0.008	-0.457	0.154

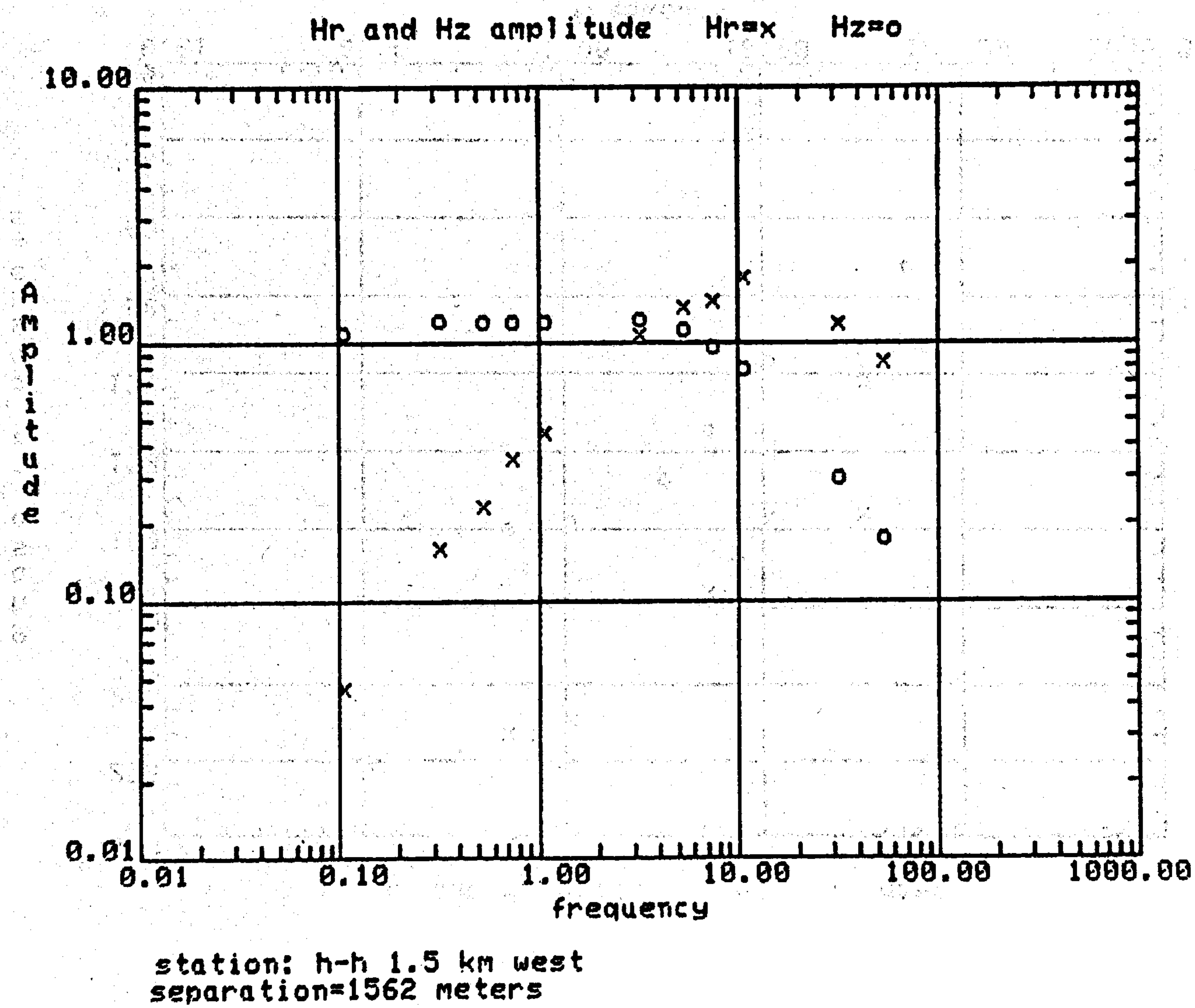
Hr and Hz amplitude Hr=x Hz=o
10.00
1.00
0.10
0.01
Amplitude
0.01
0.10
1.00
10.00
100.00
1000.00
frequency
station: h-h 1.5 km west
separation=1562 meters

XBL 806-9804

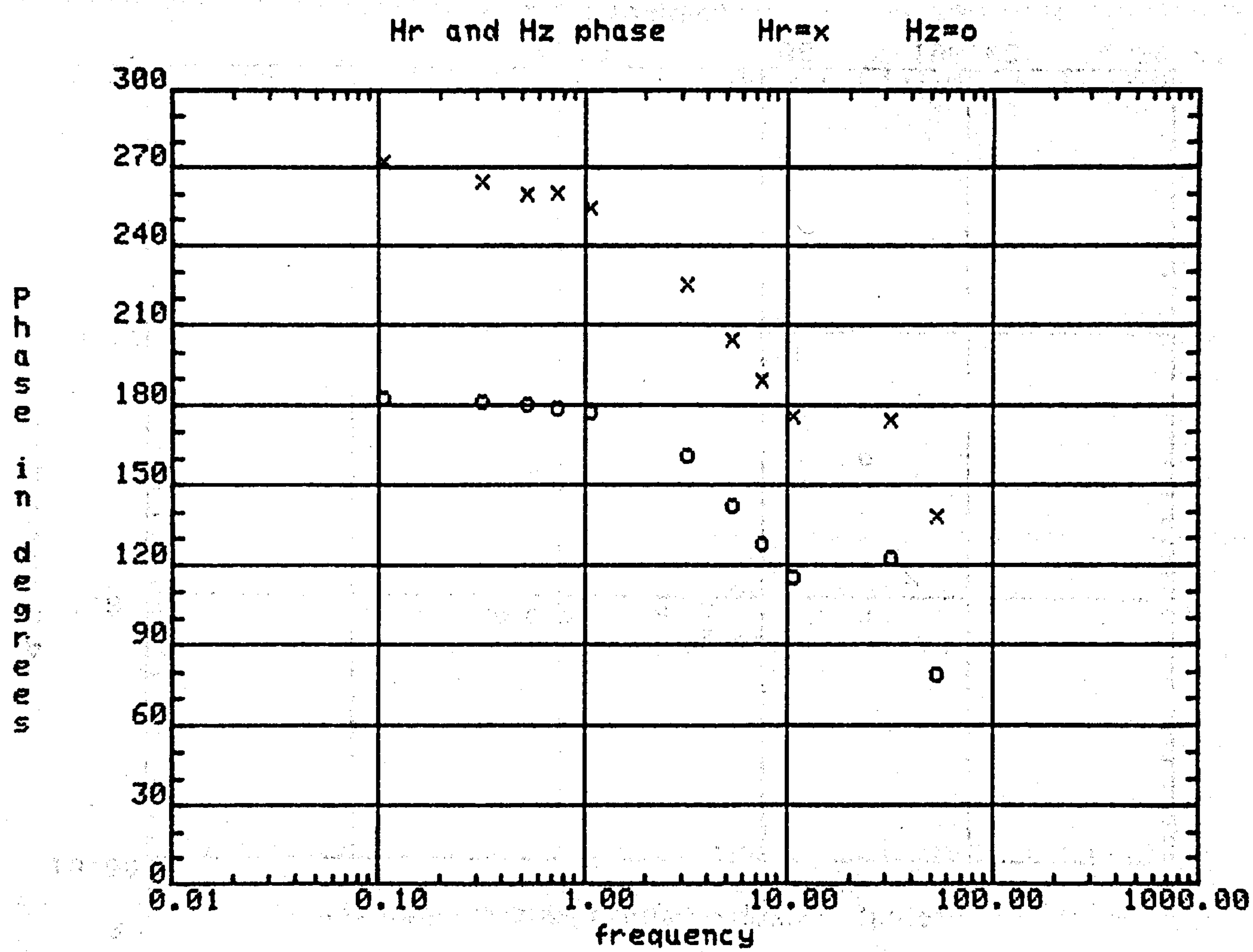

station: h-h 1.5 km west
separation=1562 meters

XBL 806-9803

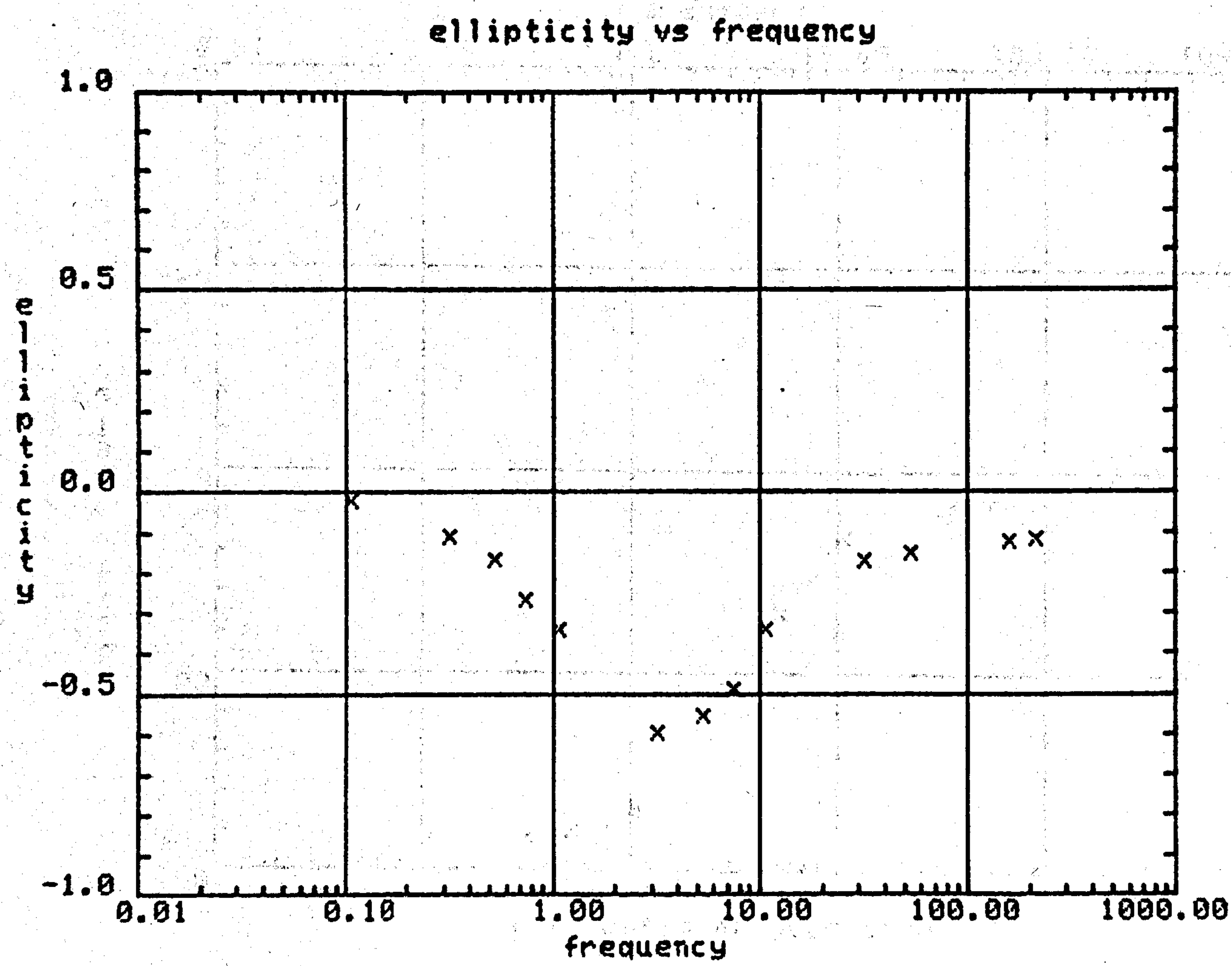

station: h-h 1.5 km west
separation=1562 meters

XBL 806-9806

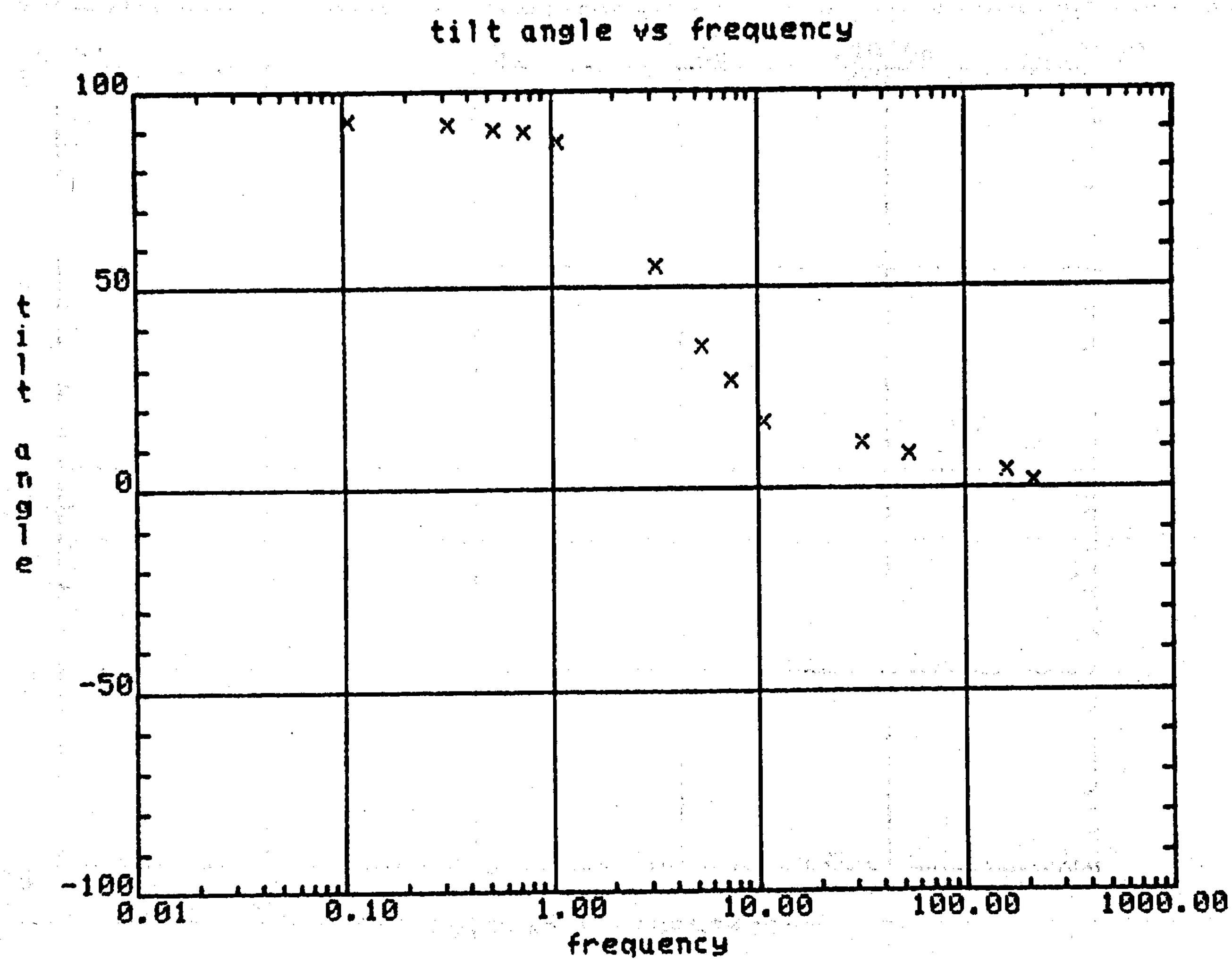

station: h-h 1.5 km west
separation=1562 meters

XBL 806-9805

APPENDIX C

One dimensional interpretation EM sounding data.

COMPARSION OF CALCULATED AND MEASURED DATA

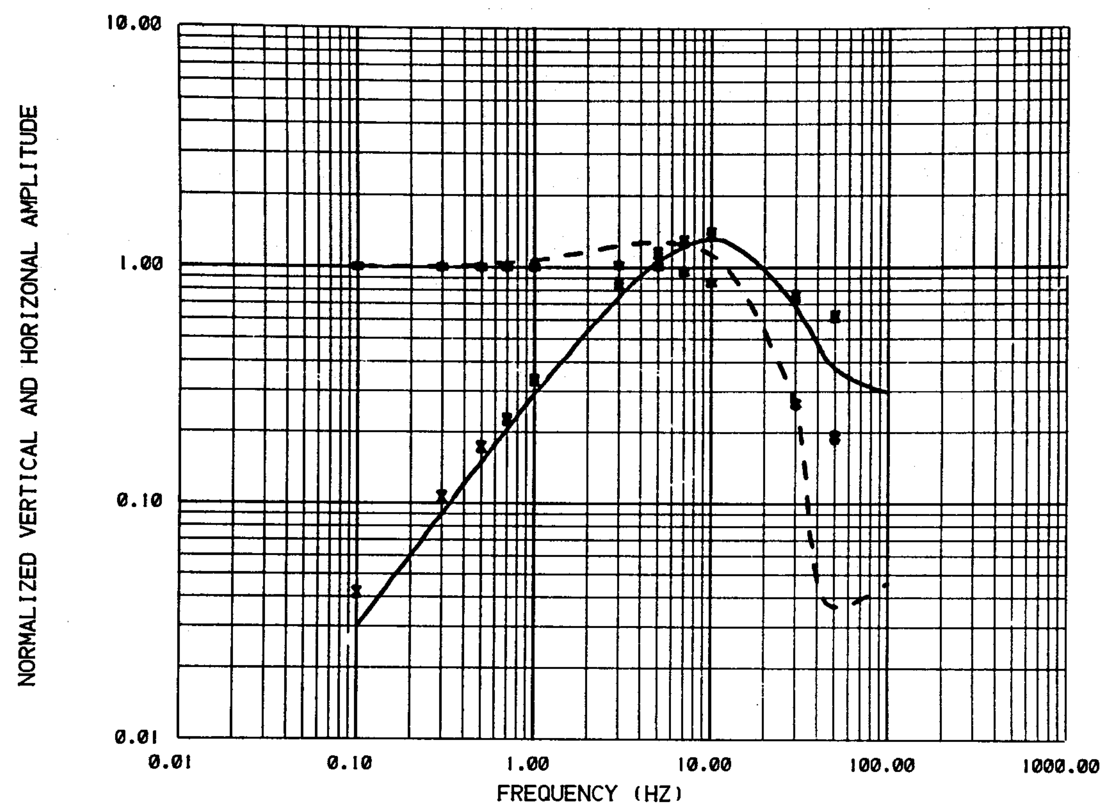

PANTHER CANYON T-T 1.5KM NORTH

CALCULATED DATA		MEASURED DATA		LAYER	RESISTIVITY(OHM-M)		THICKNESS(M)	
HR	————————	HR	X	1	4.90±	.00	233.0 ±	1.
HZ	—— —— —	HZ	*	2	150.00±	17.11	.1000E+11±	0.

DATA VARIENCE ESTIMATE 260.2

XBL 803-8997

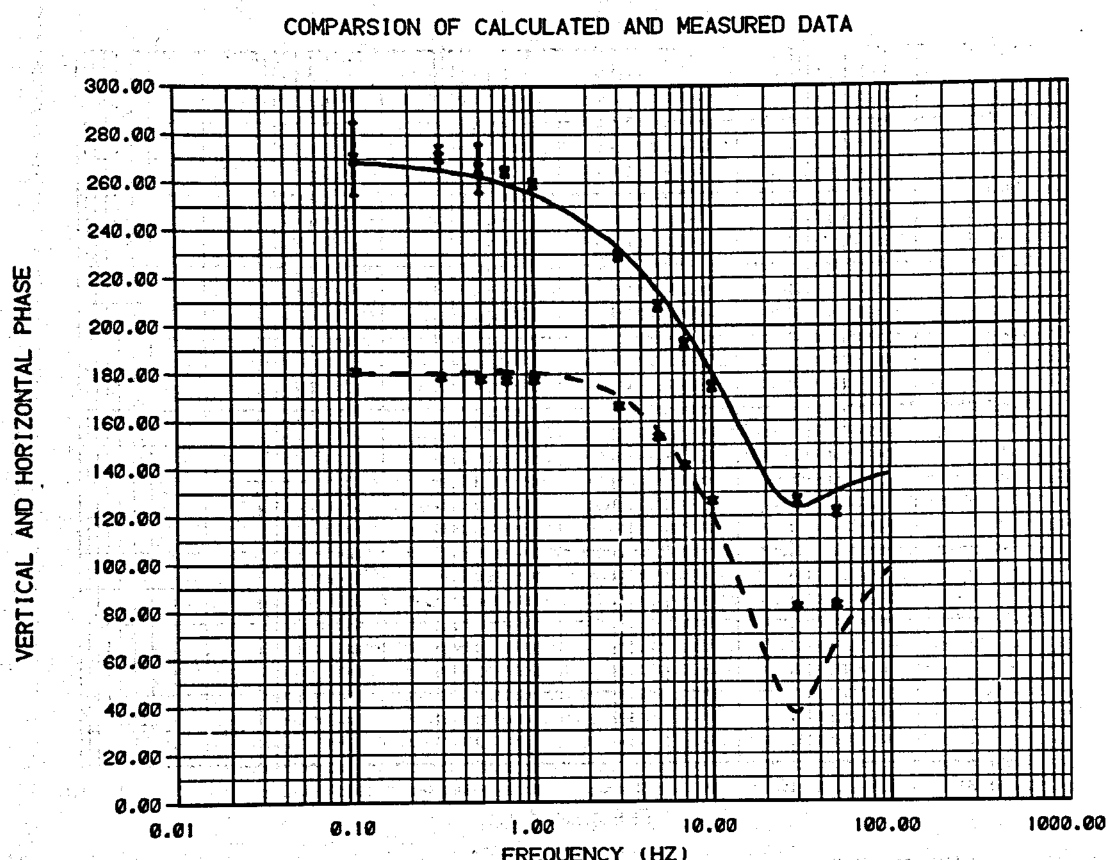

PANTHER CANYON T-T 1.5KM NORTH

CALCULATED DATA		MEASURED DATA		LAYER	RESISTIVITY(OHM-M)		THICKNESS(M)	
HR	———————	HR	X	1	4.90±	.00	233.0 ±	1.
HZ	— — —	HZ	*	2	150.00±	17.11	.1000E+11±	0.

DATA VARIENCE ESTIMATE 260.2

XBL 803-8983

COMPARSION OF CALCULATED AND MEASURED DATA

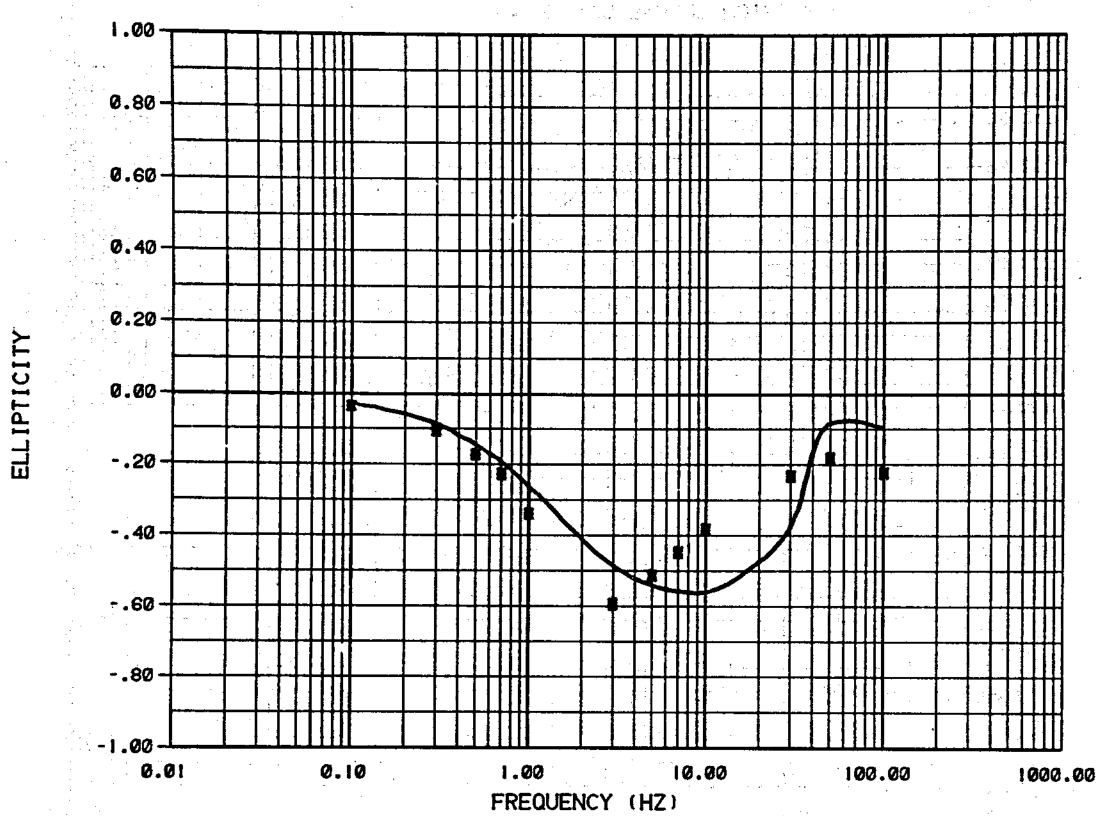

PANTHER CANYON T-T 1.5KM NORTH

CALCULATED DATA		MEASURED DATA		LAYER	RESISTIVITY(OHM-M)		THICKNESS(M)	
ELLIPTICITY	————	ELLIPTICITY	X	1	4.90*	.00	233.0 *	1.
				2	150.00*	17.11	.1000E+11*	0.

DATA VARIENCE ESTIMATE 260.2

XBL 804-9016

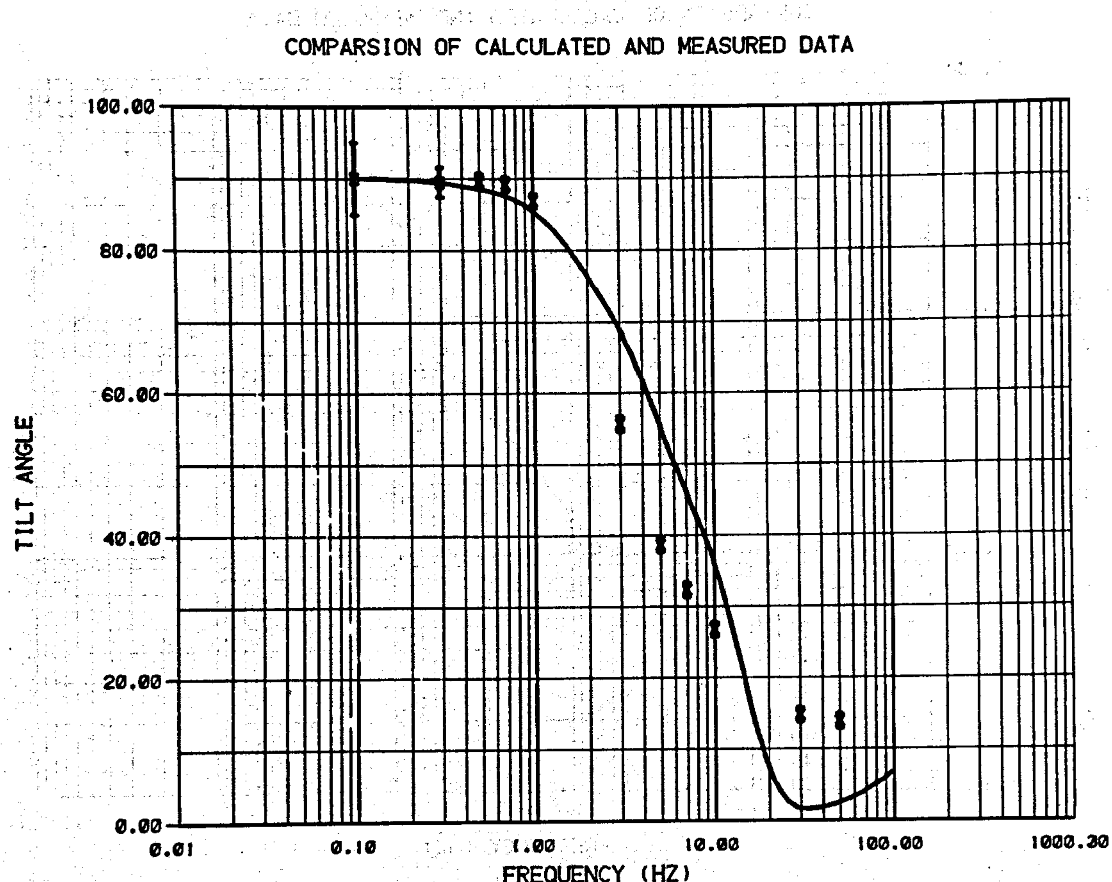

PANTHER CANYON T-T 1.5KM NORTH

CALCULATED DATA		MEASURED DATA		LAYER	RESISTIVITY(OHM-M)		THICKNESS(M)	
TILT ANGLE	———	TILT ANGLE	X	1	4.90±	.00	233.0 ±	1.
				2	150.00±	17.11	.1000E+11±	0.

DATA VARIENCE ESTIMATE 260.2

XBL 804-9015

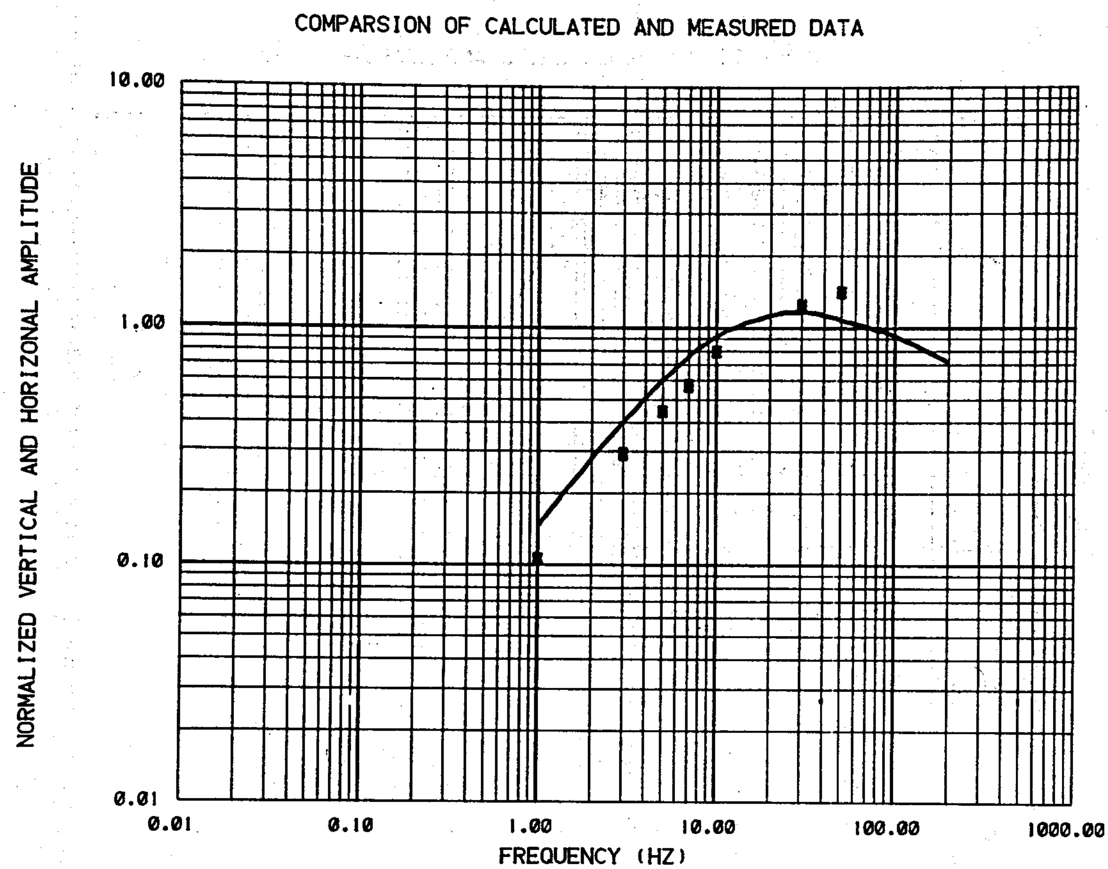

PANTHER CANYON T-T 0.5KM NORTH

CALCULATED DATA		MEASURED DATA		LAYER	RESISTIVITY(OHM-M)		THICKNESS(M)	
HR	————	HR	X	1	6.30±	.00	90.00 ±	2.
				2	2.20±	.06	200.0 ±	16.
				3	150.00±	611.83	.1000E+11±	0.

DATA VARIENCE ESTIMATE 303.4

XBL 803-8977

COMPARSION OF CALCULATED AND MEASURED DATA

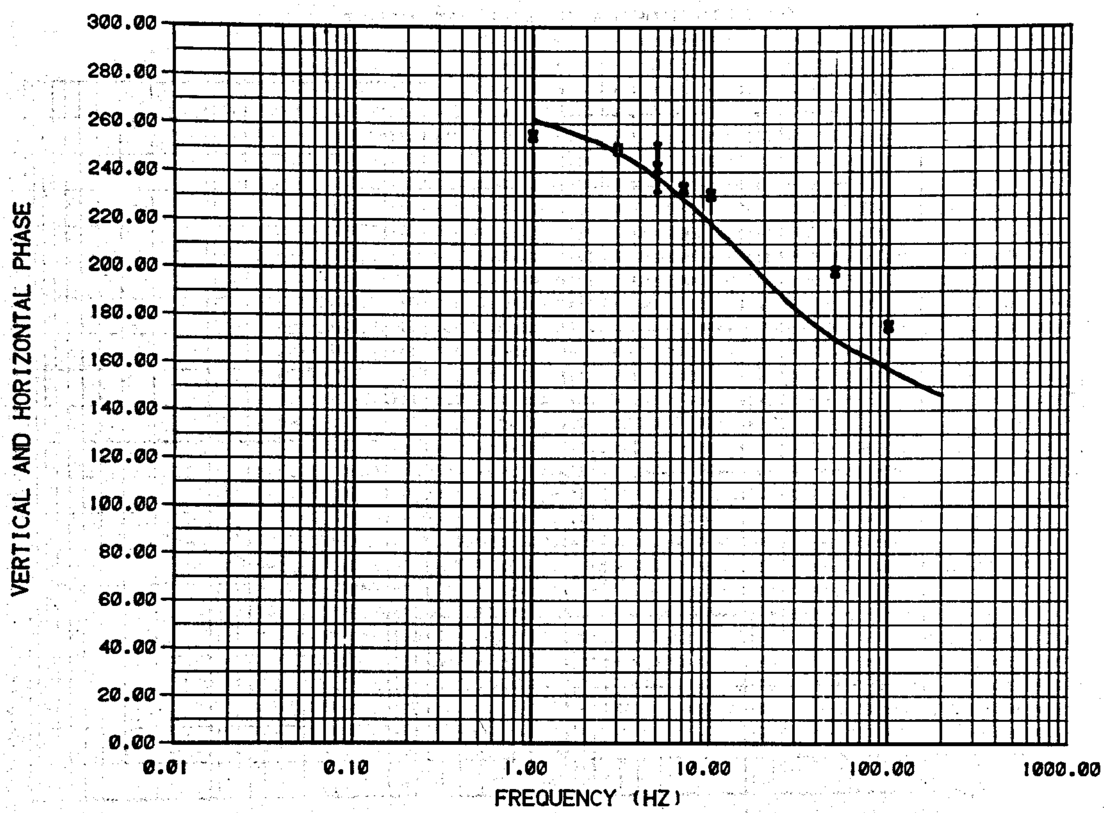

PANTHER CANYON T-T 0.5KM NORTH

CALCULATED DATA		MEASURED DATA		LAYER	RESISTIVITY(OHM-M)		THICKNESS(M)	
HR	————	HR	X	1	6.30±	.00	90.00 ±	2.
				2	2.20±	.06	200.0 ±	16.
				3	150.00±	611.83	.1000E+11±	0.

DATA VARIENCE ESTIMATE 303.4

XBL 803-8970

COMPARSION OF CALCULATED AND MEASURED DATA

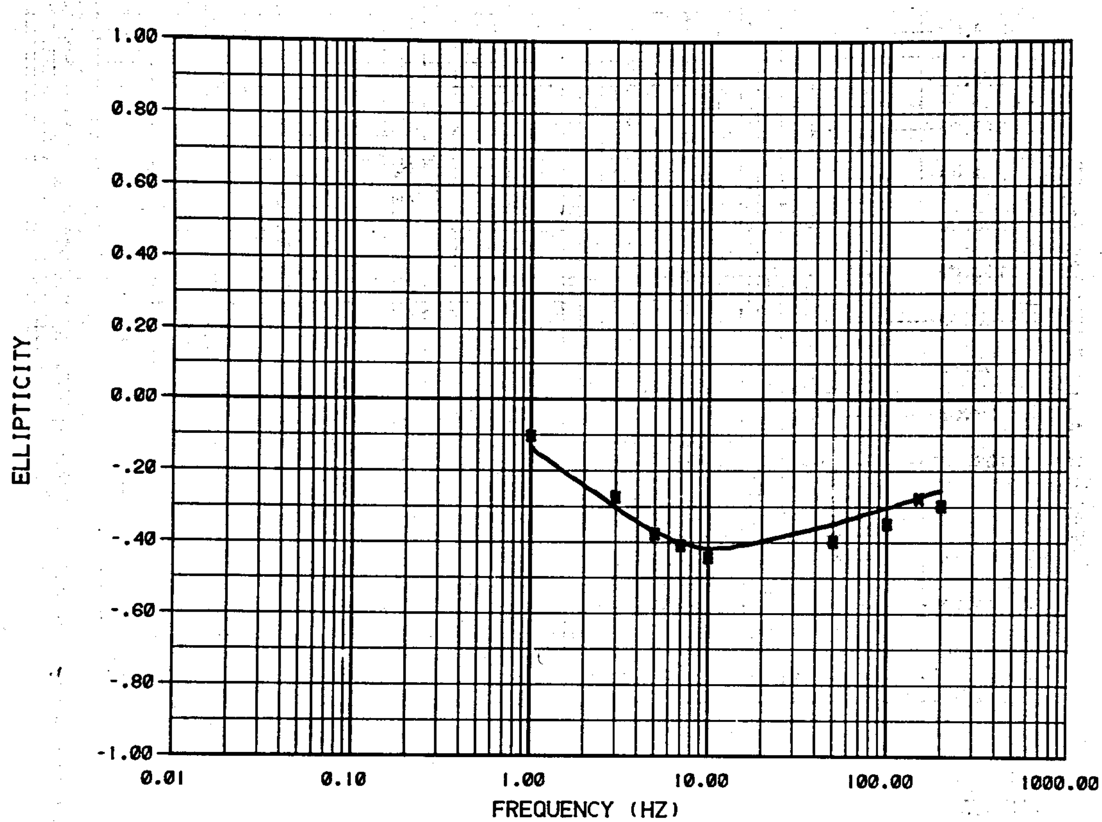

PANTHER CANYON T-T 0.5KM NORTH

CALCULATED DATA		MEASURED DATA		LAYER	RESISTIVITY(OHM-M)		THICKNESS(M)	
ELLIPTICITY	————	ELLIPTICITY	X	1	6.30±	.00	90.00	± 2.
				2	2.20±	.06	200.0	± 16.
				3	150.00±	611.83	.1000E+11±	0.

DATA VARIENCE ESTIMATE 303.4

XBL 803-8976

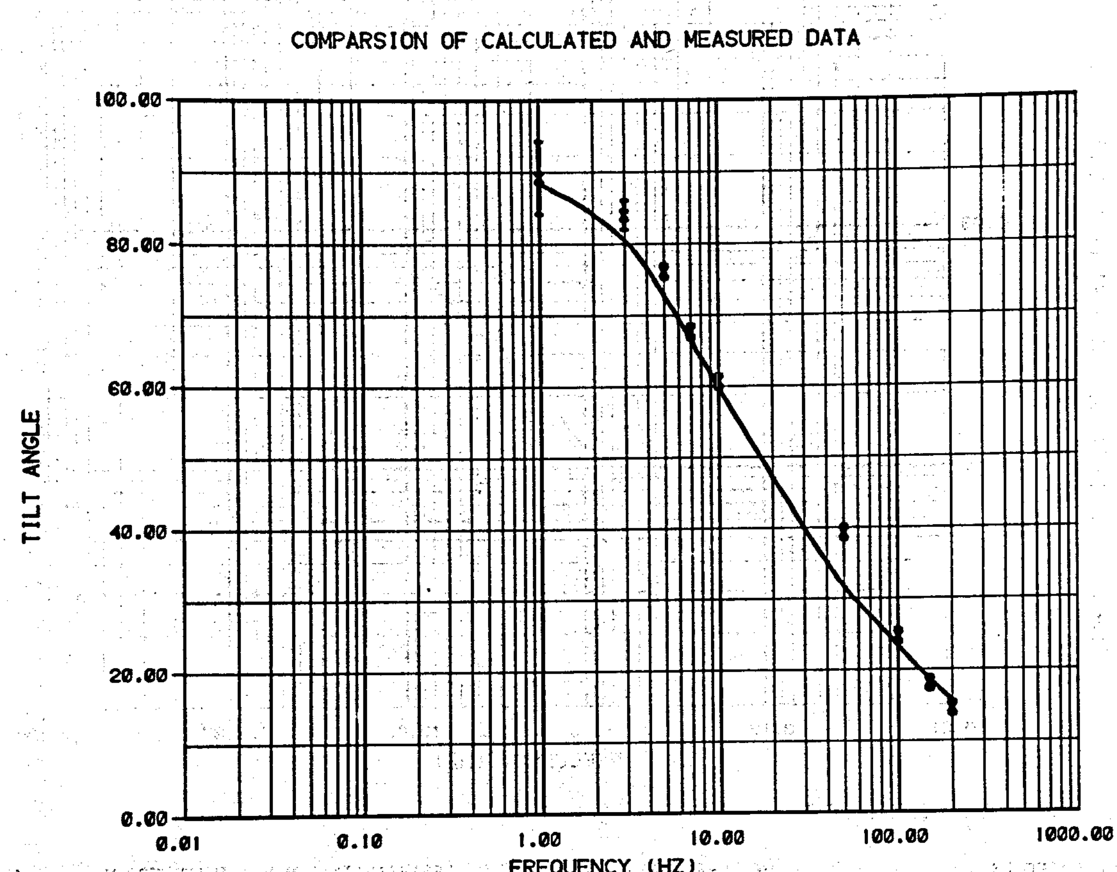

PANTHER CANYON T-T 0.5KM NORTH

CALCULATED DATA

TILT ANGLE ———

MEASURED DATA

TILT ANGLE X

LAYER	RESISTIVITY(OHM-M)		THICKNESS(M)	
1	6.30±	.00	90.00 ±	2.
2	2.20±	.06	200.0 ±	16.
3	150.00±	611.83	.1000E+11±	0.

DATA VARIENCE ESTIMATE 303.4

XBL 804-9012

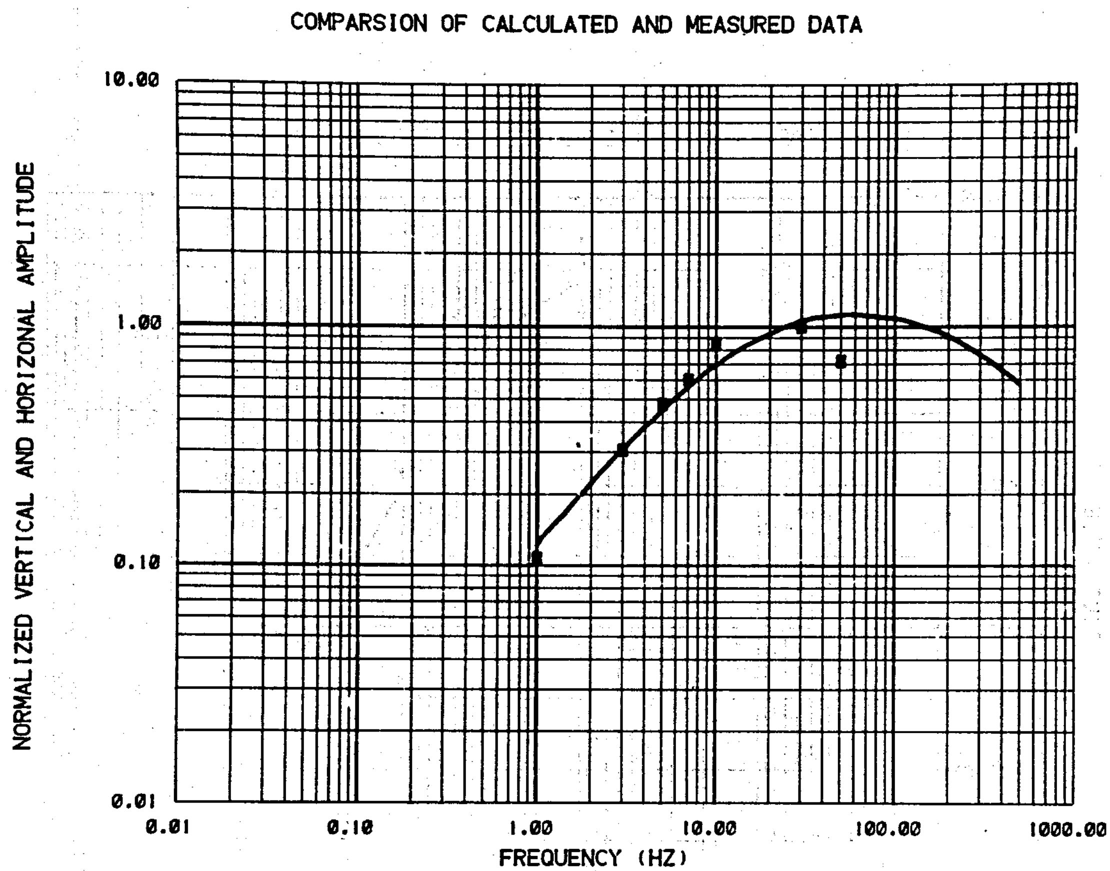

PANTHER CANYON T-T 0.5KM SOUTH

CALCULATED DATA		MEASURED DATA		LAYER	RESISTIVITY(OHM-M)		THICKNESS(M)	
HR	————————	HR	X	1	6.30±	.00	90.00 ±	1.
				2	2.20±	.03	.1000E+11±	0.

DATA VARIENCE ESTIMATE 381.7

XBL 803-8984

COMPARSION OF CALCULATED AND MEASURED DATA

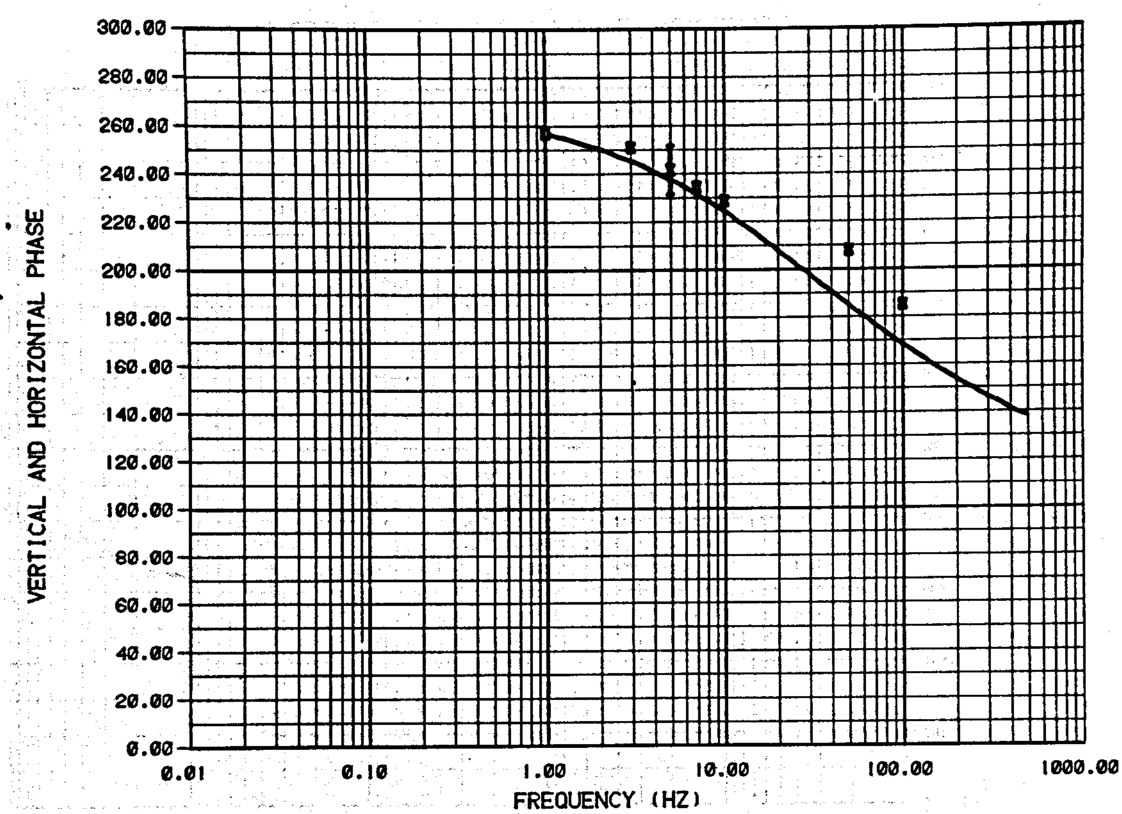

PANTHER CANYON T-T 0.5KM SOUTH

CALCULATED DATA		MEASURED DATA		LAYER	RESISTIVITY(OHM-M)		THICKNESS(M)	
HR	————————	HR	X	1	6.30±	.00	90.00 ±	1.
				2	2.20±	.03	.1000E+11±	0.

DATA VARIENCE ESTIMATE 381.7

XBL 803-8988

COMPARSION OF CALCULATED AND MEASURED DATA

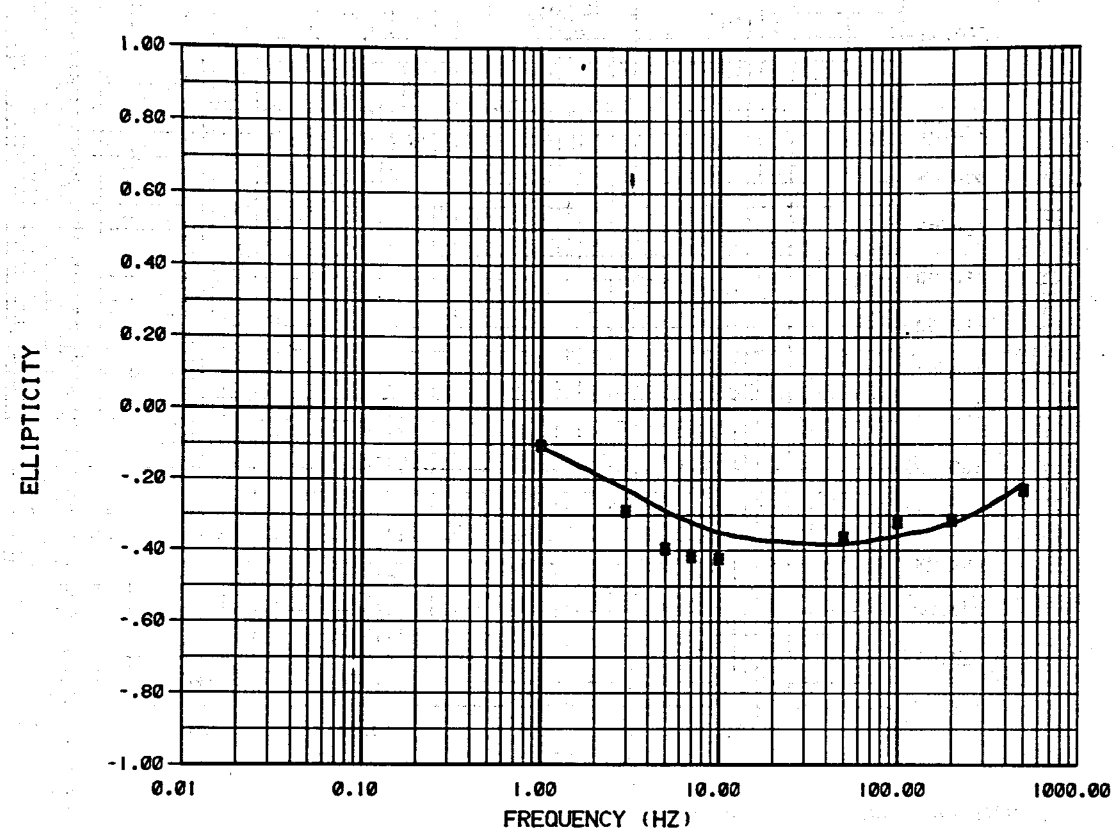

PANTHER CANYON T-T 0.5KM SOUTH

CALCULATED DATA		MEASURED DATA		LAYER	RESISTIVITY(OHM-M)		THICKNESS(M)	
ELLIPTICITY	———	ELLIPTICITY	X	1	6.30±	.00	90.00 ±	1.
				2	2.20±	.03	.1000E+11±	0.

DATA VARIENCE ESTIMATE 381.7

XBL 803-8986

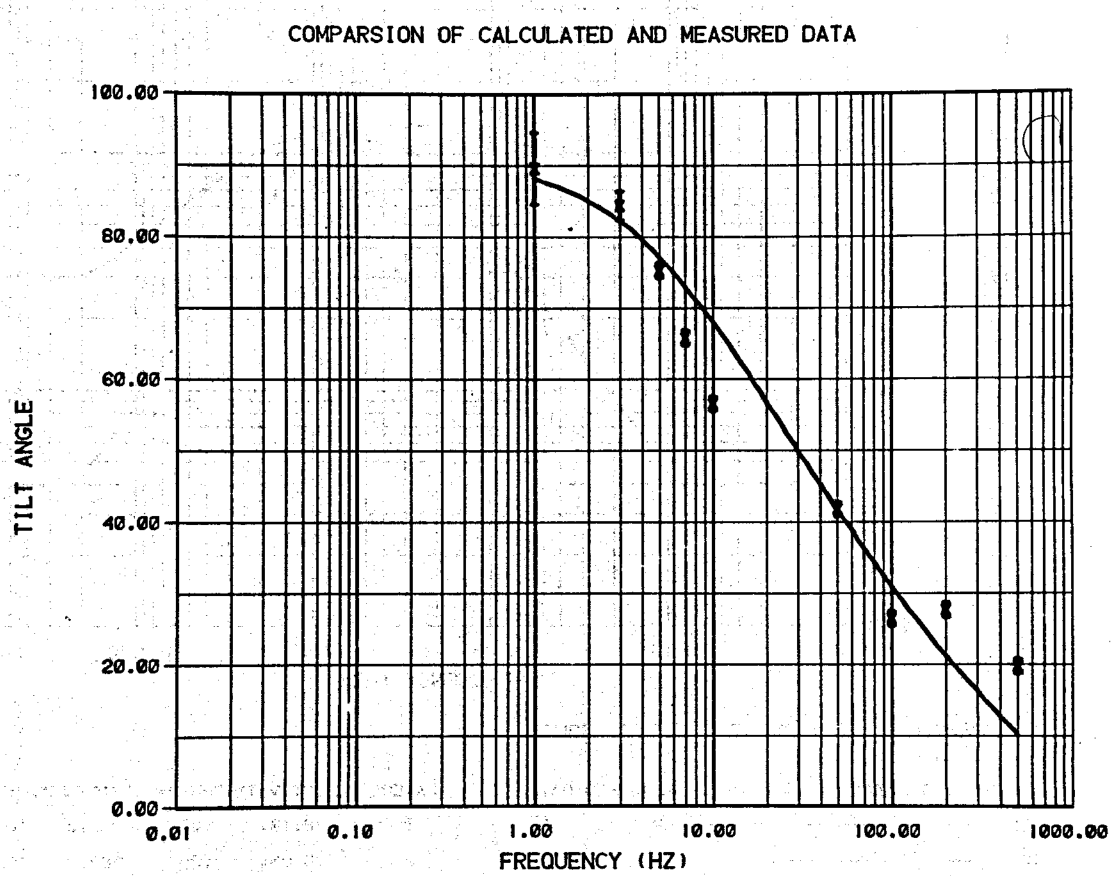

PANTHER CANYON T-T 0.5KM SOUTH

CALCULATED DATA		MEASURED DATA		LAYER	RESISTIVITY(OHM-M)		THICKNESS(M)		
TILT ANGLE	———	TILT ANGLE	X	1	6.30±	.00	90.00	±	1.
				2	2.20±	.03	1000E+11±		3

XBL 803-8985

COMPARSION OF CALCULATED AND MEASURED DATA

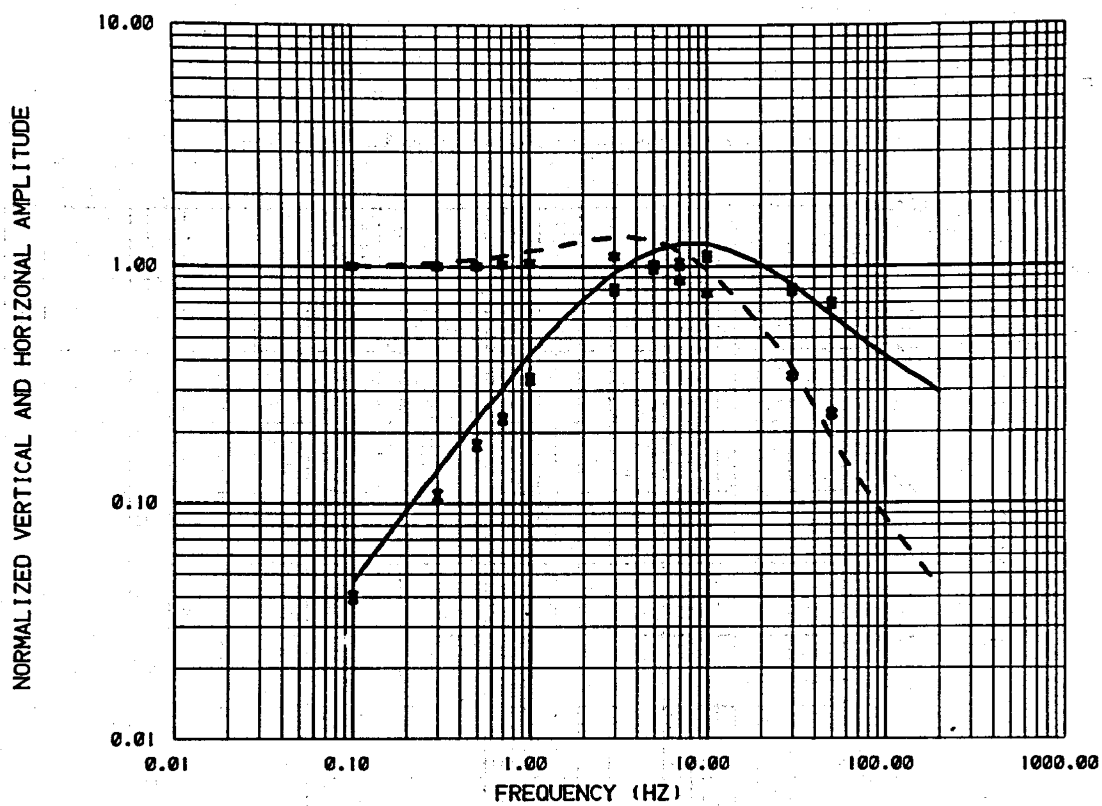

PANTHER CANYON T-T 1.5KM SOUTH

CALCULATED DATA		MEASURED DATA		LAYER	RESISTIVITY(OHM-M)		THICKNESS(M)	
HR	————————	HR	X	1	8.10±	.00	340.0	± 16.
HZ	—— —— ——	HZ	*	2	3.90±	.38	280.0	± 47.
				3	150.00±	173.45	.1000E+11±	0.

DATA VARIENCE ESTIMATE 153.8

XBL 804-9008

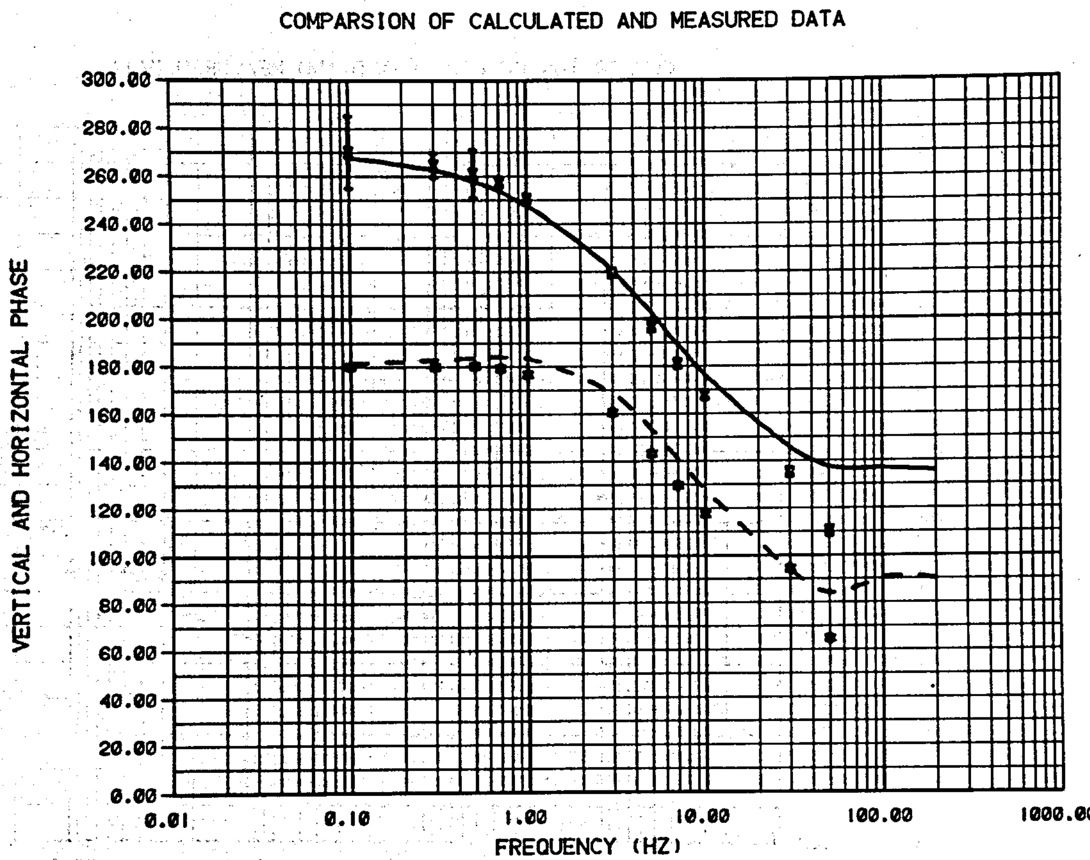

PANTHER CANYON T-T 1.5KM SOUTH

CALCULATED DATA

HR ————————

HZ — — —

MEASURED DATA

HR X

HZ *

LAYER	RESISTIVITY(OHM-M)		THICKNESS(M)	
1	8.10±	.00	340.0 ±	16.
2	3.90±	.38	280.0 ±	47.
3	150.00±	173.45	.1000E+11±	0.

DATA VARIENCE ESTIMATE 153.8

XBL 804-9013

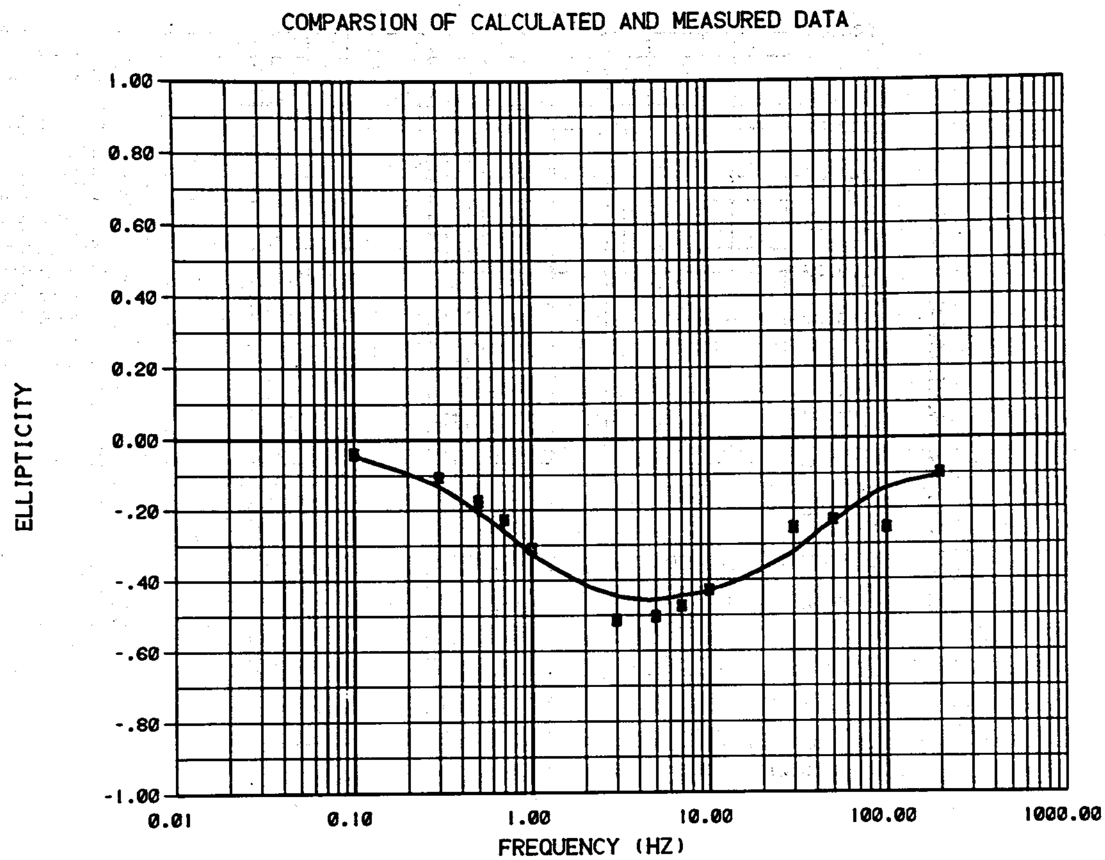

PANTHER CANYON T-T 1.5KM SOUTH

CALCULATED DATA		MEASURED DATA		LAYER	RESISTIVITY(OHM-M)		THICKNESS(M)	
ELLIPTICITY	————	ELLIPTICITY	X	1	8.10±	.00	340.0 ±	16.
				2	3.90±	.38	280.0 ±	47.
				3	150.00±	173.45	.1000E+11±	0.

DATA VARIENCE ESTIMATE 153.8

XBL 804-9005

COMPARSION OF CALCULATED AND MEASURED DATA

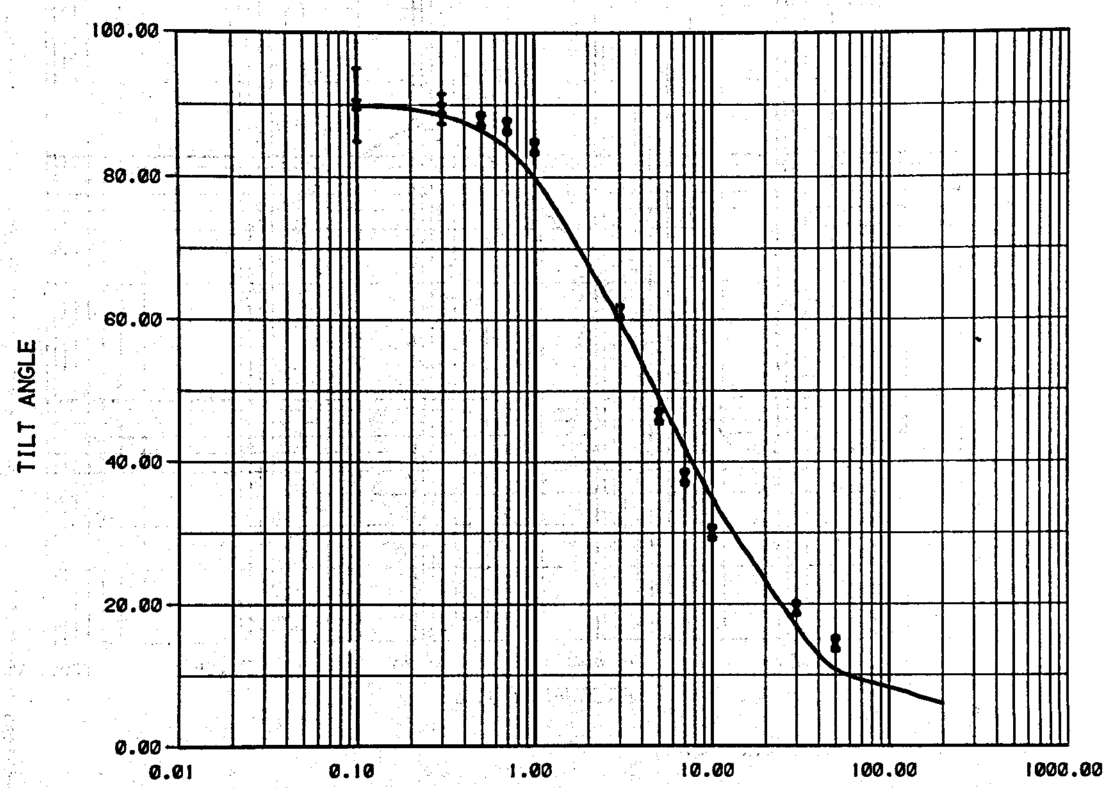

PANTHER CANYON T-T 1.5KM SOUTH

CALCULATED DATA		MEASURED DATA		LAYER	RESISTIVITY(OHM-M)		THICKNESS(M)	
TILT ANGLE	———	TILT ANGLE	X	1	8.10±	.00	340.0	± 16.
				2	3.90±	.38	280.0	± 47.
				3	150.00±	173.45	.1000E+11±	0.

DATA VARIENCE ESTIMATE 153.8

XBL 803-8971

COMPARSION OF CALCULATED AND MEASURED DATA

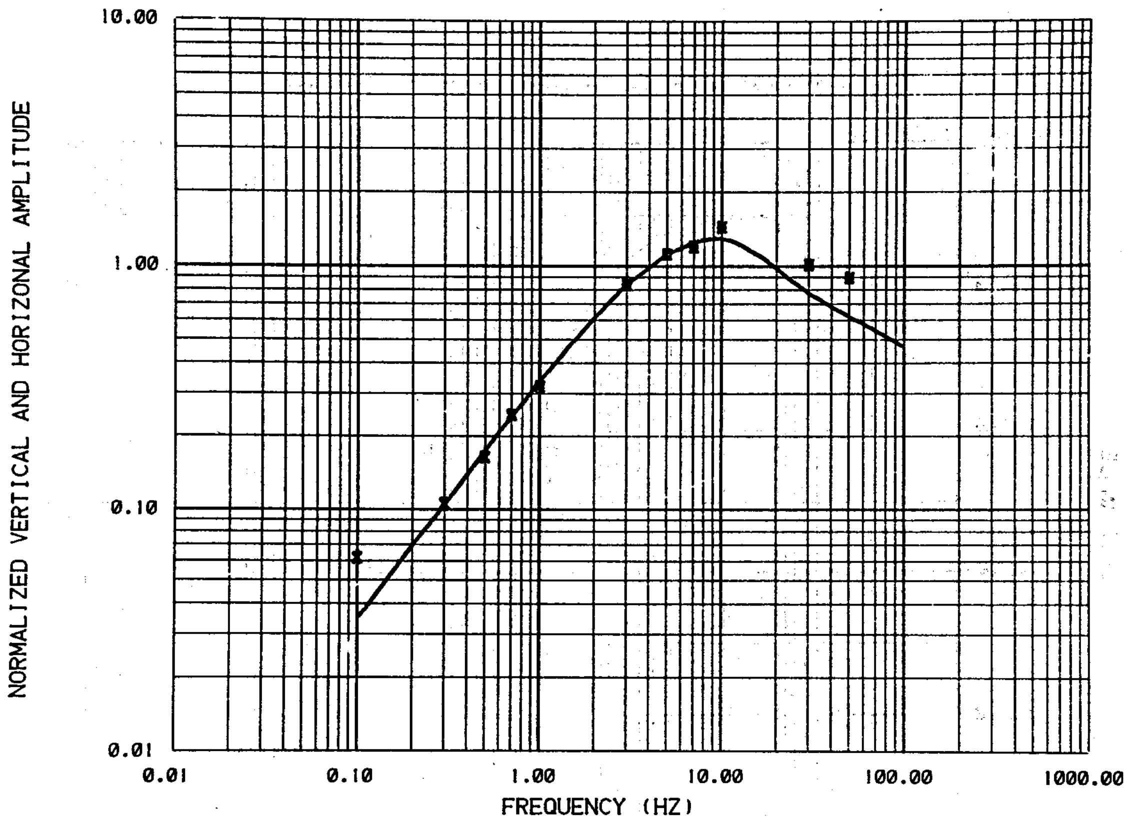

PANTHER CANYON H-H 1.5KM EAST

CALCULATED DATA		MEASURED DATA		LAYER	RESISTIVITY(OHM-M)	THICKNESS(M)
HR	————————	HR	X	1	9.00± .00	200.0 ± 15.
				2	2.70± .57	125.0 ± 34.
				3	150.00± 102.33	.1000E+11± 0.

DATA VARIENCE ESTIMATE 126.2

XBL 805-9744

COMPARSION OF CALCULATED AND MEASURED DATA

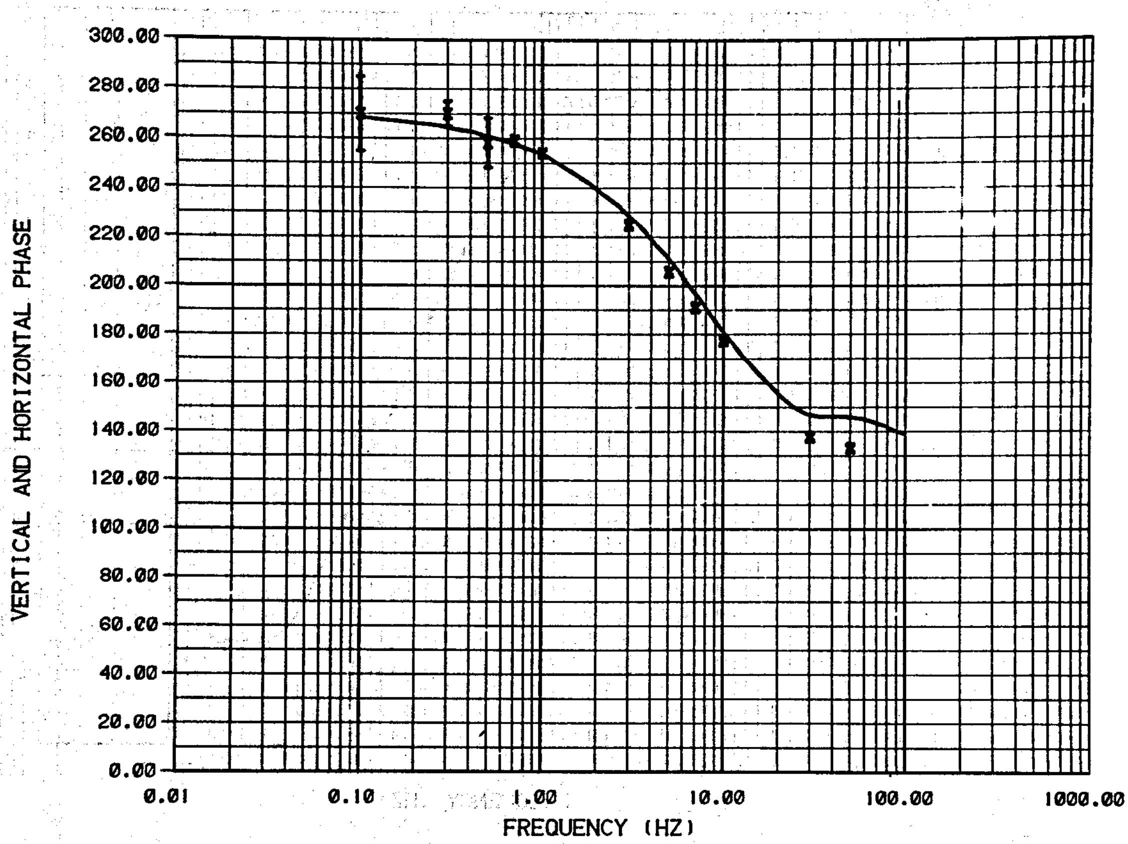

PANTHER CANYON H-H 1.5KM EAST

CALCULATED DATA	MEASURED DATA		LAYER	RESISTIVITY(OHM-M)		THICKNESS(M)	
HR ———	HR	X	1	9.00±	.00	200.0	± 15.
			2	2.70±	.57	125.0	± 34.
			3	150.00±	102.33	.1000E+11±	0.

DATA VARIENCE ESTIMATE 126.2

XBL 805-9746

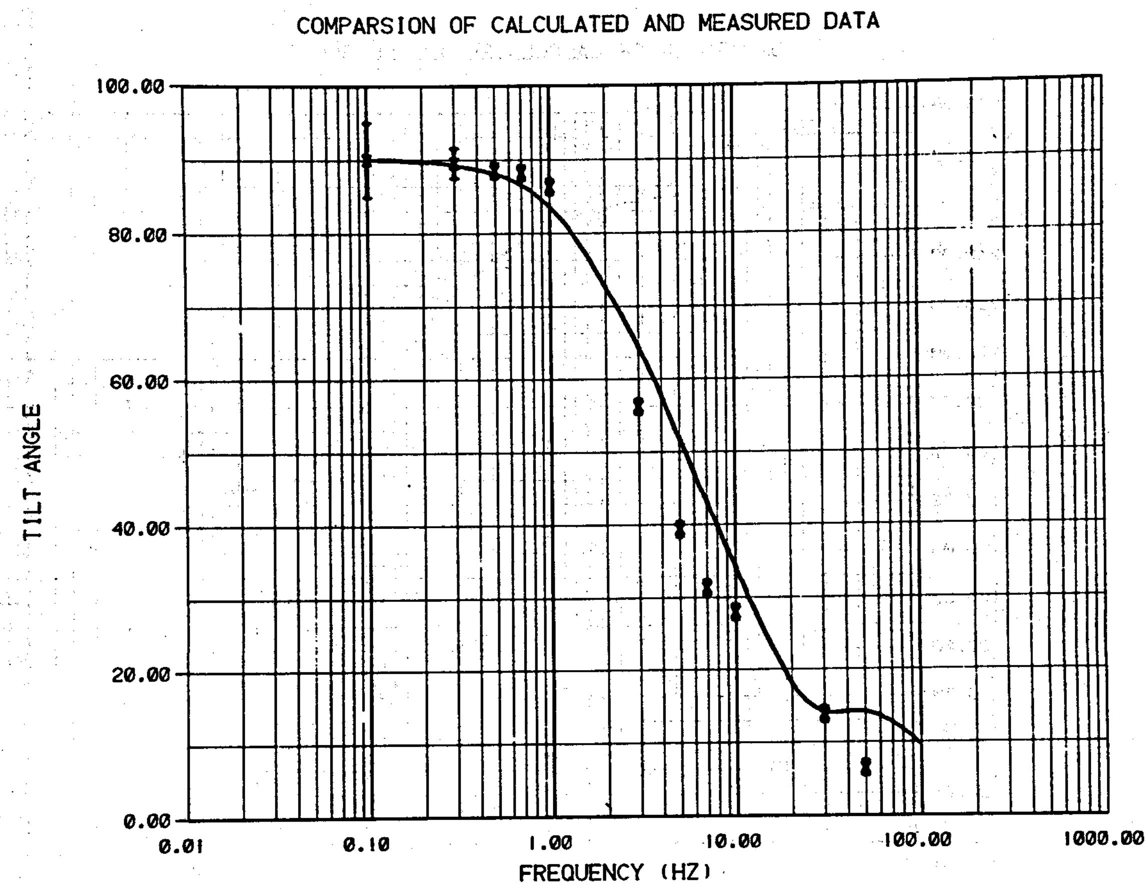

PANTHER CANYON H-H 1.5KM EAST

CALCULATED DATA	MEASURED DATA		LAYER	RESISTIVITY(OHM-M)		THICKNESS(M)	
TILT ANGLE ———	TILT ANGLE	X	1	9.00±	.00	200.0	± 15.
			2	2.70±	.57	125.0	± 34.
			3	150.00±	102.33	.1000E+11±	0.

DATA VARIENCE ESTIMATE 126.2

XBL 805-9748

COMPARSION OF CALCULATED AND MEASURED DATA

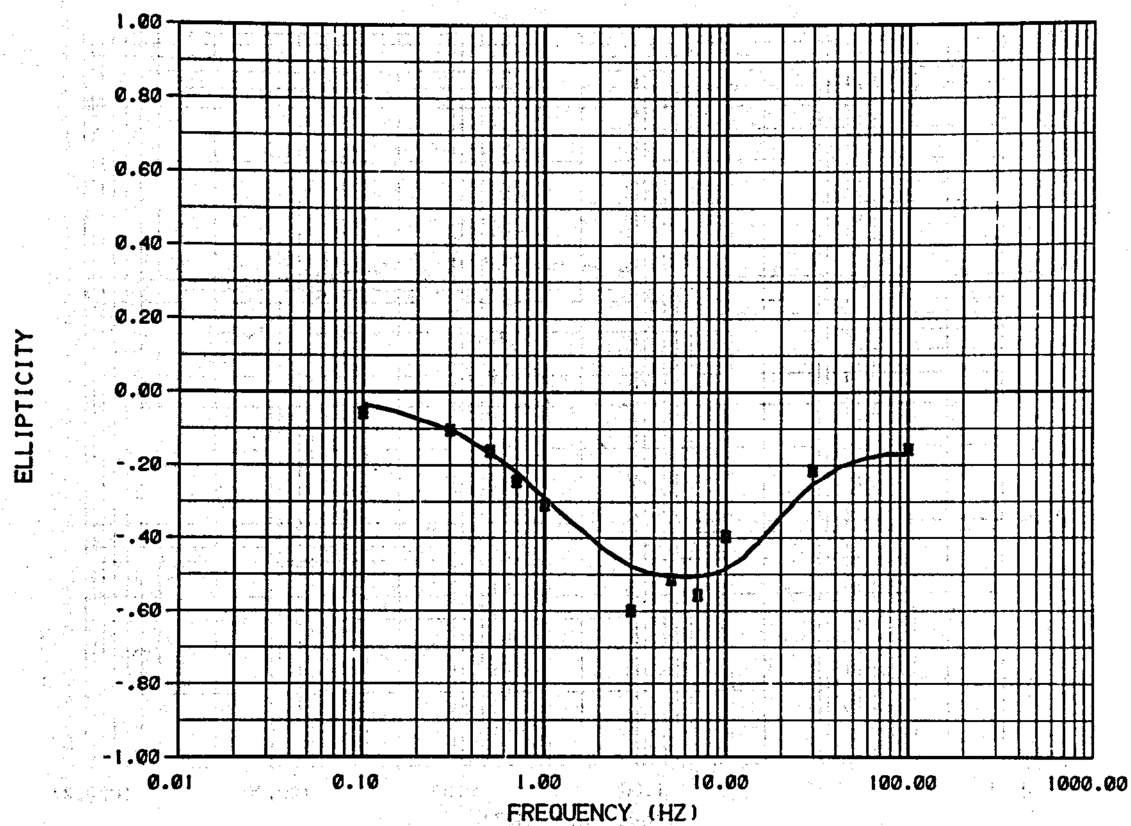

PANTHER CANYON H-H 1.5KM EAST

CALCULATED DATA ELLIPTICITY ———

MEASURED DATA ELLIPTICITY X

LAYER	RESISTIVITY(OHM-M)		THICKNESS(M)	
1	9.00±	.00	200.0	± 15.
2	2.70±	.57	125.0	± 34.
3	150.00±	102.33	.1000E+11±	0.

DATA VARIENCE ESTIMATE 126.2

XBL 805-9747

COMPARSION OF CALCULATED AND MEASURED DATA

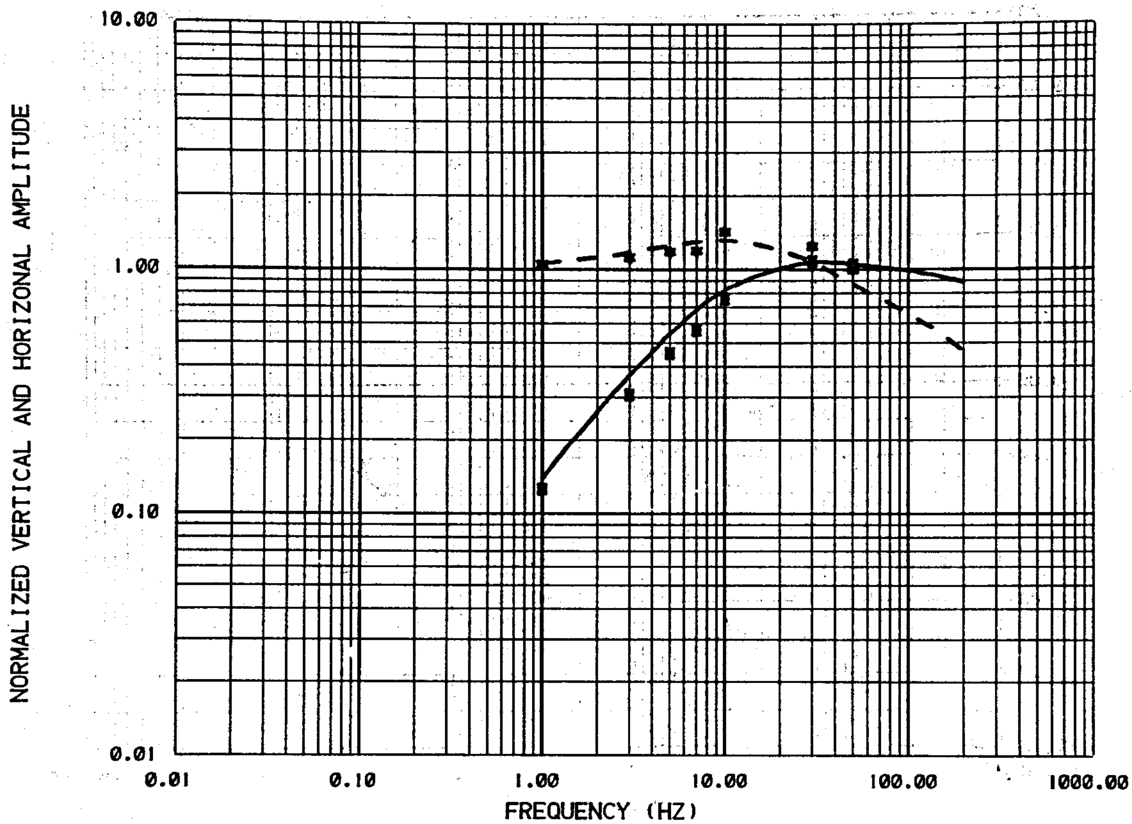

PANTHER CANYON H-H 0.5KM EAST

CALCULATED DATA		MEASURED DATA		LAYER	RESISTIVITY(OHM-M)		THICKNESS(M)	
HR	————————	HR	X	1	15.00±	.00	120.0	± 2.
HZ	— — —	HZ	*	2	2.80±	.08	200.0	± 20.
				3	10.00±	1.85	.1000E+11±	0.

DATA VARIENCE ESTIMATE 90.07

XBL 806-9848

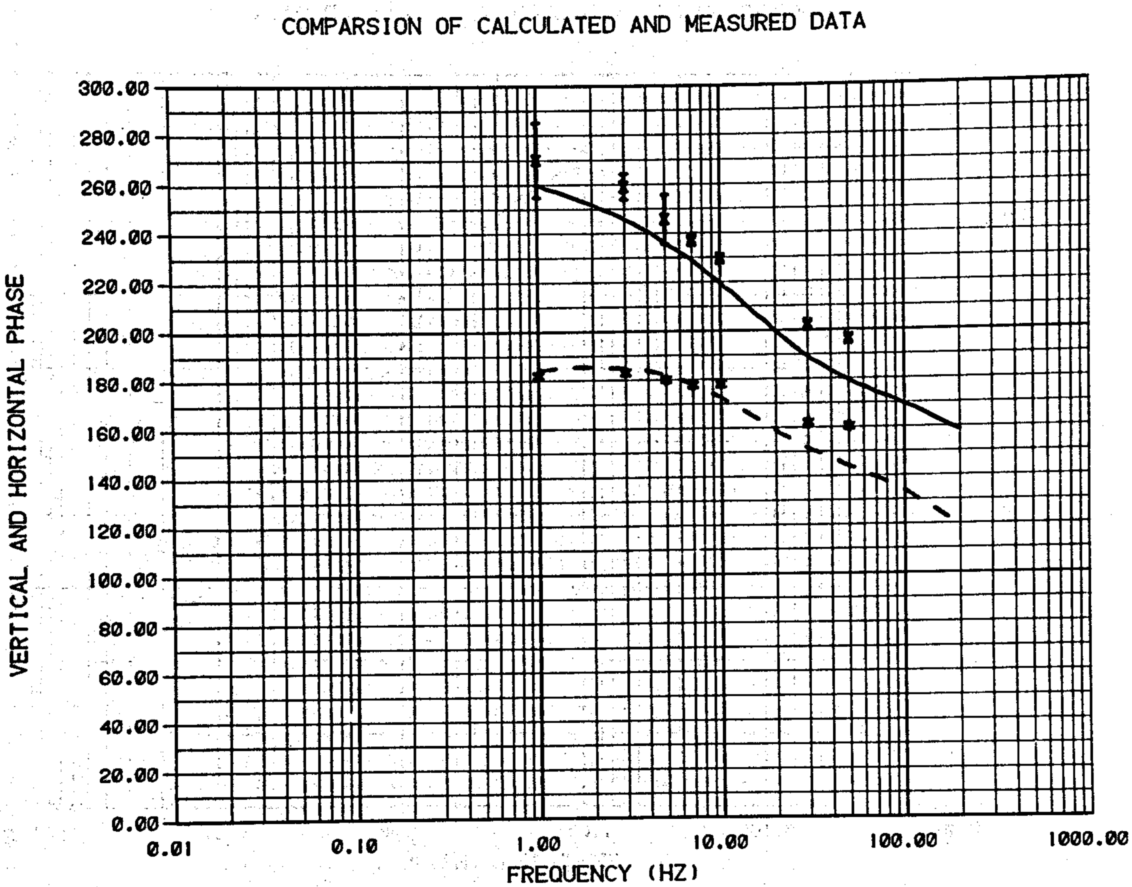

PANTHER CANYON H-H 0.5KM EAST

CALCULATED DATA		MEASURED DATA		LAYER	RESISTIVITY(OHM-M)		THICKNESS(M)	
HR	———————	HR	X	1	15.00±	.00	120.0	± 2.
HZ	— — —	HZ	*	2	2.80±	.08	200.0	± 20.
				3	10.00±	1.85	.1000E+11±	0.

DATA VARIENCE ESTIMATE 90.07

XBL 806-9847

COMPARSION OF CALCULATED AND MEASURED DATA

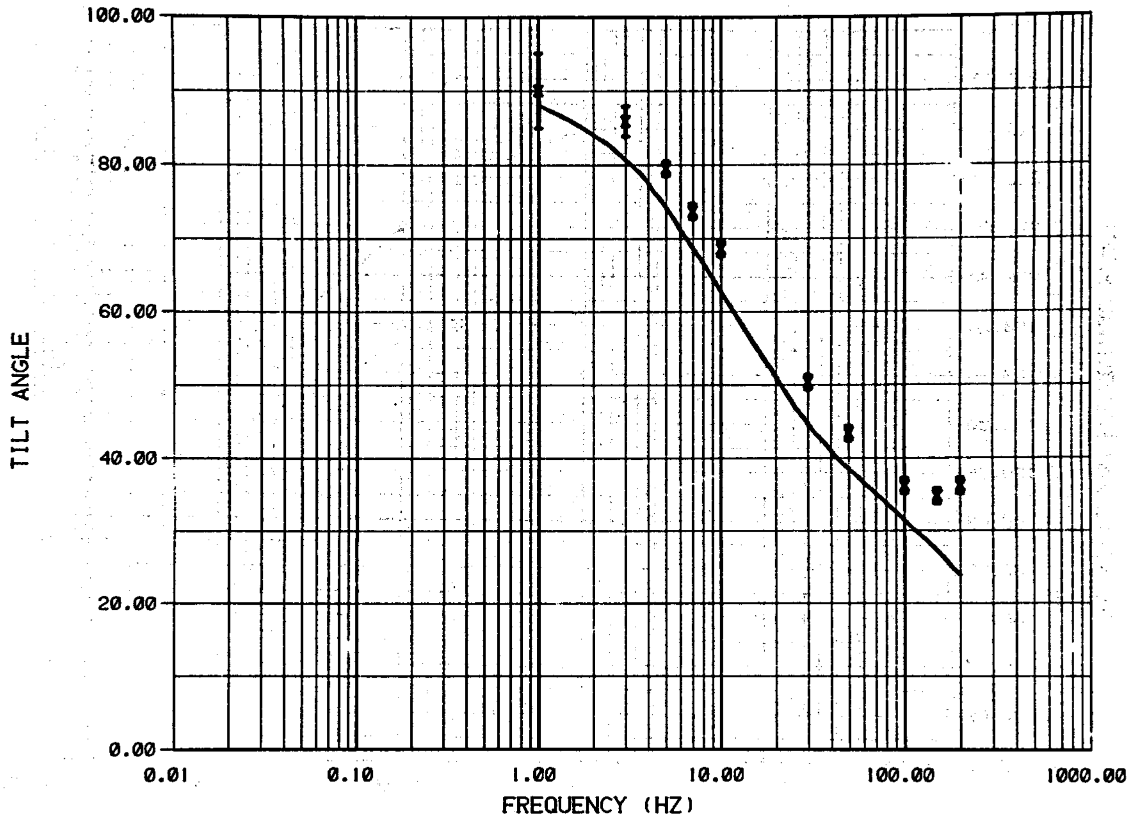

PANTHER CANYON H-H 0.5KM EAST

CALCULATED DATA		MEASURED DATA		LAYER	RESISTIVITY(OHM-M)		THICKNESS(M)	
TILT ANGLE	————	TILT ANGLE	X	1	15.00±	.00	120.0 ±	2.
				2	2.80±	.08	200.0 ±	20.
				3	10.00±	1.85	.1000E+11±	0.

DATA VARIENCE ESTIMATE 90.07

XBL 805-9741

COMPARSION OF CALCULATED AND MEASURED DATA

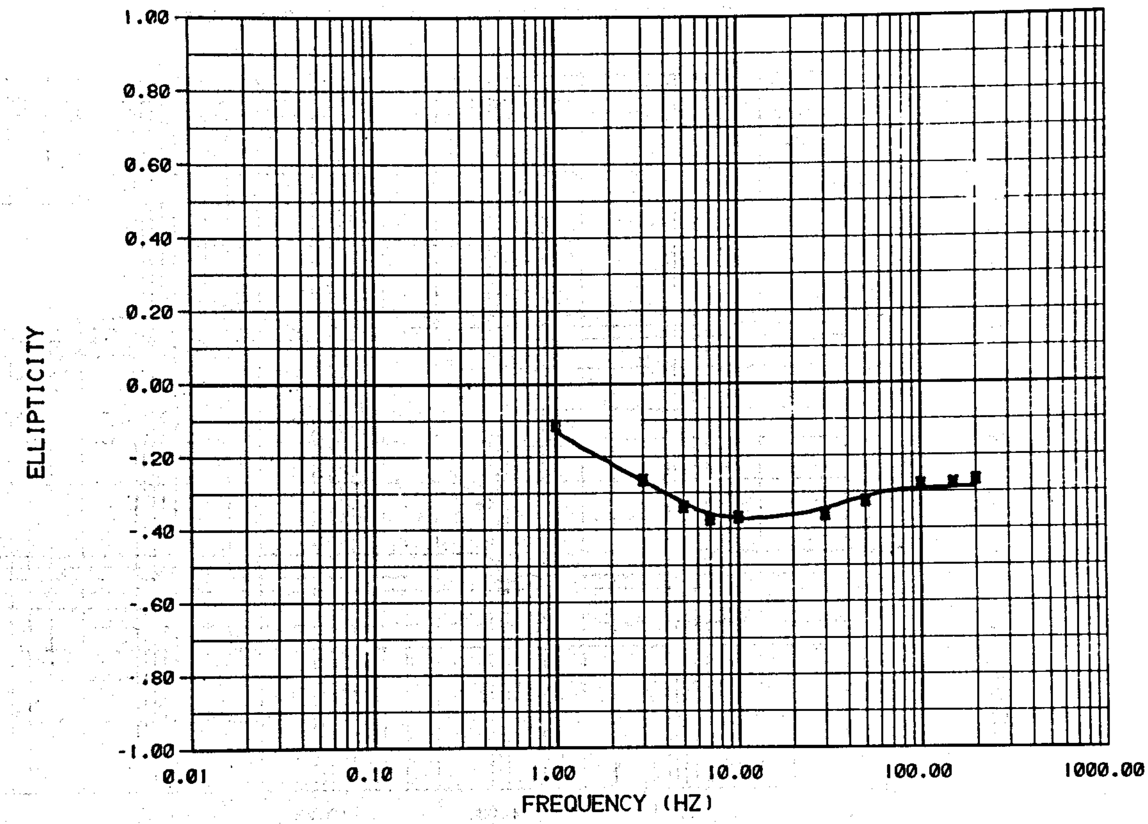

PANTHER CANYON H-H 0.5KM EAST

CALCULATED DATA	MEASURED DATA	LAYER	RESISTIVITY(OHM-M)	THICKNESS(M)
ELLIPTICITY ———	ELLIPTICITY X	1	15.00± .00	120.0 ± 2.
		2	2.80± .08	200.0 ± 20.
		3	10.00± 1.85	.1000E+11± 0.

DATA VARIENCE ESTIMATE 90.07

XBL 805-9740

COMPARSION OF CALCULATED AND MEASURED DATA

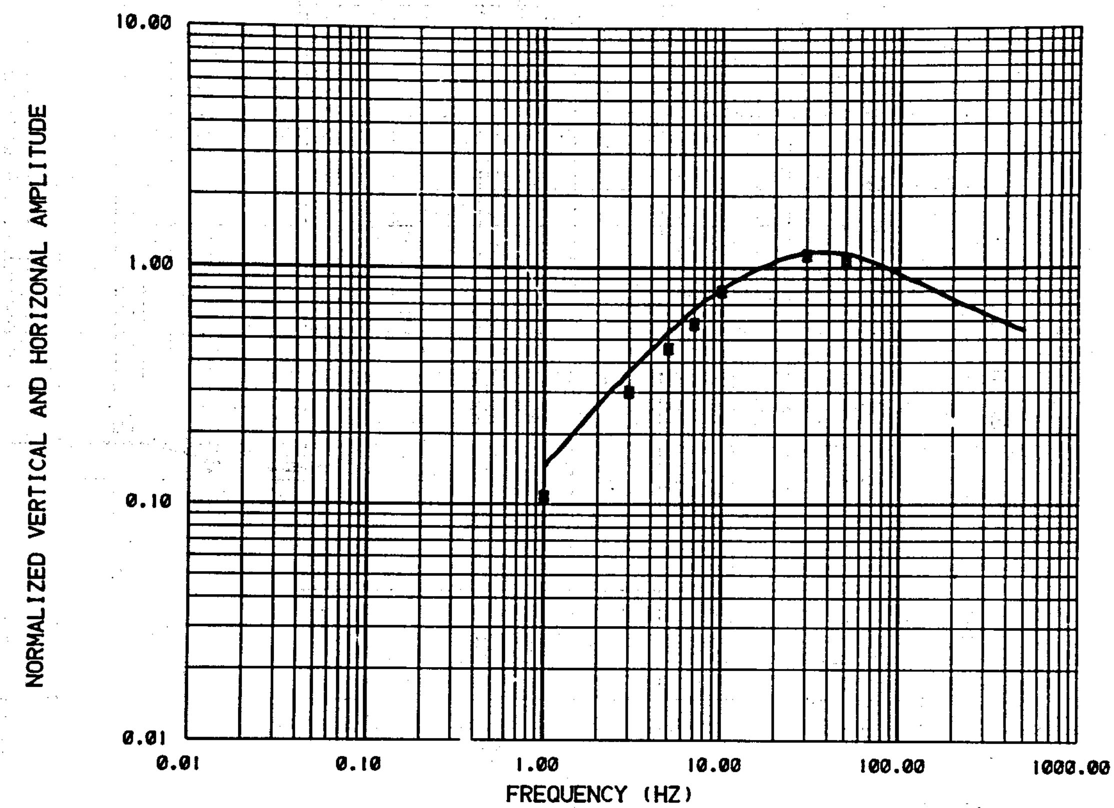

PANTHER CANYON H-H 0.5KM WEST

CALCULATED DATA		MEASURED DATA		LAYER	RESISTIVITY(OHM-M)		THICKNESS(M)	
HR	————————	HR	X	1	10.00±	.00	50.00 ±	1.
				2	3.20±	.03	.1000E+11±	0.

DATA VARIENCE ESTIMATE 504.5

XBL 803-8979

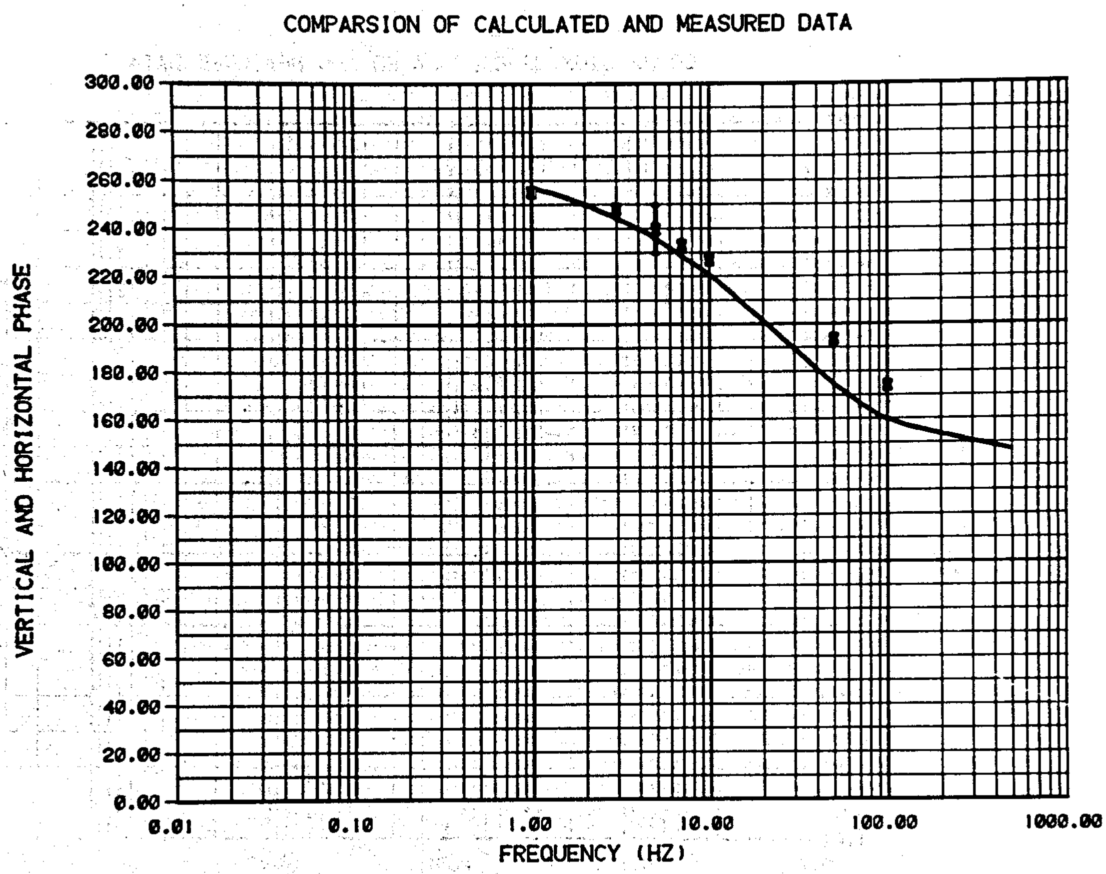

PANTHER CANYON H-H 0.5KM WEST

CALCULATED DATA	MEASURED DATA	LAYER	RESISTIVITY(OHM-M)		THICKNESS(M)	
HR ————	HR X	1	10.00±	.00	50.00 ±	1.
		2	3.20±	.03	.1000E+11±	0.

DATA VARIENCE ESTIMATE 504.5

XBL 803-8965

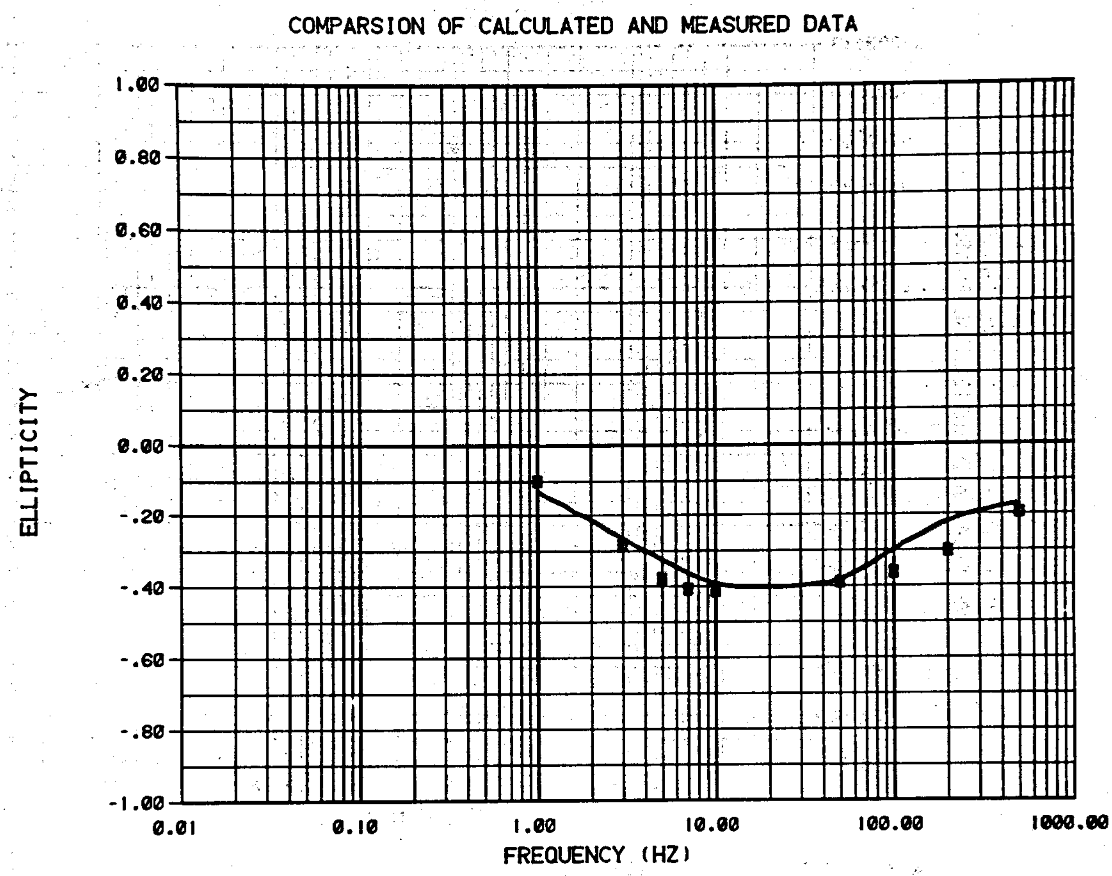

PANTHER CANYON H-H 0.5KM WEST

CALCULATED DATA		MEASURED DATA		LAYER	RESISTIVITY(OHM-M)		THICKNESS(M)	
ELLIPTICITY	———	ELLIPTICITY	X	1	10.00*	.00	50.00 *	1.
				2	3.20*	.03	.1000E+11*	0.

DATA VARIENCE ESTIMATE 504.5

XBL 804-9018

COMPARSION OF CALCULATED AND MEASURED DATA

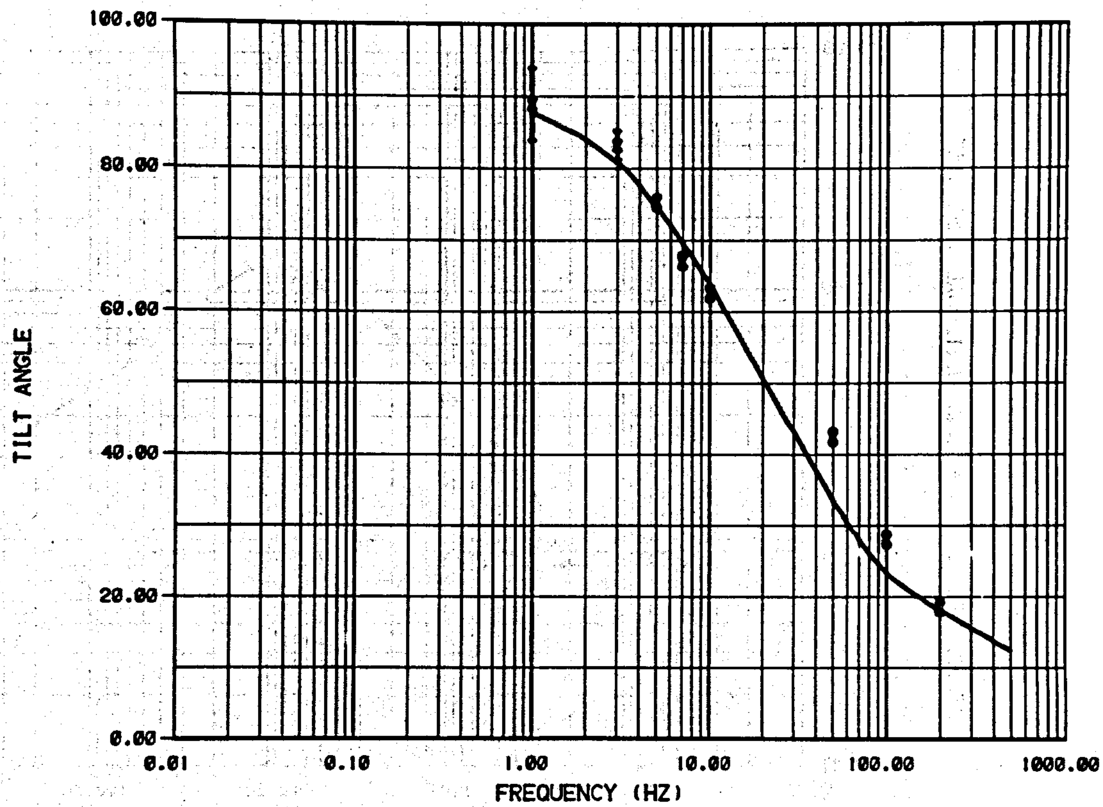

PANTHER CANYON H-H 0.5KM WEST

CALCULATED DATA		MEASURED DATA		LAYER	RESISTIVITY(OHM-M)		THICKNESS(M)	
TILT ANGLE	————	TILT ANGLE	X	1	10.00±	.00	50.00 ±	1.
				2	3.20±	.03	.1000E+11±	0.

DATA VARIENCE ESTIMATE 504.5

XBL 803-8982

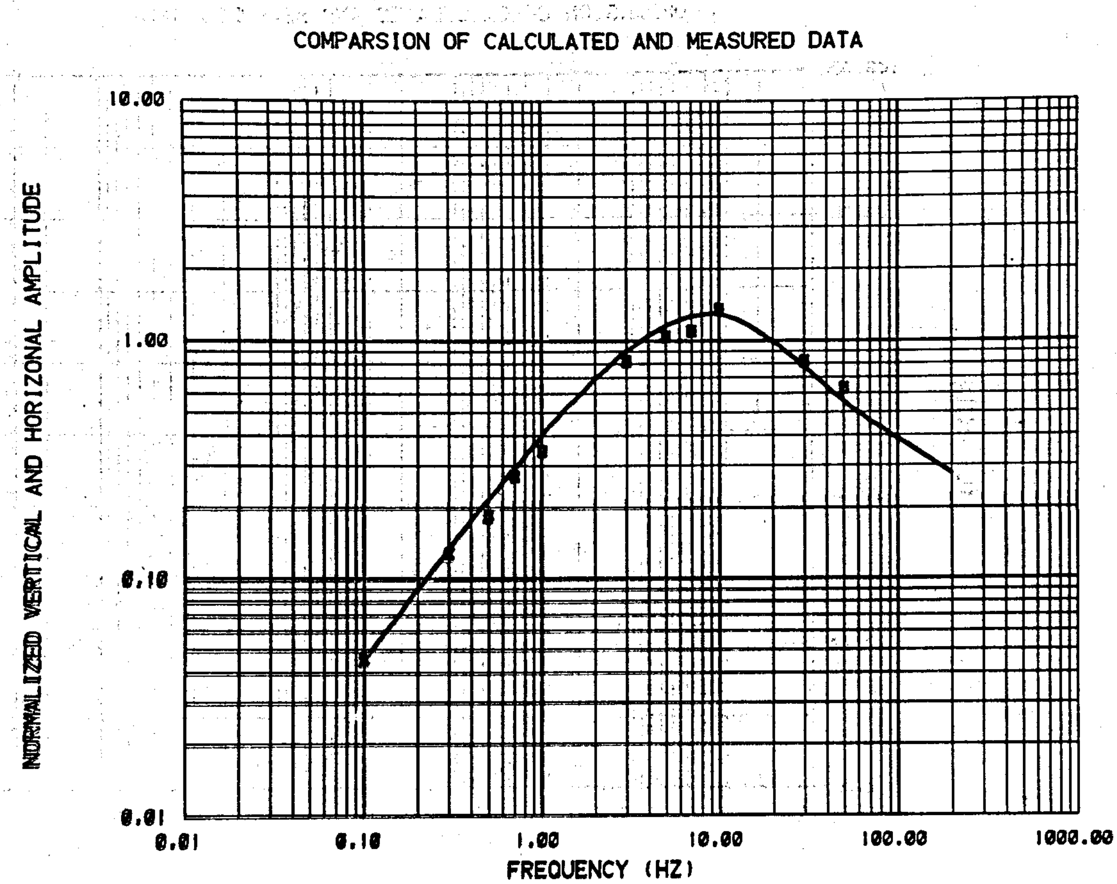

PANTHER CANYON H-H 1.5KM WEST

CALCULATED DATA		MEASURED DATA		LAYER	RESISTIVITY(OHM-M)		THICKNESS(M)	
HR	————	HR	X	1	8.00±	.00	700.0	± 42.
				2	25.00±	6.31	.1000E+11±	0.

DATA VARIENCE ESTIMATE 82.50

XBL 803-8999

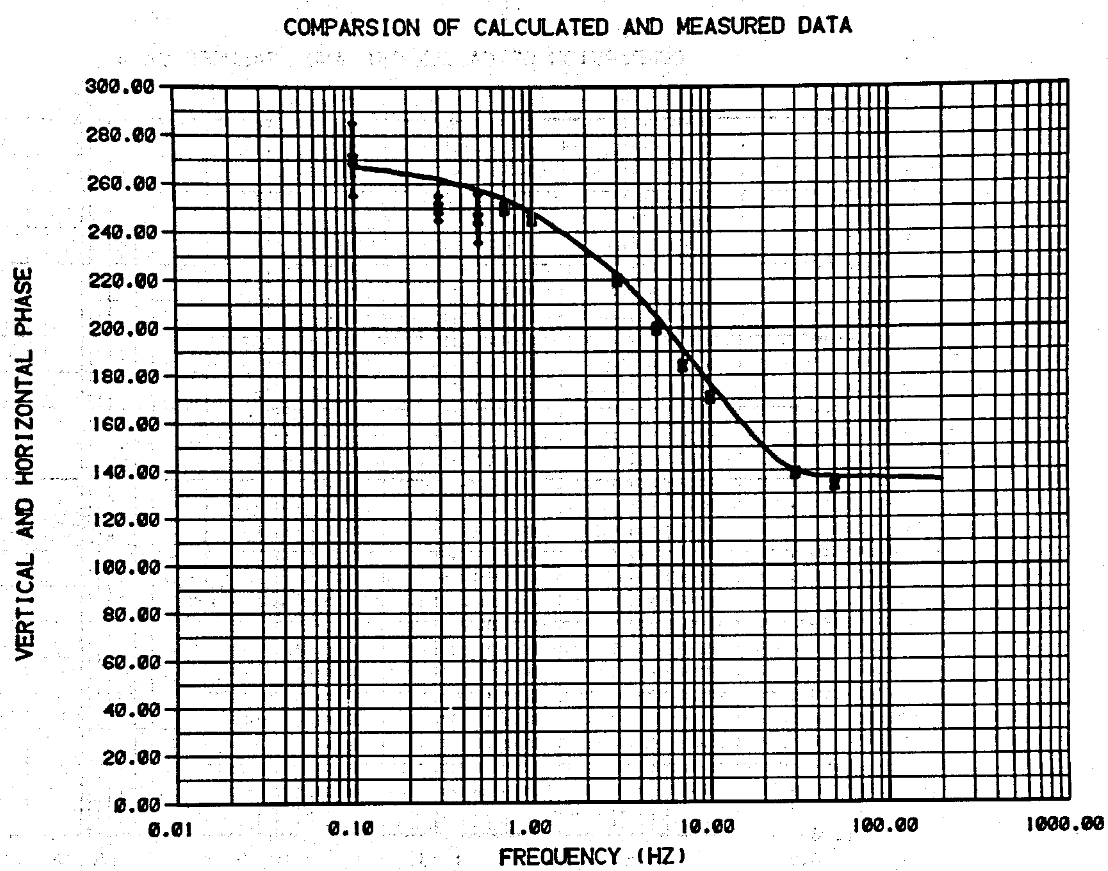

PANTHER CANYON H-H 1.5KM WEST

CALCULATED DATA		MEASURED DATA		LAYER	RESISTIVITY(OHM-M)		THICKNESS(M)	
HR	————	HR	X	1	8.00±	.00	700.0 ±	42.
				2	25.00±	6.31	.1000E+11±	0.

DATA VARIENCE ESTIMATE 82.50

XBL 804-9002

COMPARSION OF CALCULATED AND MEASURED DATA

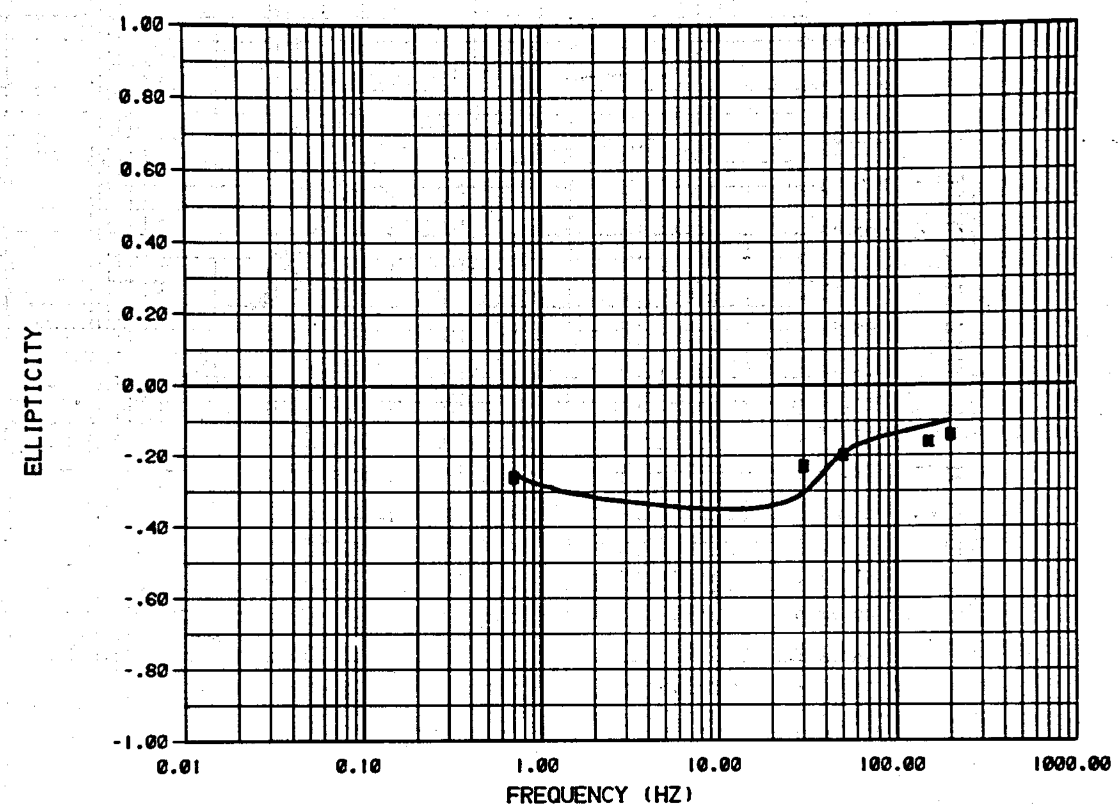

PANTHER CANYON H-H 1.5KM WEST

CALCULATED DATA		MEASURED DATA		LAYER	RESISTIVITY(OHM-M)		THICKNESS(M)	
ELLIPTICITY	————	ELLIPTICITY	X	1	8.00±	.00	700.0 ±	42.
				2	25.00±	6.31	.1000E+11±	0.

DATA VARIENCE ESTIMATE 82.50

XBL 803-8995

COMPARSION OF CALCULATED AND MEASURED DATA

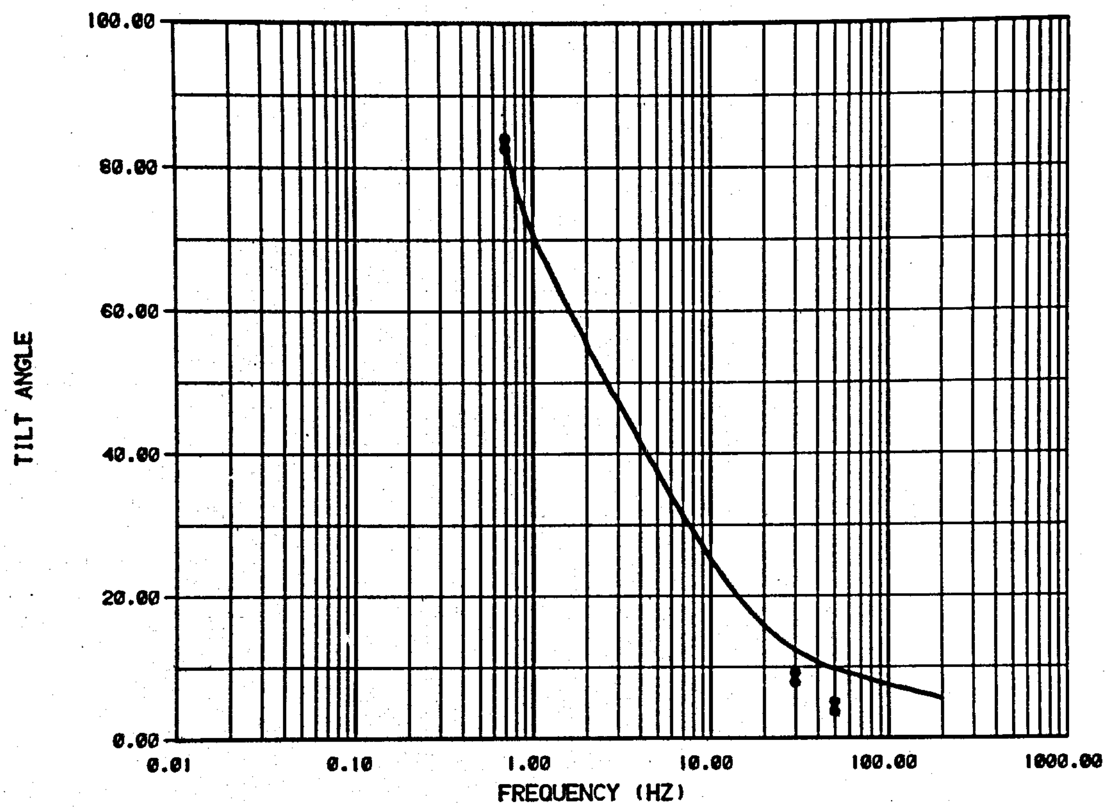

PANTHER CANYON H-H 1.5KM WEST

CALCULATED DATA		MEASURED DATA		LAYER	RESISTIVITY(OHM-M)		THICKNESS(M)	
TILT ANGLE	———	TILT ANGLE	X	1	8.00±	.00	700.0 ±	42.
				2	25.00±	6.31	.1000E+11±	0.

DATA VARIENCE ESTIMATE 82.50

XBL 803-8996